AD-A056 982 SYSTEMS RESEARCH LABS INC DAYTON OHIO F/G 5/8
A THEORY FOR LONGITUDINAL SHORT-PERIOD PILOT INDUCED OSCILLATIO--ETC(U)
JUN 77 R H SMITH F33615-77-C-3011
UNCLASSIFIED AFFDL-TR-77-57 NL

1 OF 2
AD A056 982

AFFDL-TR-77-57

LEVEL II

A THEORY FOR LONGITUDINAL SHORT-PERIOD PILOT INDUCED OSCILLATIONS

RALPH H. SMITH
SYSTEMS RESEARCH LABORATORIES, INC.
2800 INDIAN RIPPLE ROAD
DAYTON, OHIO 45440

JUNE 1977

TECHNICAL REPORT AFFDL-TR-77-57
Interim Report for Period November 1975 – April 1977

AIR FORCE FLIGHT DYNAMICS LABORATORY
AIR FORCE WRIGHT AERONAUTICAL LABORATORIES
AIR FORCE SYSTEMS COMMAND
WRIGHT-PATTERSON AIR FORCE BASE, OHIO 45433

NOTICE

When Government drawings, specifications, or other data are used for any purpose other than in connection with a definitely related Government procurement operation, the United States Government thereby incurs no responsibility nor any obligation whatsoever; and the fact that the Government may have formulated, furnished, or in any way supplied the said drawings, specifications, or other data, is not to be regarded by implication or otherwise as in any manner licensing the holder or any other person or corporation, or conveying any rights or permission to manufacture, use, or sell any patented invention that may in any way be related thereto.

This report has been reviewed by the Information Office (OI) and is releasable to the National Technical Information Service (NTIS). At NTIS it will be available to the general public, including foreign nations.

This technical report has been reviewed and is approved for publication.

Frank L. George Brian W. Van Vliet

FRANK L. GEORGE BRIAN W. VAN VLIET
Co-project Engineers

R. O. Anderson

Ronald O. Anderson, Chief
Control Criteria Branch
Flight Control Division
Air Force Flight Dynamics Laboratory

FOR THE COMMANDER

Robert F. Lopina

R. F. Lopina, Col, USAF
Chief, Flight Control Division
Air Force Flight Dynamics Laboratory

Copies of this report should not be returned unless return is required by security considerations, contractual obligations, or notice on a specific document.

AIR FORCE/56780/7 June 1978 — 450

SECURITY CLASSIFICATION OF THIS PAGE (When Data Entered)

(19) **REPORT DOCUMENTATION PAGE**

READ INSTRUCTIONS BEFORE COMPLETING FORM

(18) 1. REPORT NUMBER: AFFDL-TR-77-57

2. GOVT ACCESSION NO.

3. RECIPIENT'S CATALOG NUMBER

(6) 4. TITLE (and Subtitle): A Theory for Longitudinal Short-Period Pilot Induced Oscillations.

(9) 5. TYPE OF REPORT & PERIOD COVERED: Interim Report. Nov 1975 - Apr 1977,

6. PERFORMING ORG. REPORT NUMBER

(10) 7. AUTHOR(s): Ralph H. Smith

(15) 8. CONTRACT OR GRANT NUMBER(s): F33615-77-C-3011

9. PERFORMING ORGANIZATION NAME AND ADDRESS: Systems Research Laboratories, Inc. 2800 Indian Ripple Road Dayton, Ohio 45440

(16) (12) 10. PROGRAM ELEMENT, PROJECT, TASK AREA & WORK UNIT NUMBERS: 62201F 82190418

(11) 11. CONTROLLING OFFICE NAME AND ADDRESS: Air Force Flight Dynamics Laboratory/FGC Wright-Patterson Air Force Base Ohio 45433

12. REPORT DATE: June 1977

13. NUMBER OF PAGES

(12) 141 p.

14. MONITORING AGENCY NAME & ADDRESS (if different from Controlling Office)

15. SECURITY CLASS. (of this report): Unclassified

15a. DECLASSIFICATION/DOWNGRADING SCHEDULE

16. DISTRIBUTION STATEMENT (of this Report)

Approved for public release; distribution unlimited.

17. DISTRIBUTION STATEMENT (of the abstract entered in Block 20, if different from Report)

18. SUPPLEMENTARY NOTES

19. KEY WORDS (Continue on reverse side if necessary and identify by block number)

PIO	Manual Control	Human Dynamics
Pilot Induced Oscillation	Pilot Dynamics	Human Pilot Dynamics
Handling Qualities	Bibliography	
Flying Qualities		

20. ABSTRACT (Continue on reverse side if necessary and identify by block number)

This report presents a theory for longitudinal, short-period, pilot-induced oscillations (PIO). The theory explains how the airplane's pitch attitude and normal acceleration modes can couple with pilot dynamics to produce large-amplitude, uncontrollable oscillations. The effects of control system dynamics and feel system nonlinearities are encompassed by this theory. It is concluded that an airplane's potential for PIO can be determined based

(over)

DD FORM 1 JAN 73 1473 EDITION OF 1 NOV 65 IS OBSOLETE

SECURITY CLASSIFICATION OF THIS PAGE (When Data Entered)

Item 20 (continued)

entirely on linear systems analysis; the prediction of fully-developed PIO frequency and amplitude requires that all significant nonlinearties be considered. The theory postulates that PIO can develop either as a result of closed loop control of pitch attitude or from abrupt control or atmospheric inputs of size sufficient to excite a lightly damped, dominant, stick-free airplane mode. A number of PIO case histories are examined; it is shown that these confirm the proposed theory. The implications of the theory to flight test and to simulation are discussed. A generalized definition for PIO is given which permits distinctions to be made between pilot-vehicle system oscillations due only to attitude control and those due to attitude plus path control modes. It is suggested that the theory can be easily extended to the study of lateral-directional PIO. A bibliography of PIO source material is included with this report.

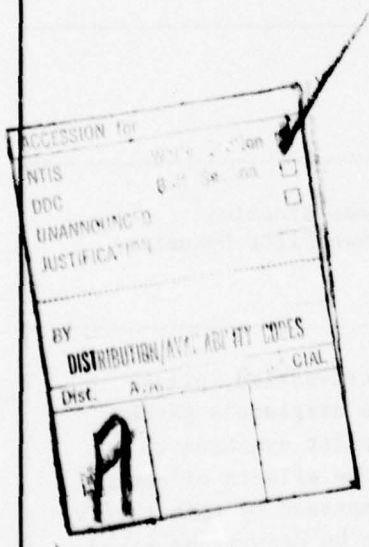

FOREWORD

This report summarizes an effort to identify the principal pilot-airplane-control system mechanics that lead to the development of the pilot induced oscillation phenomenon. The development of the PIO theory was performed on-site at the Air Force Flight Dynamics Laboratory under sponsorship of the Visiting Scientist program, Contract F33615-73-C-4155, Task 69. The testing of the theory against the base of PIO case history data and portions of the final documentation were performed under Contract F33615-77-C-3011, as part of Air Force Project 8219, Task 821904. The AFFDL project engineer for both efforts was Mr. Frank L. George (AFFDL/FGC). All work was performed by the author, Ralph H. Smith, of Systems Research Laboratories, Inc., Dayton, Ohio, during the period November 1975 through April 1977. The draft of this report was submitted in May 1977.

The author gratefully acknowledges the support given to this work by members of the AFFDL/FGC engineering staff. Mr. Frank George provided invaluable assistance at almost every phase of this project by providing basic source material, serving as a sounding board, and helping to clarify the pitfalls involved in making a successful transition from theory to airplane design. Capt. Jerry Callahan and Mr. David Mayhew were always ready with counterarguments which served to keep this work focused on the real problems; it could not have been done without their comments, criticisms and continuing support. Mrs. Ruth Kellar provided considerable assistance in the accumulation of the reports which comprise the bibliography and references of this document. Finally, the contributions of Mr. Thomas Twisdale of the Air Force Flight Test Center (DOEST) must be mentioned. Tom has, over the past several months, been testing the proposed theory against current flight test problems; his interest, enthusiasm and encouragement have provided substantial motivation for the author to broaden the scope of the initial documentation effort and to include a commentary on the difficulties of simulation or flight testing of the PIO phenomenon.

TABLE OF CONTENTS

SECTION		PAGE
I	THE PIO PROBLEM	1
	A. Background	1
	B. The Handling Qualities--PIO Dichotomy	4
	C. Report Outline	5
II	A DEFINITION	6
	A. PIO Definition	6
	B. Comments	6
III	A PILOT MODEL	8
	A. Background	8
	B. A Comment on Stick Pumping and Motion Cues	14
	C. A Pilot Model for PIO Analysis	16
	D. Model Properties	18
IV	A PIO THEORY	21
	A. PIO Categories	21
	B. Type I PIO	21
	Phase 1: Pitch Attitude System Dynamics	21
	Phase 2: Normal Acceleration System Dynamics	28
	Phase 3: Acceleration Amplitude	35
	C. Type II PIO	37
V	SUMMARY OF RULES FOR PIO ASSESSMENT	41
	A. Type I PIO (Initiated by Pitch Attitude Control)	41
	B. Type II PIO (Initiated by Maneuvering Control of Turbulence)	43
VI	NUMERICAL EXAMPLES	44
	A. The YF-17 (Approach and Landing: CAS-On)	44
	System Dynamics	44
	Type II PIO Assessment	48
	Type I PIO Assessment	48
	B. The T-38A (M = 0.85 at Sea Level)	52
	System Dynamics--Original Control System	53
	Type I PIO Assessment --T-38A	53
	Type II PIO Assessment--T-38A	68
	PIO Assessment--Modified Control System	68
	Comment on Pilot Time Delay	71

TABLE OF CONTENTS (cont'd)

SECTION		PAGE
VI	NUMERICAL EXAMPLES (cont'd)	
	C. The YF-12 (M = 0.77, Altitude = 25,000; Refueling Condition)	72
	System Dynamics	73
	Type I PIO Assessment--YF-12	79
	Type II PIO Assessment--YF-12	90
	D. Calspan PIO In-Flight Simulations	90
	Type I PIO	92
	Type II PIO	94
	Summary	95
VII	THE IDENTIFICATION OF PIO IN FLIGHT TEST OR SIMULATION	101
	A. Ground-Based Simulation	101
	B. In-Flight Simulation	105
	C. Flight Test	108
VIII	DISCUSSION AND CONCLUSIONS	111
APPENDIX:	NORMAL ACCELERATION DYNAMICS	115
BIBLIOGRAPHY		118
REFERENCES		124

LIST OF ILLUSTRATIONS

FIGURE		PAGE
1	Simplified Pilot-Vehicle System Model for Fully-Developed PIO	8
2	Multiple Loop Pilot-Vehicle System Model for Pitch Attitude Control (No Motion Cues)	11
3	The Multiple Loop Pilot Model for Pitch Attitude Control with Normal Acceleration Cue	13
4	A Pilot-Aircraft Model for PIO Analysis	16
5	Closed Loop Dynamics; $\theta \rightarrow F_s$ and $a_{z_p} \rightarrow F_s$	31
6	System Phase Components for $a_{z_p} \rightarrow F_s$	32
7	Determination of Limit Cycles in $a_{z_p} \rightarrow F_s$	34
8	Effect of ζ_{sp} and Stick Force Level on PIO	40
9	YF-17 Pitch Attitude Dynamics	49
10	YF-17 Acceleration Control System Dynamics	51
11	T-38A PIO Time History	52
12	T-38A Airframe-Control System Dynamics	54
13	T-38A Pitch Attitude Dynamics; Effect of Bobweight	55
14	T-38A Pitch Control Dynamics; Lag-Equalized Pilot, No Bobweight; Effect of Pilot Gain	56
15	Simplified Turbulence Model	57
16	PSD of a_{z_p}; No Bobweight; Lag-Equalized Pilot	58
17	PSD of a_{z_p}	58
18	T-38A Pitch Control Dynamics; Non-Equalized Pilot; No Bobweight	59
19	PSD of a_{z_p}; No Bobweight; Non-Equalized Pilot	60
20	T-38A: Total Phase Angle of the Acceleration Control Loop; Effect of Bobweight	61

LIST OF ILLUSTRATIONS (cont'd)

FIGURE		PAGE
21	T-38A Pitch Control Dynamics; Lag-Equalized, Unadapted Pilot; Full Bobweight	63
22	T-38A: A Model for Large-Amplitude Acceleration Control Dynamics	65
23	T-38A: Gain-Phase Diagrams for the Nonlinear $a_{z_p} \rightarrow F_s$ System Dynamics	66
24	T-38A: Gain-Phase Diagrams for the Nonlinear $a_{z_p} \rightarrow F_s$ System Dynamics; Modified Control System	71
25	YF-12 Pitch Attitude Control Model	74
26	YF-12 First Mode Fuselage Bending Curve	74
27	Describing Function for YF-12 Control System	78
28	YF-12 Pitch Attitude Dynamics	80
29	YF-12 $a_{z_p} \rightarrow F_s$ Dynamics; SAS-On	81
30	YF-12 $a_{z_p} \rightarrow F_s$ Dynamics; SAS-Off	83
31	YF-12: Gain-Phase Diagram for the Nonlinear $a_{z_p} \rightarrow F_s$ System Dynamics	84
32	YF-12: Large-Amplitude PIO Time History	85
33	YF-12: PSD of Pitch Attitude During Refueling	86
34	YF-12: PSD of Elevator Stick Deflection; Comparison of Theory and Flight Test Results	87
35	YF-12 Pitch Control Dynamics; Saturated SAS; Lag-Equalized Pilot	87
36	The PIO Rating Scale	91
37	A-7A Pitch Attitude Dynamics	97
38	A-7A Normal Acceleration Dynamics	98
39	A-7A Feel and Control System Schematic Description	99

LIST OF ILLUSTRATIONS (cont'd)

FIGURE		PAGE
40	Effect of Motion Drive System Washout on Simulated YF-17 $a_{z_p} \rightarrow F_s$ Dynamics	104
41	Phase Angle Comparison of $N_{\delta_e}^{a_{z_p}}(j\omega)$ for the YF-17 In-Flight Simulation	108

LIST OF TABLES

TABLE		PAGE
1	Summary of Aircraft Known to Have Encountered PIO (USA Only)	2
2	System Dynamic Data; T-38A and A4D-2	38
3	Sinusoidal Describing Function for T-38A Control System	64
4	T-38 Limit Cycle Characteristics	66
5	$\lvert a_{z_p}/\dot{\theta}\ (j\omega)\rvert$ vs ω_R	67
6	Stability Derivatives for the YF-12	75
7	CALSPAN PIO Configurations	91
8	Estimated PIO Parameters for CALSPAN Configurations; Type I PIO	93
9	Type II PIO Susceptibility Evaluation of CALSPAN Configurations	95

LIST OF SYMBOLS

SYMBOL	DESCRIPTION
A	Amplitude parameter of the a_{z_p} PSD
a_z	z-axis component of acceleration of aircraft's center of gravity, positive down; ft/sec^2 or g's
a_{z_B}	z-axis component of bobweight acceleration, positive down; ft/sec^2 or g's
a_{z_p}	z-axis component of pilot acceleration, positive down; ft/sec^2 or g's
$(a_{z_p})_{CR}$	Critical value for which $\|a_{z_p}\| > \|(a_{z_p})_{CR}\|$ can result in pilot closure of $a_{z_p} \rightarrow F_s$ loop, positive down; ft/sec^2 or g's
$a_{z_{p_e}}$	Tracking error in $a_{z_p} \rightarrow F_s$ loop closure; ft/sec^2 or g's
cg	Center of gravity
CAS	Control Augmentation System
CCV	Control Configured Vehicle
DB	Decibels
DLC	Direct Lift Control
f	Frequency, Hz
F_s	Pilot-applied control stick force, pounds
$G(j\omega)$	Forward path dynamics of the linear portions of the control system and airframe; $a_{z_p} \rightarrow F_s$ loop
$G_a(j\omega)$	The pilot's a_{z_p}-channel dynamics
$G_M(j\omega)$	The pilot's neuromuscular system dynamics
$G_q(j\omega)$	The pilot's q-channel dynamics
$G_\theta(j\omega)$	The pilot's θ-channel dynamics
g	The acceleration due to qravity, ft/sec^2 or g's
h(s)	Rate washout dynamics in SAS loop
j	$\sqrt{-1}$

SYMBOL	DESCRIPTION
K	Transfer function gain
K'	Transfer function gain
K_a	Pilot gain in the $a_{z_p} \rightarrow F_s$ loop
K_{a_o}	Value of K_a when $a_{z_p}(t)$ approaches a pure sine wave
K_B	Bobweight gain in equivalent control stick force per g
K_p	Pilot gain in the $\theta \rightarrow F_s$ loop
K_z	Gain of the $N^{a_{z_p}}_{\delta_e}(s)$ numerator
$L(j\omega)$	Linear part of the forward path dynamics of the $a_{z_p} \rightarrow F_s$ system
L_α	Dimensional lift force derivative with respect to angle of attack, $\rho U_o S C_{L_\alpha}/2m$
ℓ_o	Distance from node of the fuselage first bending curve to to the pilot; feet
ℓ_x	Distance from the aircraft cg forward to the pilot; feet
M	Mach number
M_q	$\rho S U_o c^2 C_{M_q}/4I_y$
M_w	$\rho S U_o c C_{M_\alpha}/2I_y$
$M_{\dot{w}}$	$\rho S c^2 C_{M_{\dot{\alpha}}}/4Iy$
M_α	$U_o M_w$
$M_{\dot{\alpha}}$	$U_o M_{\dot{w}}$
M_{δ_e}	$\rho S U_o^2 c C_{M_{\delta_e}}/2I_y$
$N(\omega)$	Nonlinear part of the forward path dynamics of the $a_{z_p} \rightarrow F_s$ system
N_1	Rate limiter in SAS feedback loop
N_2	Position limiter in SAS feedback loop
n_z	Normal load factor; g's
$P(j\omega)$	Pilot model in the $a_{z_p} \rightarrow F_s$ loop

LIST OF SYMBOLS (cont'd)

SYMBOL	DESCRIPTION
PIO	Pilot-Induced Oscillation
PIOR	Pilot-Induced Oscillation Rating (McDonnell Scale)
POR	Pilot Opinion Rating (Cooper-Harper scale)
PSD	Power Spectral Density
q	$d\theta/dt$ (motion only in the longitudinal plane)
q_e	Error in pilot control of q (normally = - q)
s	Laplace transform variable, $s = \sigma + j\omega$; 1/sec
SAS	Stability Augmentation System
T_I	Lag equalization time constant in $Y_p(j\omega)$; sec
T_L	Lead equalization time constant in $Y_p(j\omega)$; sec
T_{θ_2}	Time constant of the $\theta/\delta_e(s)$ transfer function numerator, short-period approximation; sec
t	Time; sec
U_o	Steady-state aircraft speed; kts or ft/sec
$W(s)$	Washout dynamics in a motion-base flight simulator
w	z-axis component of aircraft perturbation velocity vector; ft/sec
w_g	z-axis component of atmospheric turbulence; ft/sec
Y_{CL}	The closed loop system transfer function, $Y_{OL}/(1 + Y_{OL})$
Y_{OL}	Forward path dynamics of a closed loop servo system -- the open loop system transfer function
Y_p	Pilot dynamic model (linearized) in the $\theta \rightarrow F_s$ loop
z_p	Displacement of pilot from the line of zero fuselage bending, positive down; feet
Z_w	$\rho S U_o(-C_{L_\alpha} - C_D)/2m$
Z_α	$U_o Z_w$
Z_{δ_e}	$\rho S U_o^2(-C_{L_{\delta_e}})/2m$

LIST OF SYMBOLS (cont'd)

Greek Symbols

Δ	width parameter of the $a_{z_p}(t)$ PSD, $\Delta = \sigma^2_{a_{z_p}}/2A$
δe	Elevon deflection, positive trailing edge down; radians or degrees
δ_{e_c}	Pilot-commanded elevon actuator deflection
δ_{es}	Deflection of the pilot's control stick, positive forward; inches, radian or degrees
ζ_{CL}	Damping ratio of the dominant closed loop dynamic mode
ζ_{FS}	Damping ratio of the feel system modal response
ζ_R	Damping ratio of the resonant mode of pitch attitude dynamic response--open or closed loop
ζ_{sp}	Damping ratio of the stick-fixed, short-period mode
ζ'_{sp}	Damping ratio of the stick-free, short-period mode
ζ_Z	Equivalent damping ratio of the $N^{a_{z_p}}_{\delta_e}(s)$ polynomial
θ	Pitch attitude; radians or degrees
$\dot{\theta}$	$d\theta/dt$
$\ddot{\theta}$	$d^2\theta/dt^2$
θ_B	Bending-induced pitch attitude, measured at the cockpit; radians or degrees
$\ddot{\theta}_B$	$d^2\theta_B/dt^2$
θ_c	Equivalent command to the $\theta \rightarrow F_s$ closed loop system; radians or degrees
θ_e	Tracking error in the $\theta \rightarrow F_s$ closed loop, $\theta_c - \theta$; radians or degrees
θ_R	Rigid body component of pitch attitude; radians or degrees
ν	Index of subjective predictability, Δ/ω_R; dimensionless
σ	Real part of s; 1/sec
σ_A	High frequency asymptote for the simplified pilot-vehicle system for pitch control

Greek Symbols

$\sigma_{a_{z_p}}$	Root mean square value of $a_{z_p}(t)$
σ_q	Root mean square value of $q(t)$
τ	Pilot time delay in continuous tracking (usually τ_a or τ_e); sec
τ_a	Pilot time delay in the $a_{z_p} \rightarrow F_s$ loop; sec
τ_e	Pilot equivalent time delay in the $\theta \rightarrow F_s$ loop; degrees
$\phi(j\omega)$	Total open loop phase angle of the $a_{z_p} \rightarrow F_s$ loop; degrees
$\phi_m(j\omega)$	Phase margin, $180° + \angle Y_{OL}(j\omega_c)$; degrees
$\Phi_{a_z a_z}(\omega)$	PSD of $a_{z_p}(t)$
$\Phi_{w_g w_g}(\omega)$	PSD of $w_g(t)$
$\Phi_{\delta\delta}(\omega)$	PSD of $\delta_{es}(t)$
$\Phi_{\theta_c \theta_c}(\omega)$	PSD of $\theta_c(t)$
ω	Imaginary part of s; rad/sec
ω_b	Break frequency of the turbulence PSD model; rad/sec
ω_c	Crossover frequency; $\lvert Y_{OL}(j\omega_c) \rvert = 1$; rad/sec
ω_{FS}	Natural frequency of the feel system modal response; rad/sec
ω_L	The minimum frequency for which $L(j\omega) = -1/N(\omega)$ or the minimum frequency for which $\phi(j\omega) = -180°$; rad/sec
ω_{PIO}	Steady-state frequency of fully-developed PIO; rad/sec
ω_R	Resonant frequency of pitch attitude closed loop pilot-vehicle system; rad/sec
ω_{sp}	Undamped natural frequency of the stick-fixed, short-period mode; rad/sec
ω'_{sp}	Undamped natural frequency of the stick-free, short-period mode; rad/sec
ω_Z	Equivalent natural frequency of the $N_{\delta_e}^{a_{z_p}}(s)$ polynomial; rad/sec

Transfer Function Notation

$(1/T)$	Short-hand notation for $[s + (1/T)]$
$[\zeta,\omega]$	Short-hand notation for $(s^2 + 2\zeta\omega s + \omega^2)$
$N_{\delta_e}^{x_1}$	Numerator polynomial of the $x_1/\delta_e(s)$ transfer function

Miscellaneous Notation

$q,\theta \rightarrow F_s$ or $\theta \rightarrow F_s$	The closed loop, piloted control of q and θ with F_s considered as the pilot's output
$a_{z_p} \rightarrow F_s$	The closed loop, piloted control of a_{z_p} with F_s considered as the pilot's output

SECTION I
THE PIO PROBLEM

A. BACKGROUND

The pilot-induced oscillation (PIO) phenomenon has long been one of the most fascinating and baffling puzzles in manual control technology. The PIO problem is complex, surrounded by controversy, and has been poorly understood. It is a subject that is very important to understand because of the potential impact a PIO problem can have on an aircraft's development. Historically, PIO problems have tended to first appear in the final stages of flight test and evaluation and are, therefore, very expensive to correct. There has been no way to predict PIO encounter; it has not been clear whether simulation is a viable way to diagnose PIO tendencies.

It is not known when PIO was first encountered in manned flight. The documentation of PIO appears to have begun in earnest following World War II at a time when combat aircraft performance was being extended by every possible means and when fully-powered hydraulic control systems were being tested and introduced into service.

A partial list of United States aircraft that have experienced PIO-related difficulties is given in Table 1. In some cases, the PIO resulted from experimental modifications made to the designated aircraft and, therefore, is not necessarily a characteristic of that aircraft as it is normally used. Many other undocumented PIO encounters have occurred. It is probably safe to say that PIO should be expected to occur with each new aircraft until the problem becomes sufficiently understood to preclude it by design.

A bibliography of both longitudinal and lateral-directional PIO is included in this report. The reports listed are representative of the base of data and information available on the subject. No attempt was made to list every report that addresses the PIO problem. The reports are listed in alphabetical order according to the surname of the first-listed author. A report listed in this bibliography will be referred to in the remainder of this

TABLE 1. SUMMARY OF AIRCRAFT KNOWN TO HAVE ENCOUNTERED PIO (USA Only)

1.	XP-42	15.	F-106A
2.	P-63A-1	16.	F-4C
3.	SB2C-1	17.	B-58
4.	F4U-4B	18.	T-37A
5.	A3D	19.	T-38
6.	C-97	20.	A4D-1/2
7.	F4H	21.	KC-135A
8.	A2F	22.	F-5A
9.	F-86D	23.	X-15
10.	F-100C	24.	M2-F2
11.	F-101B	25.	YF-12
12.	F-102A	26.	YF-16
13.	XF-104	27.	YF-17*
14.	F-104B	28.	A-7

*As simulated with the NT-33A only.

section by the prefix B(for example, B12). A separate Reference section will list principal documents supporting the analyses of this report; some of these will also be found in the Bibliography.

The PIO problem is one in which an oscillation of the aircraft occurs (e.g., porpoising, dutch-roll, etc.) that is difficult or impossible for the pilot to stop. A central characteristic of the phenomenon is that the airplane is stable both stick-fixed or stick-free; hence the name pilot-induced oscillation.

Opinion varies widely on the causes of PIO. The dynamics of the control system have been implicated by numerous investigations as a principal cause for PIO (e.g., B4, B5, B8, B15, B20, B21, B32, B34, B35, B46, B57, B65, and B71). Feel or control system nonlinearities have been noted as important to PIO by most investigators; among these, B15, B54, B66, and B71 are of particular interest. Bobweights have been identified by several investigators as possible PIO initiators (e.g., B4, B15, B20, B21, B38, B54, and B57). Surprisingly few citations have been made of basic airframe dynamics as causes

for PIO; B46 is one of the few references to suggest that airframe properties are at fault. In B15, the role of the airframe is considered as an important part of the overall dynamic system; in B22 a PIO criterion is proposed that emphasizes the role of airframe dynamics. A few studies have suggested the importance of pilot task requirements to PIO (B5, B15, B54, B66, and B71). "Abrupt" control inputs have often been connected with the onset of PIO (e.g., B15, B27, B54, B66, and B71). The PIO rating scale -- shown in Figure 36 and first introduced at McDonnell Aircraft during the F-4 development -- emphasizes the significance to PIO of abrupt control (B21).

The piloting cue that is most central to PIO is a point on which sharp disagreement is found in the literature. Normal load factor response has been cited directly or by implication by numerous investigators; among these, B4, B5, B8, and B54 are representative. The importance of load factor as the primary piloting cue is discounted in B12 where it is suggested that pitch attitude is the primary cue. The closed loop criterion for PIO proposed in B22 is based largely on pitch attitude tracking.

One notable area of universal agreement (at least in the literature) is the importance of visualizing the pilot as a force producing dynamic element. It is suggested in B15, however, that the pilot should also be considered as a deflection producing servomechanism in analyzing for possible PIO-prone aircraft-controller combinations.

A lateral-directional PIO, known to exist in actual flight, has been duplicated in a fixed-base simulation in at least one instance (B47) and possibly others as well (B73?). However, to this author's knowledge, a longitudinal PIO has never been created in a fixed-base simulation, although at least one serious, undocumented attempt to do so was made. What was called a longitudinal PIO in a fixed-base simulation was obtained by Hirsch and McCormick (B39) in a fascinating study; this was a contrived experiment, however, in which rapid and non-physical, on-line variations of $1/T_{\theta_2}$ were made in order to catalyze a sustained system oscillation--apparently because a PIO could not be initiated otherwise! The non-existence of longitudinal mode mode PIO in fixed-base simulations is regarded by this author as a fact of

some importance. It is also noteworthy that Fortenbaugh (B30) failed to create PIO in a normal-acceleration-deprived simulation which did include the pitch rotational acceleration $\ddot{\theta}$.

The overall state of the art of PIO understanding may be best inferred by the reader after he has studied the public debate by Ashkenas and A'Harrah (B12, B7, and B13). This valuable record suggests that there are many ways in which the nature of PIO may be visualized and that each of these can contribute to our ultimate understanding of the phenomenon.

B. THE HANDLING QUALITIES--PIO DICHOTOMY

It is not at all clear whether PIO necessarily results from basically poor handling qualities. The evidence is that it does not. That is, PIO has occurred with aircraft that have passed flight test certification and may therefore be presumed to have generally acceptable handling qualities (the T-38A is an example--Ref. 1).

On the other hand, if an aircraft is very difficult to control (Cooper-Harper ratings worse than about 8) must we conclude that it is PIO-prone? Can we determine from flight test whether such an aircraft has a PIO problem or whether it merely has poor handling qualities in the control of attitude? Does it matter?

There are two complicating factors involved in attempting to answer such questions. First, the relation between the pilot's task and any tendency to excite latent PIO in a flight or simulator experiment is unknown since we know neither if latent PIO exists nor, if it does, how it may be excited. Second, we have no rule for discriminating between a control problem due to poor attitude control dynamics and one due to PIO tendencies when these are encountered in flight test or simulation. Thus, we cannot be sure that we are testing the proper control situations or that we can identify a potential PIO configuration when one is encountered. This is a nontrivial matter since it may affect the character of system change requirements and the impact that the aircraft might have if delivered to the training or service communities.

The tendency in past work has been to identify any pilot-aircraft oscillation as a PIO without a great deal of discrimination. Of course, the wings-bending, rivet-popping, fully-developed PIO is easily identified when it occurs (by definition). This is not the usual PIO encounter, however. We need a method for the unambiguous separation of attitude control problems from those that we choose to call PIO. Clearly, a workable definition for PIO is required.

C. REPORT OUTLINE

In the remainder of this report, only the longitudinal mode, short-period PIO will be considered. A formal definition for PIO will be proposed in Section II which will, it is hoped, permit resolution to be made between the PIO-prone aircraft and the one that merely has deficient handling qualities in the control of attitude. A model for pilot dynamics will be presented in Section III that is useful for the analysis of PIO. Connections between this model and the more familiar ones found in the literature of pilot dynamics will be discussed. Particular attention will be devoted to the so-called synchronous tracking mode of pilot behavior that has been linked with PIO in past works. Section IV will present a physical and mathematical theory for PIO that is consistent with available data. Two classifications of PIO will be introduced in an attempt to account for the mechanisms by which a PIO can be catalyzed in actual flight. A compendium of rules for the assessment of PIO will be summarized in Section V as an aid to applications of the PIO theory. A number of numerical examples will be given in Section VI to indicate that known PIO problems are "predictable" with the proposed theory; equally important, one example will be given to confirm that an aircraft not known to have experienced PIO difficulties is indeed excluded as a PIO candidate by present theory. Section VII will discuss some general problem areas of importance to the experimental identification of PIO from the viewpoint of the proposed theory. Finally, Section VIII will summarize what has been concluded elsewhere in this report.

A derivation of the pilot-centered normal acceleration transfer function is presented in the Appendix. Approximate factors for the acceleration transfer function are also derived there.

SECTION II
A DEFINITION

The lack of a suitable definition for PIO has been a major obstacle to understanding the phenomenon. It appears, however, that a nontrivial PIO definition can only be formulated after the physical problem is understood with a certain degree of sophistication. We are therefore faced with the task of developing an understanding of a problem we cannot yet define. Needless to say, this author went down many blind alleys before arriving at the theoretical description of PIO that forms the main body of this report. Based on the results of Section IV, then, a consistent PIO definition can be devised as follows:

A. PIO DEFINITION

> PIO is an unwanted, inadvertent and atypical closed loop coupling between a pilot and two or more independent response variables of an aircraft.

It is presumed that a fully-developed PIO will either tax the pilot's ability to control it--and thereby leave little or no margin for accomplishment of the primary piloting task--or it will be entirely beyond his control capabilities. In the latter case, the only successful recovery technique is for the pilot to remove himself from the control loop, either by clamping or releasing the control.

B. COMMENTS

This definition eliminates from the PIO classification all those single variable feedback control systems for which lightly damped closed loop oscillations are intrinsic (even with a high-gain autopilot!) but which are not otherwise susceptible to PIO. The definition of PIO as "unwanted" excludes the "stick pumping" phenomenon (Refs. 2 and 3) from the PIO category.

The "independent" response variables referred to in the PIO definition are intended to correspond with the usual aircraft degrees of freedom, their derivatives, or linear combinations of these. A derivative of one of these variables is not, by definition, independent of the variable itself.

By this definition one might suspect that a certain element of chance is involved in PIO encounter; this author suspects that this is, indeed, the case. Thus, we must test for PIO with great care to be certain that the conditions necessary to sustain it are satisfied.

It is not by chance that this definition dictates that PIO requires a level of piloting task that is more complex than mere control of attitude. It is contended that PIO can only occur for those circumstances in which the pilot is very concerned about precision control of aircraft path or path-related acceleration components.

Past occurrences of PIO have been with aircraft that were otherwise stable; with future aircraft employing relaxed static margin, PIO could occur following control system failures for which the aircraft would be unstable. Such a control problem is still admitted to the PIO category by the definition here; however, for such aircraft stability could not be restored following PIO encounter by clamping or releasing the controls.

SECTION III

A PILOT MODEL

A. BACKGROUND

It was assumed in References 4 and 5 that the essential piloting cue in PIO is pitch attitude; it was further assumed that a sufficient model for pilot dynamics in the fully-developed PIO is a pure gain; i.e., $Y_p(j\omega) = K_p$ such that the stick force $F_s(t)$ is just $K_p\theta_e(t)$. No pilot dynamic equalization (lead or lag) or time delay was considered necessary for analysis of the causes of a PIO once it was known to exist; it was suggested that normal acceleration might also serve as a piloting cue, although it would not likely be so important as pitch attitude. A final assumption was that the pilot's primary response is stick force F_s. The resulting pilot-vehicle system block diagram is shown in Figure 1; the locus of closed loop roots of the system is indicated in the generic sketch for the case of no significant nonlinearities or control dynamics, and with the short-period approximation employed for airframe dynamics.

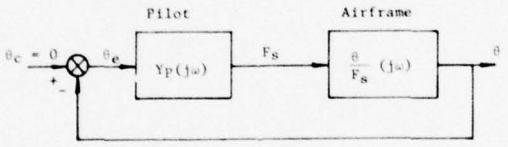

$Y_p(j\omega) \cong K_p$ (The "Synchronous" Pilot)

$$\frac{\theta}{F_s}(j\omega) = \frac{\theta}{\delta_e}(j\omega)\,\frac{\delta_e}{F_s}(j\omega) \cong \left(\frac{\delta_e}{F_s}\right)_0 \frac{M\delta_e\left(j\omega + \frac{1}{T\theta_2}\right)}{j\omega[(j\omega)^2 + 2\zeta_{sp}\omega_{sp}j\omega + \omega_{sp}^2]}$$

$\frac{\delta_e}{F_s}(j\omega)$ = control/feel dynamics

$\left(\frac{\delta_e}{F_s}\right)_0$ = static gain of $\frac{\delta_e}{F_s}(j\omega)$

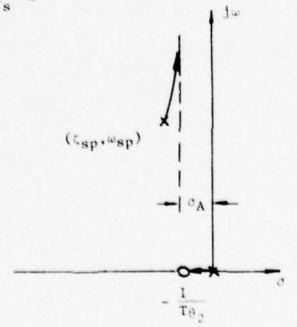

High Frequency Asymptote: $\sigma_A = \left(2\zeta_{sp}\omega_{sp} - \frac{1}{T\theta_2}\right) \div 2$

From Reference 4 and 5

Figure 1. Simplified Pilot-Vehicle System Model for Fully-Developed PIO

The non-equalized, no time delay model for pilot dynamics--the so-called "synchronous pilot"--has since been criticized by other researchers as being too unsophisticated. One must be careful not to confuse "unsophisticated" with "elegant." The synchronous pilot model is, in this author's opinion, the elegant product of very sophisticated reasoning. It was developed by the same people (and organization) responsible for the development of the engineering theory for pilot dynamics (Ref. 6); the pure gain form of the model was believed to be in reasonable agreement with the very limited time response data available for actual PIO experiences. The model contains two features that are probably essential to the understanding of PIO:

1. The overwhelming importance to the development of PIO of pitch attitude loop dynamics is explicit in the model.
2. The frequency at which PIO is likely to occur is largely determined by the pitch attitude loop closure.

Each of these points will be discussed later in this report.

Ashkenas (Ref. 5) used the linear, pilot-vehicle representation of Figure 1 to make his point that PIO cannot occur in the absence of control system dynamics--linear or nonlinear; that is, the system of Figure 1 can never become unstable for real aircraft (with the possible exception of closely-coupled canards). However, his basic assumption was that PIO results solely from pitch attitude tracking; he further implied that for PIO to occur it is necessary that either a locus crossing of the imaginary axis must occur in Figure 1 as a result of higher order system dynamics or a limit cycle in the control of pitch attitude must occur as a result of control system nonlinearities. In either case, Ashkenas' theory underscored the importance to PIO mechanics of $1/T_{\theta_2}$ -- a parameter usually ignored in experimental work of that period and known to be of major significance to the pitch tracking task handling qualities. This viewpoint was the genesis of the PIO criterion, based entirely on pitch control, proposed in B22 as a specification for aircraft design.

A'Harrah (Ref. 7) disagreed sharply with Ashkenas on the significance to PIO of $1/T_{\theta_2}$, the pitch attitude cue, and control system dynamics or nonlinearities. He contended, based on experimental results obtained using a "g-seat" (visual plus normal acceleration cues) in which ω_{sp}, ζ_{sp} and F_s/g were varied at constant $1/T_{\theta_2}$, that the dominant cue is normal acceleration--not pitch attitude. The ensuing argument was never entirely resolved. However, Cornell Aeronautical Laboratory flight tests (Ref. 17) have since established that PIO does not necessarily result from short-period dynamics which force σ_A to lie in the unstable-half plane (see Figure 1). In addition, as Ashkenas noted, the violation of A'Harrah's PIO boundaries is not sufficient for PIO to be created. We might suspect, therefore, that neither viewpoint is entirely correct.

Recent flight tests (Ref. 8) encountered a serious PIO in landing flare with an all-linear simulation of the YF-17. This is hard evidence that control system nonlinearities may not be necessary to the development of PIO. Control system phase lags were, however, identified in Reference 8 as the PIO catalyst.

There are two obvious difficulties with the synchronous pilot model:

1. It provides no insight into the mechanisms by which a fully developed PIO can be initiated.
2. The assumption that the pilot's time delay in single loop tracking can approach zero may be indefensible on philosophical grounds.

The first deficiency limits our ability to predict PIO, to understand it, or to develop design rules for avoiding it. The second bears comment. In tracking of periodic inputs, it has been observed that the pilot's time delay appears to approach zero with practice (Ref. 9); this has been attributed to the pilot's adaptation of a more sophisticated form of control called precognitive (knowledge of input) tracking. This conclusion, however, implies that the pilot knows what his time delay is; otherwise, he has no way of eliminating it. This is assumed here to be a philosophical impossibility. Are you, for example, reading this passage now or did you read it yesterday and only believe you are reading it now?

The assumption of synchronous control behavior is based on the assumption that the human pilot, in single loop tracking, may be represented as a single input/single output device as shown in Figure 1. He can, of course (Ref. 6). Problems arise, however, when we attempt to <u>interpret</u> physical data against the theoretical framework provided by such a model. Reference 10 challenges the validity of the servo model for pilot dynamics (Ref. 6) as a description for the physiological processes involved in human pilot dynamics. It is suggested in Reference 10 that when the pilot is modeled as a multi-sensor device a unity of understanding will emerge to link physical response data with a rational, theoretical description for pilot dynamics. It is suggested that the resulting model will be completely consistent with the servo model of Reference 6 in all phenomenological respects.

A consequence of the theory of Reference 10 is that the input to the human pilot is most appropriately represented as an information vector (in a manner completely consistent with modern state space analyses of system dynamics). Thus, when pitch attitude is displayed to the <u>pilot</u> (in the absence of motion cues), pitch attitude and pitch rate should be used as inputs to the <u>pilot model</u> if a mathematical simulation of attitude control is to be performed (Figure 2). The transfer devices labeled $G_q(j\omega)$ and $G_\theta(j\omega)$ are intended to represent the dynamics involved in the visual detection and control of $q(t)$ and $\theta(t)$, respectively. These elements, especially $G_q(j\omega)$, may be nonlinear; however, as a first approximation they may both be replaced with constant gains (Ref. 10). When the q-loop is closed (analytically), the resulting model for F_s/θ_e is equal to $Y_p(j\omega)$ as given by the servo theory (Ref. 6).

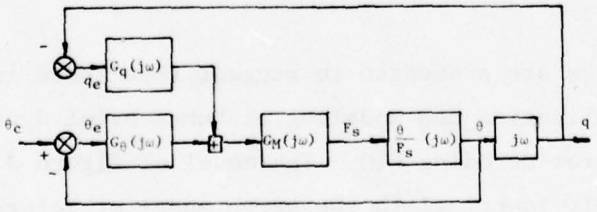

Pilot Dynamic Elements:

$G_q(j\omega)$ = ?

$G_\theta(j\omega)$ = ?

$G_M(j\omega)$ = neuromuscular system dynamics

Figure 2. Multiple Loop Pilot-Vehicle System Model for Pitch Attitude Control (no Motion Cues)

The model of Figure 2, when compared with the conventional servo model of Reference 6, may seem needlessly complex. It is not, in fact, for reasons discussed in Reference 10. The purpose of the model was not to contribute to the advancement of the computational aspects of man/machine systems analyses, but to enable the forecasting or explanation of the qualitative relationships found in tasks important to vehicle handling qualities. As an example, consider how the model of Figure 2 might be used to devise an explanation for the physical observation that the time delay between $F_s(t)$ and $\theta_e(t)$ approaches zero in sine wave tracking experiments. Consider the following facts:

1. With a periodic input to a stable servo system, the average system error will be zero when the controller is a pure gain.
2. $q_e(t)$ leads $\theta_e(t)$ by 90 degrees; the corresponding time advance is $\pi/2\omega_R$ seconds (ω_R = frequency of the periodic input).
3. Control of only $q(t)$ ensures control of $\theta(t)$ except for possible low frequency drift in error.

We might speculate, therefore, that for reasons that are as yet unclear, the human pilot really only controls error rate (in a sine wave tracking experiment) in the continuous, closed loop sense. He can null drift in error with control amplitude modulation. Further, if his time delay in rate tracking is $\pi/2\omega_R$ seconds then it will appear that he controls system error with zero time delay -- the synchronous pilot -- if one insists that the system be structured as shown in Figure 1. This is an entirely plausible, physical and theoretical explanation for synchronous, precognitive tracking with visual inputs to the human controller.

The foregoing remarks are presented to suggest that there is an alternative approach to visualization and modeling of human pilot dynamics, and that this may be useful for decoding PIO. The model of Figure 2 is, by definition, quantitatively identical to the servo model of Reference 6 for visual tracking of pitch attitude. A major advantage of the model for the study of PIO is the manner in which it may be extended to account for the effects of motion cues (linear and angular accelerations). The rules for this are:

1. Each additional cue forms a path parallel with those for q and θ (Figure 2). The associated dynamics are those of the motion sensor mechanism with an input-adaptive gain.
2. The response for each motion cue path is connected with the signal pathway to the neuromuscular system through a "switch." This switch is postulated to exist within a "central processor." Its nature is such that it may appear to permit coordinated control of all feedback cues or, under stressful conditions, permit only motion cue control.

This situation is depicted in Figure 3 for the case where the motion cue is assumed to be normal acceleration a_{z_p} at the pilot's location (observe the sign convention). The task is assumed to be regulation of pitch attitude in the presence of atmospheric turbulence; therefore, no command input need be shown on the figure. Figure 3 suggests that if the "switch" were set such

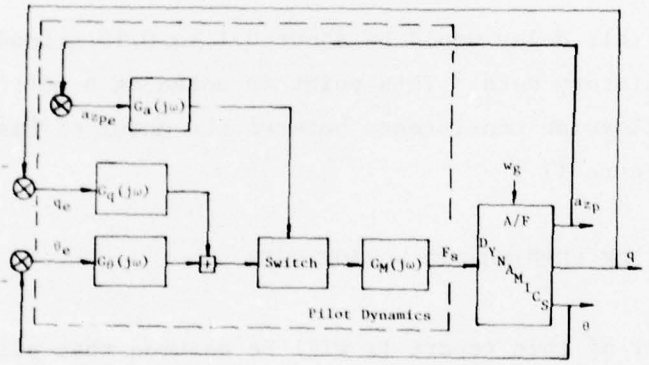

a. The Basic Model

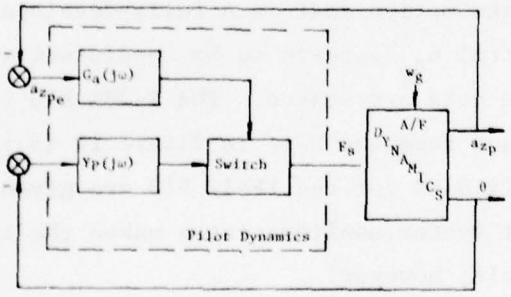

b. The Model with q-Loop Closed and Neuromuscular System Dynamics Neglected

Figure 3. The Multiple Loop Pilot Model for Pitch Attitude Control with Normal Acceleration Cue

that only acceleration is controlled in a fully-developed PIO, then F_s would appear to be synchronous with θ when a phase lag exists in $G_a(j\omega)$ of magnitude

$$180° + \angle \frac{a_{z_p}}{\theta} (j\omega_{PIO})$$

The equivalent time delay is

$$\tau_a = \left[180° + \angle \frac{a_{z_p}}{\theta} (j\omega_{PIO})\right] \div (57.3\ \omega_{PIO})$$

A typical value for this delay would be about 0.1 to 0.15 seconds, based on *available PIO case history data*. This point is noted as a matter of interest and to establish a timewise consistency between the model of Figure 3 and that of Ashkenas (Figure 1).

B. A COMMENT ON STICK PUMPING AND MOTION CUES

In the remainder of this report it will be assumed that pilot-felt normal acceleration a_{z_p} is the only motion cue that must be considered in the analysis of PIO. The assumption that in a fully-developed PIO the pilot primarily seeks to control a_{z_p} appears to be consistent with available evidence, although hard data are scarce. The T-38A PIO time history contained in Reference 4 and repeated here in Figure 11 is the best such example available. Time history data for the YF-12 PIO are given in Reference 11; the presence of control system nonlinearities makes the interpretation of these data very difficult, however.

There is, to this author's knowledge, not a single example in the aircraft handling qualities literature to support the inclusion of rotational acceleration $\ddot{\theta}$ as a primary piloting cue in a closed loop VFR tracking task. $\ddot{\theta}$ was postulated in Reference 2 to be of signal importance to aircraft handling qualities and as the cue most closely linked with the control stick pumping phenomenon. However, stick pumping was exhaustively analyzed in Reference 3 (unfortunately never released for publication) where it was determined that no case for $\ddot{\theta}$ as the pumping cue could be made that was consistent with flight test records and pilot comments for carrier approach and landing.

However, it was observed that to a good approximation the amplitudes of $a_{z_p}(t)$ oscillations for the F-4B in actual carrier approach were nearly constant and equal to a value only slightly greater than the perception threshold for spine-wise linear acceleration. The corresponding $\ddot{\theta}$ amplitude was about ten times the known perception threshold.

The explanation offered (Ref. 3) for the pumping phenomenon in carrier approach was that the pilot's creation and monitoring of a small, oscillatory a_{z_p} provided him with an adaptive cue for the rapid and sensitive detection of aircraft settle due to downwash aft of the carrier ramp. Without this cue, the delay time in the detection of monotonic a_{z_p} due to downwash would be prohibitively large. The detection of settle with this pilot-created, adaptive cue appears to result in a throttle feedforward command to counter the tendency to depart from the desired flight path. Subjective support for this conclusion is offered in the pilot commentary of Reference 12.

The importance of stick pumping to the PIO phenomenon is that it appears to help unify our understanding of how skilled pilots may selectively choose those aircraft responses that are most directly related to their concept of the flight control task.

It will be assumed without further comment that the pilot's response is stick force F_s. The merits of the assumptions regarding a_{z_p} and F_s may be

judged by the resulting success of the PIO theory, contained in the next chapter, as a framework for understanding the PIO case histories discussed in Section VI.

C. A PILOT MODEL FOR PIO ANALYSIS

The structural form for the pilot-aircraft system dynamics is assumed to be the same as that shown in Figure 3b. In the remainder of this report the neuromuscular dynamics will be neglected; i.e.,

$$G_M(j\omega) \equiv 1$$

A further assumption, consistent with the theory of Reference 10, is that the pilot's acceleration channel dynamics are

$$G_a(j\omega) = K_a(a_{z_{p_e}})\, e^{-\tau_a j\omega}$$

i.e., an input-dependent gain with a time delay. The resulting PIO model is shown in Figure 4. The visual tracking portion of the pilot's dynamics

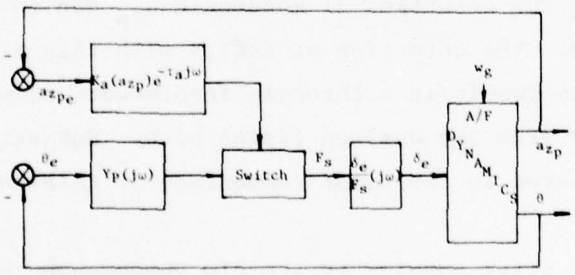

$$Y_p(j\omega) = \frac{K_p(T_L j\omega + 1)}{T_I j\omega + 1}\, e^{-\tau_e j\omega} \quad \text{(Simplified from Ref. 6)}$$

$K_a(a_{z_p}) \cong 0$ when the PSD of $a_{z_p}(t)$ is broadband

$K_a(a_{z_p}) = K_{a_0}$ when the PSD of $a_{z_p}(t)$ is narrowband

Figure 4. A Pilot-Aircraft Model for PIO Analysis

$Y_p(j\omega)$ is chosen to be consistent with the conventional servo model representation; it is assumed that the parameters of $Y_p(j\omega)$ can be selected to be consistent with the "adjustment rules" contained in Reference 6.

The functional dependency between K_a and $a_{z_{p_e}}$ was inspired by a model for visual detection of signal coherence introduced in Reference 9 as a model for precognitive tracking of a periodic input. It arises from the assumption that the process by which a human identifies a stimulus is similar to the operation of a linear, optimal filter. Based on optimal filtering theory, a model for the acceleration portion of the pilot model is

$$G_a(j\omega) = \frac{F_s}{a_{z_{p_e}}}(j\omega) = K_{a_o}\left(\frac{\sin \tau_a\Delta/2}{\tau_a\Delta/2}\right)(\cos\omega_R\tau_a)e^{-\tau_a j\omega}$$

where ω_R and Δ are the center frequency and "width" of the $a_{z_p}(t)$ power spectrum as indicated in the sketch:

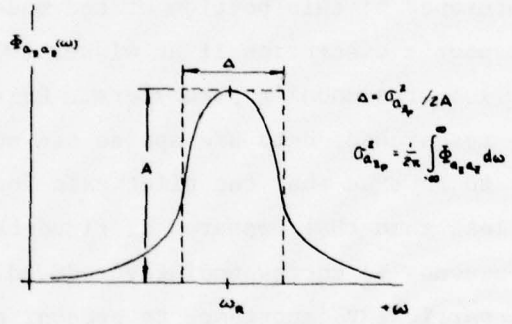

When $a_{z_p}(t)$ has a broadband spectrum, Δ is large, A is small and the corresponding pilot gain $F_s/a_{z_{p_e}} \to 0$. When $a_{z_p}(t)$ has a narrowband spectrum, Δ is small, A is large and $F_s/a_{z_{p_e}}$ is maximum. In a time-wise sense, a narrowband signal is one that is nearly periodic--much like a sinusoid having a randomly varying amplitude and phase. A closed-loop, pilot-aircraft system that is "resonant," or that has a lightly-damped, dominant mode, might have pitch attitude and normal acceleration responses with narrowband spectra.

The time delay τ_a is unknown; it may be a function of the center frequency τ_R or it may be a constant. As an interim model, it is suggested that $\tau_a = 0.25$ seconds; this is the value used in all of the PIO examples in Section VI.

D. MODEL PROPERTIES

It is postulated that in pre-PIO flight, the pilot-vehicle system's loop dynamics are dominated by the pitch attitude loop closure (θ,q → F_s); that is, we postulate that prior to PIO-initiation either (1) the power spectral density of $a_{z_p}(t)$ is broadband; therefore, $K_a(a_{z_p}) \rightarrow 0$ and there is no substantial acceleration tracking, or (2) the mode "switch" is usually set to activate the pitch attitude loop to the near-exclusion of acceleration tracking.

As was stated above, the visual portion of the pilot model, $Y_p(j\omega)$, is assumed to be completely consistent with the servo model for pilot dynamics as documented in Reference 6; this portion of the model may be refined for applications at the user's discretion if he wishes to account for the effects of motion (a_{z_p} and $\ddot{\theta}$) on the model's parameters. Rules for doing this have not been thoroughly researched; data are sparse and somewhat contradictory. Generally, it seems to be true that the pilot gain for pitch tracking in flight is slightly less than that measured in fixed-base simulation; the system crossover frequency is correspondingly reduced. The matter is not considered to be of particular importance to present purposes and will not be discussed further.

The properties of the mode "switch" (Figures 3 and 4)--if it exists--are unknown. It should be noted that this switch--hypothesized to simulate higher processes within the central nervous system--may be redundant if the validity of the input-adaptive acceleration gain is accepted. It will be retained in this report because both possibilities should be admitted until better information becomes available and because it makes no tangible difference to our final result. The function of the switch is to provide a

rational connection between system and pilot dynamics resulting mainly from pitch attitude tracking and those due mainly to normal acceleration tracking. It is assumed that, because of pilot tension (i.e., attentiveness, anxiety, etc.), and flight control task constraints, the pilot switches from pitch to acceleration control in a logical manner; it is further assumed that this switching can be modeled as indicated in Figure 4 with an appropriate switching logic.

An interesting and plausible model for mode switching is suggested by Reference 9; the authors suggest that an input stimulus to a pilot-vehicle system may be considered to be "subjectively predictable" when ν, the index of subjective predictability, ≤ 0.3.

$$\nu = \frac{\Delta}{\omega_R} \leq 0.3$$

If we assume that the coherence properties of a stimulus are synthesized within the higher centers (i.e., not by the stimulus sensor), then it is reasonable to assume that the same model for subjective predictability should apply to both motion and visual cues. Speculating further, one may expect that in a state of incipient PIO the pilot will begin to emphasize a_{z_p} control because it is "predictable" and under normal circumstances would therefore be controllable. Thus, $\nu \leq 0.3$ might serve as the required switching logic. Note, however, that ν is determined from the properties of the normal acceleration spectrum for pitch attitude tracking, only. It follows that pilot-aircraft system configurations that are prone to closed loop "resonance" in pitch attitude tracking tasks are automatically PIO candidates.

A final point about the switching hypothesis should be considered. When an actual PIO is initiated in a real airplane, the pilot hasn't the luxury of contemplating system responses, assessing whether he is in a PIO mode, and selecting an appropriate control action. Probably, many pilots will think there is something the matter with the airplane (e.g., SAS failure) and will

continue doing whatever it was that catalyzed the oscillations--and this is entirely reasonable. Thus, if the airplane is felt to sink uncontrollably following PIO initiation in flare, the pilot will pull back-stick to arrest the normal acceleration. In terms of the switching hypothesis, this suggests that when danger due to flight path departure is judged to be immediate, the attitude control mode will probably become secondary; it is conceivable that in a fully developed PIO such as experienced on several occasions with the T-38A (Ref. 1), the pilot "switches into" control of normal acceleration and cannot easily satisfy his internal logic for switching back to pitch attitude control. This limiting-case description for fully developed PIO may not be strictly correct; it will, however, almost certainly provide a system of necessary conditions which must be satisfied if a fully-developed PIO is to be possible.

SECTION IV

A PIO THEORY

A. PIO CATEGORIES

If the Pandora's box of possible PIO causes and effects found in the literature is to be systematically addressed, cataloged, and understood, it is necessary that we consider the mechanisms by which PIO is created. For this purpose, two broad classes of PIO are defined as follows:

- o Type I--PIO induced by dynamic response of the closed loop pilot control of pitch attitude.
- o Type II--PIO induced by non-tracking control or disturbance.

It was implied in Section III that the model for pilot-aircraft dynamics shown in Figure 4 was intended to address Type I PIO. It appears (and is assumed) that the model may also be applied to the analysis of Type II PIO provided that the "switch" is permitted to initiate a_{z_p} control starting from a no-tracking condition.

The control or disturbance inputs required to initiate a Type II PIO would be describable as "abrupt" and of magnitude sufficient to excite any resonant stick-free dynamic modes of the aircraft system.

B. TYPE I PIO

Phase 1: Pitch Attitude System Dynamics

It is postulated that Type I PIO begins with highly resonant closed loop dynamics resulting from pitch attitude tracking, only. If the pilot-vehicle system can be shown to be nonresonant, then Type I PIO is unlikely. The relevant system block diagram is that of Figure 4 with the switch set to preclude a_{z_p} feedback control. The pilot model for θ control

$$Y_p(j\omega) = \frac{K_p(T_L j\omega+1)}{T_I j\omega + 1} e^{-\tau_e j\omega}$$

is parameterized according to the "adjustment rules" of Reference 6 (modified, if desired, to account for motion cue effects on closed loop properties). The describing function parameters K_p, τ_e, T_L, and T_I and the closed loop parameters ω_c (crossover frequency), phase margin and gain margin are all dependent upon the aircraft dynamics $\theta/F_s(j\omega)$; the process by which these are selected is iterative and the selection process is not necessarily unique. For present purposes of developing and demonstrating a theory for PIO, we need not be too fussy about this process; for an analysis of possible PIO problems with a new aircraft for which no flight tests have been made, the parameterization of $Y_p(j\omega)$ is extremely important and must be done with great care.

Following parameter selection for $Y_p(j\omega)$ the closed loop dynamics must be computed:

$$\frac{\theta}{\theta_c}(j\omega) = \frac{Y_p(j\omega)\,\frac{\delta_e}{F_s}(j\omega)\,\frac{\theta}{\delta_e}(j\omega)}{1 + Y_p(j\omega)\,\frac{\delta_e}{F_s}(j\omega)\,\frac{\theta}{\delta_e}(j\omega)}$$

where it is understood that $\theta_c(t)$ represents an equivalent command input to the system of Figure 4 due to (vertical) w-gusts:

$$\theta_c(j\omega) = \frac{-\theta}{w_g}(j\omega) \cdot w_g(j\omega)$$

The gust response transfer function is (employing the short-period approximations)

$$\frac{-\theta}{w_g}(j\omega) \cong \frac{M_w}{(j\omega)^2 + 2\zeta_{sp}\omega_{sp}j\omega + \omega_{sp}^2}$$

The turbulence power spectral density $\Phi_{w_g w_g}(\omega)$ can be chosen as the Dryden or Von Karman or any other model that may best represent the specific flight condition to which this theory is to be applied. The corresponding θ_c power spectral density is

$$\Phi_{\theta_c\theta_c}(\omega) = \left|\frac{\theta}{w_g}(j\omega)\right|^2 \Phi_{w_g w_g}(\omega)$$

Following closure of the pitch loop, the (uncontrolled) acceleration response power spectral density (due only to closed loop control of pitch attitude) may be obtained as follows:

$$\frac{a_{z_p}}{\theta_c}(j\omega) = \frac{N_{\delta_e}^{a_{z_p}}(j\omega)}{N_{\delta_e}^{\theta}(j\omega)} \frac{\theta}{\theta_c}(j\omega)$$

$$= \left(\frac{Z_{\delta_e} - \ell_x M_{\delta_e}}{M_{\delta_e}}\right)\left(\frac{\omega_Z^2}{\frac{1}{T_{\theta_2}}}\right)\left[\frac{s\left[\left(\frac{s}{\omega_Z}\right)^2 + \frac{2\zeta_Z}{\omega_Z}s + 1\right]}{T_{\theta_2}s + 1}\frac{\theta}{\theta_c}(s)\right]_{s=j\omega}$$

$$\Phi_{a_z a_z}(\omega) = \left|\frac{a_{z_p}}{\theta_c}(j\omega)\right|^2 \Phi_{\theta_c\theta_c}(\omega)$$

$$= \left|\frac{Z_{\delta_e} - \ell_x M_{\delta_e}}{M_{\delta_e}}\right|^2 \left|\frac{M_w \omega_Z^2}{\omega_{sp}^2 \frac{1}{T_{\theta_2}}}\right|^2 \left|\frac{s\left[\left(\frac{s}{\omega_Z}\right)^2 + \frac{2\zeta_Z}{\omega_Z}s + 1\right]}{(T_{\theta_2}s+1)\left[\left(\frac{s}{\omega_{sp}}\right)^2 + \frac{2\zeta_{sp}}{\omega_{sp}}s + 1\right]}\frac{\theta}{\theta_c}(s)\right|_{s=j\omega}^2 \Phi_{w_g w_g}(\omega)$$

A typical pitch attitude loop closure will yield $|\theta/\theta_c(j\omega)| \cong 1$ (0 db) for $\omega < \omega_c$ (the crossover frequency); there may be a closed loop amplitude rise at ω_c associated with small closed loop damping ratio. At frequencies greater than ω_c the closed loop response will be heavily attentuated except (possibly) at frequencies corresponding to lightly damped modes due to the feel system,

actuator dynamics, structural dynamics, etc. A typical case is illustrated in the following sketch. (The zero db lines are intended to be representative for the case where a_{z_p}/θ_c is in units of g/degree.)

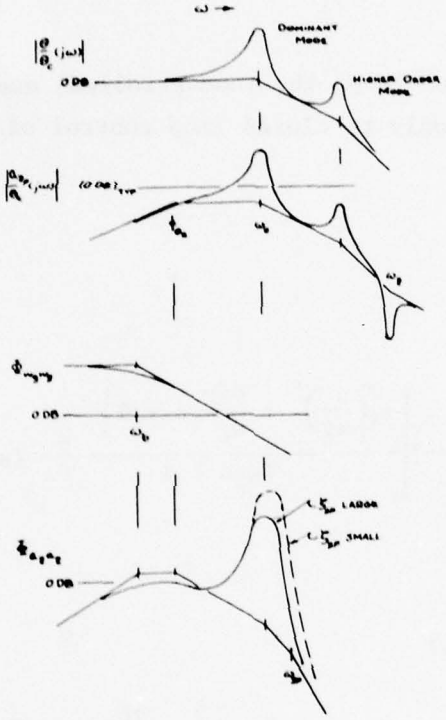

The progression from pitch attitude loop dynamics to the normal acceleration power spectral density is illustrated.

These sketches illustrate a number of points that are of value to understanding the connection between pitch attitude dynamics and the potential for Type I PIO:

- Any feature of pitch attitude loop dynamics which promotes loop resonance (amplitude ratio peaks on the closed loop Bode) is a potential cause of PIO. This would include poor pitch dynamics and excessive pilot gain, for example.

- Values of $1/T_{\theta_2}$ that approach ω_c will promote peaks in the a_{z_p} power spectrum. Small $1/T_{\theta_2}$ relative to ω_c has a slight attenuating effect.

- Small ζ_{sp} will promote a_{z_p} resonance--particularly when $\omega_{sp} \cong \omega_c$.

- Higher frequency modes due to feel or control system dynamics, for example, are heavily attenuated by the turbulence power spectral roll-off; *i.e., they are not easily excited* by turbulence.

- The turbulence spectrum break frequency ω_b is not too important to the development of a_{z_p} resonance; small ω_b decreases the amplitudes of $a_{z_p}(t)$ but has minor effect on subjective predictability of a_{z_p} according to the proposed index.

- As a rule of thumb it appears that large $1/T_{\theta_2}$ and small closed loop dominant mode damping ratio promote the development of $a_{z_p}(t)$ with narrowband signal qualities and will therefore promote Type I PIO.

The center frequency amplitude, A, and width parameter, Δ, may be estimated from the power spectrum of a_{z_p} by any convenient means. It is suggested that $\sigma^2_{a_{z_p}}$ be estimated by direct integration:

$$\sigma^2_{a_{z_p}} = \frac{1}{2\pi} \int_{-\infty}^{\infty} \Phi_{a_Z a_Z}(\omega)\, d\omega$$

Then $\Delta = \sigma^2_{a_{z_p}} / 2A$ and $\nu = \Delta/\omega_R$. [Note that the turbulence power spectral density is not important to the estimate of ν provided that the "shape" of $\Phi_{a_z a_z}(\omega)$ without regard for amplitude near ω_R is not very turbulence sensitive.]

If $\Phi_{a_z a_z}(\omega)$ has no discernible center frequency for all realistic parameterizations of $Y_p(j\omega)$ then Type I PIO is unlikely. If the a_{z_p} spectrum has more than one candidate "center frequency," and if two or more of these resonances satisfy the predictability criterion $\nu \leq 0.3$, then all the corresponding center frequencies must be used to evaluate the phase criterion to be discussed later in this section.

As a practical matter it may be impossible by analysis to certify that the pitch attitude system cannot be made to yield a suitably narrowband a_{z_p} response. In those cases, what is required is that bounds on ω_R be established (especialiy its maximum value).

A shortcut to the above analysis methodology is possible; it is recommended for those flight control tasks where uncertainties exist about the importance of turbulence to the basic piloting problem. For example, in flare the importance of good pitch attitude loop dynamics is almost an inarguable point. But flare is initiated by control feedforward from the pilot; there may be no substantial turbulence. We may assume, however, that pitch regulation will be necessary to compensate for errors generated by control resulting from pitch command errors. The corresponding pitch command error spectrum is unknown; a conservative estimate would be to model it as broadband noise, set $\Phi_{\theta_c \theta_c}(\omega) \equiv 1$ in the above equation, and estimate ν as before. The resulting $\Phi_{a_z a_z}(\omega)$ for the problem previously sketched would be as shown:

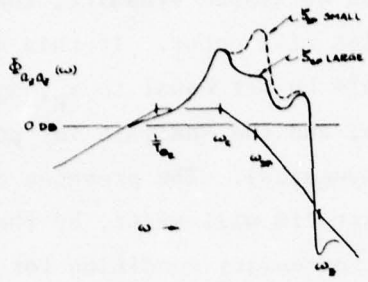

Acceleration Power Spectral Density
for Broadband Input

This sketch suggests that the estimation of A, ω_R and Δ may not be unique.

An even simpler criterion for subjective predictability could be based on the dominant mode damping ratio ζ_{CL} for closed loop pitch attitude control. Until better data can be developed it is suggested that $a_{z_p}(t)$ is subjectively predictable when

$$\zeta_{CL} \leq 0.2$$

The corresponding resonant frequency should be set equal to the dominant mode's undamped natural frequency. The validity of this criterion should be assessed on a case-by-case basis. Clearly, there may be combinations of ω_c, $1/T_{\theta_2}$, ζ_{sp}, and ω_{sp} where it will be inadequate.

If control or feel system nonlinearities exist that have significant effect on closed loop pitch dynamics, then the estimation procedure for ν and ω_R must be modified. No attempt will be made here to explain how this may be done. Describing function techniques (Reference 13) may be employed or the pilot-vehicle system may be simulated on an analog or digital computer and an "experimental" estimate made. If nonlinearities have a significant

effect on pitch tracking dynamics then (almost by definition) the handling qualities will suffer; this situation might require correction as a prelude to future exploration of PIO behavior.

If severe nonlinearities exist in the pitch attitude control loop that cannot be ignored in estimation of system dynamics, then it is conceivable that pitch attitude limit cycles will occur. If this does, indeed, happen the limit cycle frequency should be set equal to ω_R, $a_{z_p}(t)$ should be assumed to be subjectively predictable, and the analysis for possible PIO should proceed to phase 2 ($a_{z_p} \rightarrow F_s$ dynamics). The presence of a limit cycle in control of θ does not imply that PIO will exist, by the PIO definition; it would only mean that the first necessary condition for PIO had been satisfied. The distinction is important.

By now it is probably clear that the analysis of pitch dynamics is somewhat artistic. A suitable pilot model $Y_p(j\omega)$ must be parameterized to represent both the normal and possible bizarre forms of pilot dynamics in the pre-PIO phase of attitude control; this is not exactly a problem amenable to state-of-the-art solutions. A turbulence model must be selected to realistically simulate the frequency nature of expected gust disturbances; the break frequency ω_b is the most important turbulence parameter for this analysis. Fortunately, it appears that so long as $\Phi_{w_g w_g}(\omega)$ is "representative" that it is not too critical to an evaluation of PIO potential. Finally, the power spectral density predicted for a_{z_p} must be examined to diagnose whether it is suitably narrowband--and therefore subjectively predictable; the rules for doing this are primitive, at best. Thus, the problem of modeling the pitch attitude system is very much one where engineering judgment is indispensable to success. Fortunately for some of us, judgment is not quite so vital in phase 2 of Type I PIO assessment.

Phase 2: Normal Acceleration System Dynamics

If the closed loop control of pitch attitude is found to produce a subjectively predictable normal acceleration response, then it is postulated that the pilot will, at some time, attempt to track a_{z_p}. This process has

been modeled (Figure 4) with a switching function such that either θ or a_{z_p} is controlled, but not both. It was previously mentioned that the hypothesized a_{z_p}-dependent pilot gain K_a might be used as a switch to "turn on" the feedback control of a_{z_p}.

It is further postulated that when the pilot begins to track a_{z_p} his "rule" for system closure is that the crossover frequency of the a_{z_p} loop must equal ω_R--the resonant frequency of the $a_{z_p}(t)$ response due to pitch attitude control, alone. It is assumed that he selects K_a to establish this condition. The appropriate pilot model for a_{z_p} control is simply

$$\boxed{\frac{F_s}{a_{z_{pe}}}(j\omega) = K_a\, e^{-\tau_a j\omega}}$$

It is suggested that, until better information becomes available, an appropriate delay is

$$\boxed{\tau_a = 0.25 \text{ seconds}}$$

This value appears to be consistent with the T-38A PIO tracking data (Refs. 1 and 4); more important, however, is the observation that it seems to correlate the results of the numerical studies (Section VI) with actual PIO experiences. It is conceivable that τ_a is functionally dependent upon ω_R. A possibility is that

$$\tau_a = \frac{\pi}{2\omega_R}$$

This dependency arises from consideration of the pilot's motion sensor as an optimal, linear filter. This model for τ_a will not be used further in this report.

A necessary condition for the existence of Type I PIO may be simply stated as follows:

$$\boxed{\omega_R \geq \omega_L}$$

where ω_L is the minimum frequency for which

$$L(j\omega) = \frac{-1}{N}$$

It is understood that $L(j\omega)$ represents the linear portion of the $a_{z_p} \rightarrow F_s$ loop and that N is a sinusoidal describing function representation of the nonlinear part. That is, the $a_{z_p} \rightarrow F_s$ system is assumed to have been arranged in the following form:

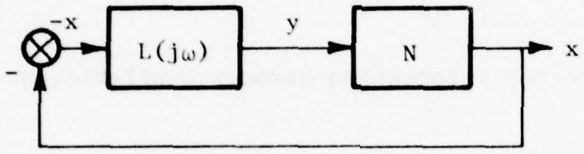

The Equivalent $a_{z_p} \rightarrow F_s$ System

[When nonlinearities are imbedded in inner loops within the feel or automatic control systems, this formulation can be difficult to accomplish.] If no important nonlinearities exist, then

$$N \equiv 1$$

$$y \equiv x = a_{z_p}$$

and

$$L(\omega) = \frac{F_s}{a_{z_{p_e}}} (j\omega) \frac{\delta_e}{F_s} (j\omega) \frac{a_{z_p}}{\delta_e} (j\omega)$$

In general, the describing function N will be a function of oscillation frequency and amplitude; i.e., $N = N(\omega, a_{z_p})$. In the examples contained in this report, however, N will be amplitude dependent only; i.e., $N = N(a_{z_p})$.

Observe that the criterion $\omega_R \geq \omega_L$ is merely necessary for PIO and is not a guarantee that PIO will occur. Further discussion of this point will be deferred until Phase 3 of the Type I PIO assessment is introduced.

With a linear system the criterion $\omega_R \geq \omega_L$ is equivalent to specifying that the phase margin must be zero or negative if Type I PIO is to occur.

The interaction between the $\theta \rightarrow F_s$ and $a_{z_p} \rightarrow F_s$ loops is illustrated in Figure 5 for a lightly damped linear system (representative feel system and actuator dynamics are shown; a first order Padé approximation is assumed for the time delay). Figure 5 is intended to be a generic sketch, only, and is not drawn to scale. The figure suggests that when the "switch" of pilot control from θ to a_{z_p} occurs, the $a_{z_p} \rightarrow F_s$ system will be stable when the resonant frequency of $\theta \rightarrow F_s$ is less than the frequency for which the $a_{z_p} \rightarrow F_s$ locus first crosses the imaginary axis. When, however, the resonant frequency of $\theta \rightarrow F_s$ is greater than the value at which the $a_{z_p} \rightarrow F_s$ locus crossing occurs then $a_{z_p} \rightarrow F_s$ will be unstable if the pilot switches from control of θ to control of a_{z_p} at that condition. This is the linearized description for PIO initiation.

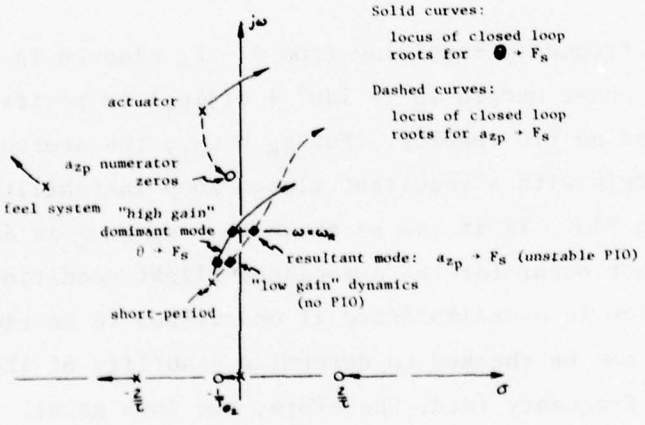

Figure 5. Closed Loop Dynamics; $\theta \rightarrow F_s$ and $a_{z_p} \rightarrow F_s$

The contributions of the feel system, control system, pilot, and airframe dynamics to PIO, for a linear system, are conveniently displayed on a plot of total, open loop system phase angle ϕ versus frequency:

$$\phi(j\omega) = (\text{pilot phase lag}) + (\text{feel system phase}) + (\text{control system phase}) + (\text{airframe phase})$$

$$\phi(j\omega) = -57.3\tau_a\omega + \angle \frac{\delta_e}{F_s}(j\omega) + \angle \frac{a_{z_p}}{\delta_e}(j\omega) \sim \text{degrees}$$

A typical plot of $\phi(j\omega)$ might appear as shown below in Figure 6.

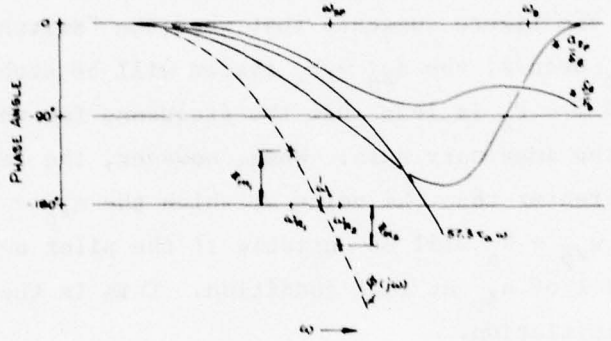

Figure 6. System Phase Components for $a_{z_p} \rightarrow F_s$

If the a_{z_p} resonant frequency resulting from $\theta \rightarrow F_s$ closure is ω_{R_1}, then the $a_{z_p} \rightarrow F_s$ system phase margin $\phi_{m_1} = 180° + \phi(j\omega_{R_1})$ is positive, the a_{z_p} system is stable, and no PIO results. For $\omega_R = \omega_{R_2}$, the sketch illustrates a negative phase margin with a resultant closed loop instability; this, by the PIO definition, is a PIO. If it can be shown that $\omega_R \geq \omega_L$ is impossible, then Type 1 PIO cannot occur for the associated flight condition. This phase margin criterion is oversimplified if one wishes to be rigorous. Nyquist's criterion can be checked to determine stability of the a_{z_p} loop, given the crossover frequency (and, therefore, the loop gain). In general, this appears to be an unnecessary complication; if ω_R is greater than the minimum frequency for which $\phi_m = 0$ then $a_{z_p} \rightarrow F_s$ is unstable if closure is made at frequency ω_R.

When feel and control system nonlinearities are known to exist, their effects on $a_{z_p} \rightarrow F_s$ system dynamics must be considered. Their effect is to introduce amplitude-dependent and frequency-dependent gains and phases into the control loops for both θ and a_{z_p}. It was already noted that the effect of nonlinearities on $\theta \rightarrow F_s$ dynamics should not generally be too significant for small motion amplitude unless the basic handling qualities are poor. For $a_{z_p} \rightarrow F_s$ dynamics, however, we cannot prescribe a priori what the character of the system dynamics might be; allowance must be made for the possibility that surface or rate limits can be encountered due to large amplitude excursions, for example.

Generally, reasonable sinusoidal describing function models can be obtained for each important nonlinearity and the system dynamics can then be formulated in the series model shown previously, combining all the linear elements into $L(j\omega)$ and representing the sinusoidal describing functions by N. Then limit cycles of the $a_{z_p} \rightarrow F_s$ loop are easily found from plotting amplitude versus phase angle for both $L(j\omega)$ and the negative inverse of N on the same diagram. Points of intersection between these two curves correspond to frequencies and amplitudes of motion at which $L(j\omega) = -1/N$. The smallest of these intersection frequencies is defined to be ω_L. A typical case is illustrated in Figure 7 for the case where the feel system contains an amplitude-dependent nonlinearity and no others.

In Figure 7, the oscillation frequency ω is the parameter of the gain-phase plot of $L(j\omega)$; oscillation amplitude a_{z_p} or pilot control amplitude parametizes the $-1/N$ plot. Three points of intersection between these two curves are indicated. Points 1 and 3 are stable limit cycles; point 2 is an unstable limit cycle.

Limit cycles found from a describing function analysis such as that indicated above do not necessarily represent PIO conditions. For a PIO to actually occur it is necessary (but not sufficient) that the resonance frequency ω_R of the pitch closed loop be equal to or greater than that of the lowest frequency limit cycle (ω_L). Actually, a better prescription for

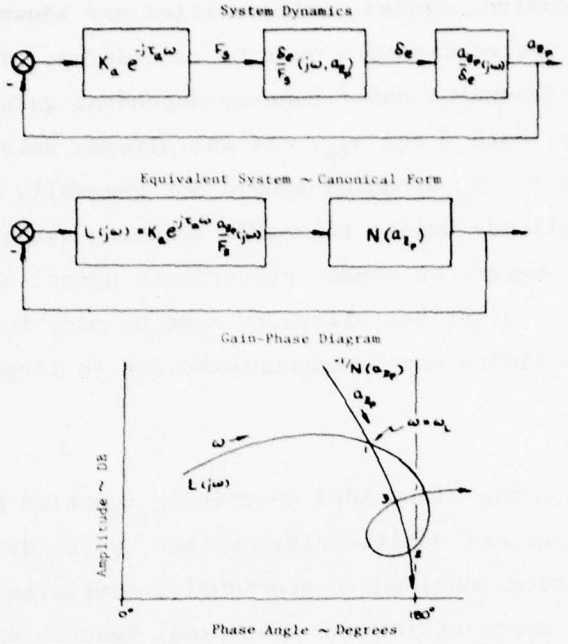

Figure 7. Determination of Limit Cycles in $a_{z_p} \rightarrow F_s$

nonlinear systems might be $\omega_L - \varepsilon < \omega_R$, where ε is a "small" number; that is a limit cycle can be initiated if the system is initially oscillating at a frequency "near" the limit cycle frequency. It may not be possible to specify what a suitable "nearness" criterion would be and, as a practical issue, it is not important here (to do so might require the development of a criterion based on Lyapunov's second method, for example). This nuance will be ignored.

If $\omega_R > \omega_L$ then a PIO may exist with initial frequency ω_R. The oscillations may orbit into a stable limit cycle or continue to increase in either amplitude or frequency (or both). It will often happen that, for the linear approximation to the nonlinear system dynamics, the frequency for $\phi = -180°$ will be $>\omega_L$. In those cases, instability of the linear system will imply that PIO exists with the nonlinear system; the use of the describing function analysis is redundant in such cases for the determination of PIO unless one wishes to estimate the PIO stability, frequency, and amplitude.

Phase 3: Acceleration Amplitude

The final necessary condition for Type I PIO is postulated to be that the amplitude of a_{z_p} oscillations due to pitch attitude control must be greater than some "critical" value $(a_{z_p})_{CR}$. The "critical" value $(a_{z_p})_{CR}$ is assumed to correspond to a pre-set pilot tolerance level such that when the amplitude of $a_{z_p}(t)$ oscillations is less than $(a_{z_p})_{CR}$ the pilot is insensitive or indifferent to it.

The conventional viewpoint of the human pilot is that he is highly adaptive. It follows that $(a_{z_p})_{CR}$ may be task-dependent. For example, oscillations of a_{z_p} that are tolerable without pilot control in air-to-air combat may be totally unacceptable in aerial refueling or in flare. A logical corollary to this reasoning is that $(a_{z_p})_{CR}$ will vary among pilots and among pilot communities; a student pilot, for example, might be hypothesized to emphasize a_{z_p} control more than might a service or test pilot. Thus, it might be concluded on this basis that the student is more susceptible to PIO than an experienced pilot. This may be so, of course; but it need not be so for the stated reason. If this viewpoint of the adaptive pilot is accepted, then a contradiction must be admitted; viz., an explanation must be offered for why less experienced pilots do not catalyze more PIO's as a result of $a_{z_p} \rightarrow F_s$ tracking in view of the fact that the $a_{z_p} \rightarrow F_s$ loop dynamics are almost universally poor and prone to instability. Rather than compound this potential philosophical felony, the writer suggests that perhaps we should reconsider the adaptive capabilities of the pilot.

It is proposed that, if $a_{z_p}(t)$ is of magnitude sufficient to be consciously felt by the pilot, and if it is subjectively predictable by him, then he may attempt to control it. If a realistic in-flight threshold of a_{z_p} sensation is assumed to be 0.01 g (Ref. 14), then it follows that $(a_{z_p})_{CR}$ = 0.01 g for any flight control task.

Using the data summarized in Reference 10, it is possible to conclude that as a first approximation the pilot opinion rating of a pitch attitude tracking task is given by the formula

$$POR = 3.8\sqrt{\sigma_q} \qquad \sim \text{Cooper-Harper scale}$$

The overall validity of this formula and the theory on which it is based need not concern us here. If the formula is accepted, then it follows that $\sigma q = 0.833$ degree/second is the maximum acceptable value for rms pitch rate (i.e., for POR = 3.5). It follows that a_{z_p} will be both detectable by the pilot and of concern to him when, to a first approximation.

$$\left|\frac{a_{z_p}}{\dot{\theta}}\ (j\omega_R)\right| \sigma_q > 0.01$$

$$\boxed{\left|\frac{a_{z_p}}{\dot{\theta}}\ (j\omega_R)\right| > 0.012}$$

where $|a_{z_p}/\dot{\theta}|$ is in units of g/degree/second. This criterion can only be verified with flight test experience. It will be shown in Section VI that the validity of the criterion is confirmed by the numerical examples (which represent the major existing PIO data base!).

The most important single parameter to the response ratio $a_{z_p}/\dot{\theta}$ is shown in the Appendix to be $1/T_{\theta_2}$. To a good approximation

$$\frac{a_{z_p}}{\dot{\theta}}\ (s) = \frac{-\ell_x}{2}\left[\frac{s^2 + \frac{1}{T_{\theta_2}}\, s + \frac{2U_o}{\ell_x}\frac{1}{T_{\theta_2}}}{s + \frac{1}{T_{\theta_2}}}\right]$$

Thus, the present PIO theory has implicated $1/T_{\theta_2}$ as a central parameter in two of the three criteria necessary for obtaining a Type I PIO (the first and the third). (See Appendix for information concerning the approximations above.)

C. TYPE II PIO

The tasks addressed here are those in which closed loop control of pitch is not an a priori requirement for PIO onset. This might include high-g maneuvers of an open loop control sort, trim malfunction, system transients resulting from SAS/CAS start-up or shutdown, etc. The common thread, however, is that the control (or disturbance) must be "suddenly applied" and of amplitude sufficient to excite the stick-free dynamic modes of the aircraft.

The analysis requirements for the investigation of Type II PIO are much simpler than those of the last section. Basically the procedure is the same except that there is no messy attitude loop closure to be performed.

It is assumed that the potential for Type II PIO may be determined as follows:

1. Compute the power spectral density of a_{z_p} using a normalized, broadband noise representation for $F_s(j\omega)$--to simulate the required "abrupt" character; that is

$$\Phi_{a_z a_z}(\omega) = \left| \frac{a_{z_p}}{F_s}\ (j\omega) \right|^2 \times 1$$

2. Determine the resonance frequency and the subjective predictability index ν from $\Phi_{a_z a_z}(\omega)$ exactly as was done for Type I PIO.

3. If $\nu \leq 0.3$ then Type II PIO cannot be ruled out as a possibility; then it is necessary to determine ω_L for $L(j\omega) = -1/N(\omega)$ as was done for the acceleration control loop for Type I PIO.

4. If $\nu \leq 0.3$, $\omega_R \geq \omega_L$ and $|a_{z_p}/\dot{\theta}(j\omega_R)| > 0.012$ g/degree/second, then Type II PIO should be considered probable for the given flight condition at some time during the aircraft's lifetime.

An alternative procedure which is simpler and which may be just as satisfactory is to determine whether any stick-free dynamic mode exists which significantly contributes to $\Phi_{a_z a_z}(\omega)$ and which has a damping ratio $\zeta_R \leq 0.2$. As a rule of thumb, the modal frequency must be less than about 10 rad/sec for such a mode to produce significant effect on $\Phi_{a_z a_z}(\omega)$ due to high frequency attenuation of a_z. If such a mode exists, then the a_{z_p} response should be considered to be subjectively predictable, ω_R should be set equal to the modal frequency, and the additional criteria for Type II PIO examined; viz., is $\omega_R \geq \omega_L$ and does $|a_{z_p}/\dot{\theta}(j\omega_R)|$ exceed 0.012 g/degree/second? If so, then Type II PIO is probable.

The simplified predictability criterion of $\zeta_R \leq 0.2$ was selected based on the T-38A and A4D-2 PIO experiences. Table 2 contains data extracted from page 54 of Reference 15. The airframe and feel system dynamics are shown for the flight conditions where each airplane experienced serious PIO; these data are given for the original and the modified control systems. It is clear

TABLE 2. SYSTEM DYNAMIC DATA; T-38A AND A4D-2

Airplane	STI TM 239-3 T-38A, aft c.g.		Douglas LB-25452 A4D-2, c.g. slight aft	
Control System	Orig	Mod	Orig	Mod
Airframe Dynamics:				
Stick Fixed ω_{sp}	7.0	7.0	7.94	7.94
Stick Fixed ζ_{sp}	0.40	0.40	0.40	0.40
Stick Free ω'_{sp}	9.8	7.5	8.8	4.8
Stick Free ζ'_{sp}	0.10	0.28	0.16	0.34
Feel System Dynamics: (in flight)				
ω_{FS}	17.7	24	18.4	19.2
ζ_{FS}	0.23	0.17	0.22	0.14

from these data that the stick-free, short-period mode probably dominates the character of $a_{z_p}(t)$ responses to abrupt control or turbulence inputs. The further assumptions are made that both the T-38A and the A4D-2 were susceptible to Type II PIO (and this appears to be a self-consistent assumption) and that the problems were cured (or at least alleviated) by the control system modifications performed. An inspection of these data suggests that

- o ζ_R = 0.16 will permit Type II PIO (A4D-2, original sitck-free damping ratio).
- o ζ_R = 0.28 is sufficient to eliminate (or reduce) Type II PIO tendencies (T-38A, modified stick-free damping ratio).

It follows that ζ_R between 0.16 and 0.28 will represent a susceptibility boundary.

Substantiation for this criterion is available from Reference 16. Bobweights were identified as a possible contributing cause for PIO for those cases where they degrade the stick-free short-period dynamics. The overall importance of stick force per steady-state g, minimum dynamic stick force per g, and short-period damping ratio was cited. The suggested correlation is shown in Figure 2 of Reference 16, p. 161 and in Figure 8 below; the PIO rating scale used is that given in Figure 36. These data were obtained from a flight test program documented in Reference 17. It is, to this writer, clear from this data plot that stick force per g is a tenuous basis for a PIO criterion. The data show only three PIO or near-PIO cases; one of these lies in the "safe" region of F_s/g. One no-PIO case lies on the 1.4 lb/g boundary. There are four cases with PIOR = 3-3.5 lying in the region of $(F_s/g)_{min} > 3.0$ lb/g. If one assumes that a correlation exists between PIOR and damping ratio <u>regardless of</u> <u>F_s/g</u> then it is clear from these data that a damping ratio of about 0.2 should represent a PIO boundary. This is indicated in the figure. This damping ratio should be interpreted, in general, as that of the resonant mode; i.e., as ζ_R. When the variations of PIOR with ζ_R shown above are interpreted against present theory, the data are completely consistent. These data potentially represent both Type I and Type II PIO conditions due to the nature of the flight test procedures used; the flight tests did appear to emphasize open-loop maneuvering to a considerable extent, however. Since

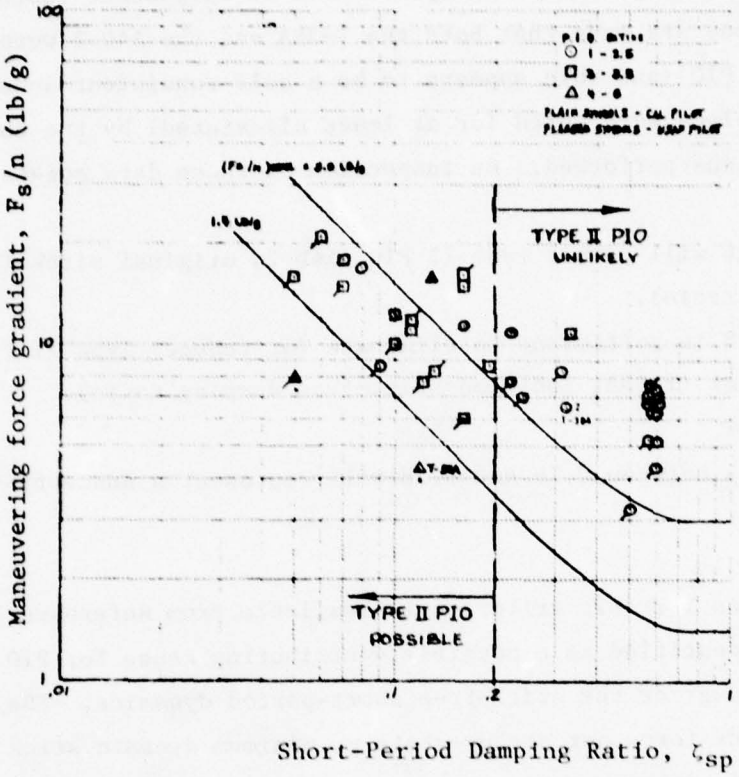

Figure 8. Effect of ζ_{sp} and Stick Force Level on PIO

$\zeta_R \leq 0.2$ has been postulated to be a necessary, but not sufficient, condition for Type II PIO, it is reasonable to expect that the three non-PIO cases tested with $\zeta_{sp} < 0.2$ did not satisfy the additional Type II PIO criteria ($a_{z_p} \rightarrow F_s$ phase or $|a_{z_p}/\dot{\theta}(j\omega_R)| > 0.012$). Similarly, the one data point with $\zeta_{sp} > 0.2$ and PIOR > 2.5 may possibly result from tendencies toward development of a Type I PIO.

It should be noted that the YF-12 and the YF-17 (as simulated by CALSPAN) both experienced serious PIO. The short-period damping ratio for the YF-17 is estimated to be almost 0.9, while that of the YF-12 is about 0.4 -- both in the PIO configurations. The interpretation of these data against criteria based only on F_s/g is impossible. Both cases, however, are readily understood when compared against the PIO criteria suggested as a result of the Type I and Type II distinctions for PIO. These case histories will be discussed in some detail in Section VI.

SECTION V

SUMMARY OF RULES FOR PIO ASSESSMENT

This chapter is presented as a summary and compendium of rules for the assessment of aircraft and flight control systems with respect to their potential for PIO encounter. It is a condensation of the theory of the last chapter. It is assumed that the flight conditions and aircraft-control system configurations to be investigated are known and that all the dynamic models required for application of the theory have been measured or estimated.

A. TYPE I PIO (INITIATED BY PITCH ATTITUDE CONTROL)

1. Select an appropriate model for piloted control of pitch attitude (e.g., Reference 6).

2. Close the pitch attitude loop.

3. Compute the power spectral density $\Phi_{a_z a_z}(\omega)$ of normal acceleration at the pilot's location due to control of pitch attitude (i.e., with no closed loop control of acceleration). Use a representative model for vertical turbulence.

4. From $\Phi_{a_z a_z}(\omega)$ estimate ω_R (the resonant frequency)--if one exists. If none exists for any realistic choice of pilot dynamics (allowing for gain changes or drop-out of equalization, for example, due to pilot tension, etc.) then type I PIO is unlikely. If ω_R exists, then estimate the subjective predictability index ν. If $\nu > 0.3$ go to step 4a; otherwise continue with step 5.

4a. Estimate the resonant mode damping ratio ζ_R. If $\zeta_R > 0.2$ then conclude that Type I PIO is unlikely; the evaluation can be continued at step 5 if conservatism is required or if one has little confidence in the pilot model parameterization. If $\zeta_R \leq 0.2$ go to step 5.

5. If there are no feel or control system nonlinearities present that may have significant effect on pilot-vehicle system dynamics in high-g, oscillatory states of motion, continue with step 5a; otherwise go to step 5b.

5a. (Linear system dynamics) Plot the total open loop system phase angle Bode $\phi(j\omega)$ for the $a_{z_p} \rightarrow F_s$ loop dynamics. $\phi(j\omega)$ will be the sum of phase angles due to the pilot, the feel system dynamics, the control system (or CAS) dynamics, and the airframe dynamics (including any SAS feedback loops). The pilot phase should be assumed to result entirely from a 0.25 second delay (i.e., -57.3×0.25). If the phase margin $180° + \phi(j\omega_R) > 0$ then Type I PIO is unlikely and the analysis for Type I PIO is complete. If $180° + \phi(j\omega_R) < 0$ then Type I PIO is possible and the analysis should proceed with step 6. If $180° + \phi(j\omega_R)$ is greater than, but approximately equal to zero, then this may suggest that the airplane will exhibit PIO tendencies, although a fully-developed PIO may be unlikely. In that case, it becomes a matter of judgment as to what course to follow in a design or development program.

5b. (Nonlinear system dynamics) On a gain-phase plot of $L(j\omega)$ and $-1/N$--the linear and negative inverse of the nonlinear portions of the $a_{z_p} \rightarrow F_s$ system, respectively--determine the smallest frequency ω_L at which these two curves intersect. If $\omega_R > \omega_L$, a Type I PIO is possible and the analysis must continue with step 6. If $\omega_R < \omega_L$ then Type I PIO is unlikely and the analysis for Type I PIO is complete (the cautionary note of 5a applies to this inequality determination, however). The pilot model for the analysis of $a_{z_p} \rightarrow F_s$ dynamics should be

$$\frac{F_s}{a_{z_{pe}}}(j\omega) = K_a \, e^{-\tau_a j\omega}$$

It is suggested that $\tau_a = 0.25$ seconds is a satisfactory choice.

6. If $|a_{z_p}/\dot{\theta}(j\omega_R)| \leq 0.012$ g/degree/sec then conclude that Type I PIO is unlikely. If this ratio is > 0.012, then conclude that Type I PIO is a very strong possibility.

B. TYPE II PIO (INITIATED BY MANEUVERING CONTROL OR TURBULENCE)

1. Compute the power spectral density of a_{z_p} for the stick-free airplane dynamics; assume that the airplane is excited by a wideband noise with power spectral density $\equiv 1$ (to simulate "abrupt" inputs). That is, assume

$$\Phi_{a_z a_z}(\omega) = \left| \frac{a_{z_p}}{F_s} (j\omega) \right|^2$$

2. Continue the analysis exactly as described above for Type I PIO, starting at step 4 and replacing "Type I" with "Type II."

3. Simplified alternative procedure: if the damping ratio of the dominant, resonant mode of a_{z_p}/F_s is ≤ 0.2, then Type II PIO is possible. Call this damping ratio ζ_R and continue the analysis as described above for Type I PIO, starting with step 5 and replacing "Type I" with "Type II." If the damping ratio is >0.2, then conclude that Type II PIO is unlikely. For conservatism one could define ω_R as the dominant mode's <u>damped</u> frequency and proceed to step 5 of the Type I PIO analysis above.

SECTION VI

NUMERICAL EXAMPLES

A. THE YF-17 (APPROACH AND LANDING: CAS-ON)

The reader should note that the YF-17 never experienced a PIO problem to this writer's knowledge. The NT-33A variable stability airplane, configured to simulate the YF-17, did encounter serious PIO difficulties in flare (Ref. 8). Calspan diagnosed the problem as excessive control system phase lag due to the CAS mechanization. They modified the (simulated) control system dynamics to reduce the lag contribution to longitudinal dynamics and found that this eliminated the PIO. This occurred prior to the first flight of the prototype airplane. Based on the variable stability airplane simulations the YF-17 flight control system was similarly modified prior to the first flight. Throughout the rest of this report, this PIO case history will be referred to as the YF-17 PIO without further qualification. The YF-17 case is particularly interesting because the airplane-control system dynamics as simulated were entirely linear.

System Dynamics

It is unfortunate that a quality description of the YF-17 airframe and control system dynamics was not available for analysis and presentation within this report. The only data available to this writer were those contained in Reference 8; this included only the pitch attitude transfer function with no stability derivatives. In order to reconstruct the corresponding normal acceleration transfer function some assumptions are required as follows:

1. From Reference 8,

$$\frac{\dot{\theta}}{\delta_e}(s) = \frac{M\delta_e\,(s + .84)}{s^2 + 2(.89)(1.98)s + 1.98^2}$$

$$\frac{1}{T_{\theta_2}} = 0.84$$

$$\omega_{sp} = 1.98$$

$$\zeta_{sp} = 0.89$$

M_{δ_e} is unknown

$$U_o = 140 \text{ kt} = 237 \text{ f/s}$$

2. Assume $\ell_x = 15.7$ ft (the pilot's location forward of the c.g.).

3. Assume

$$N_{\delta_e}^{a_{z_p}}(s) = (Z_{\delta_e} - \ell_x M_{\delta_e}) \left[s^2 + \frac{1}{T_{\theta_2}} s + \frac{2U_o}{\ell_x} \frac{1}{T_{\theta_2}} \right]$$

4. Assume $Z_{\delta_e} = -26.9$ and $M_{\delta_e} = -5.31$. These are representative values for a similar airplane (F-5) in power approach (Ref. 18).

5. Estimate

$$N_{\delta_e}^{a_{z_p}}(s) = 56.5 \left[s^2 + 0.84s + 25.4 \right]$$

$$\zeta_Z = 0.08$$

$$\omega_Z = 5.04$$

$$\frac{a_{z_p}}{\delta_e}(s) = \frac{56.5 \left[s^2 + 2(.08)(5.04)s + 5.04^2 \right]}{\left[s^2 + 2(.89)(1.98)s + 1.98^2 \right]}$$

$$\frac{a_{z_p}}{\dot{\theta}}(j\omega) = \frac{-10.64 \left[(j\omega)^2 + 2(.08)(5.04)j\omega + 5.04^2 \right]}{j\omega + 0.84}$$

Note that the acceleration dynamics estimated here for the YF-17 are not exactly those that were simulated in the reference 8 flight tests. The simulated acceleration numerator was that of the basic NT-33A -- in the absence of a direct lift control capability or the use of model-following techniques (which were apparently not used). The present analysis, using estimated YF-17 dynamics, will establish that according to present theory the YF-17 with the original control system was indeed PIO-prone. The question of in-flight simulator fidelity will be further examined in Section VII where it will be concluded that the Calspan simulation was qualitatively correct.

6. To a first approximation, assume the feel and control dynamics to be simplifications of those given in Reference 8:

$$\frac{\delta_e}{F_s}(s) = \frac{\delta_{es}}{F_s}(s)\,\frac{\delta_e}{\delta_{es}}(s) = \left(\frac{1\text{ in.}}{9\text{ lb}}\right) \times \frac{\delta_e}{\delta_{es}}(s)$$

$$\frac{\delta_e}{F_s}(s) = \frac{K'\,[s^2 + 2(.44)(11)s + 11^2]}{[s^2 + 2(.7)(4)s + 4^2]}\,\frac{(s+2)(s+2.3)}{(s+.9)(s+5)} \qquad \sim \text{original}$$

$$\frac{\delta_e}{F_s}(s) = \frac{K'\,(s+18)}{(s+10)}\,\frac{(s+2)(s+2.3)}{(s+.9)(s+5)} \qquad \sim \text{modified}$$

K' is unknown (and not required in this analysis).

7. Summary:

$$\frac{\theta}{F_s}(s) = \frac{K(2)(2.3)[.44,11]}{(0)[.89,1.98](5)[.7,4]} \qquad \sim \text{original}$$

$$\frac{\theta}{F_s}(s) = \frac{K(2)(2.3)(18)}{(0)[.89,1.98](5)(10)} \qquad \sim \text{modified}$$

$$\frac{a_{z_p}}{F_s}(s) = \frac{K[.08,5.04](2)(2.3)[.44,11]}{[.89,1.98](.9)(5)[.7,4]} \quad \sim \text{original}$$

$$\frac{a_{z_p}}{F_s}(s) = \frac{K[.08,5.04](2)(2.3)(18)}{[.89,1.98](.9)(5)(10)} \quad \sim \text{modified}$$

where the short hand notation employed above is:

$(1/T)$ means $(s + 1/T)$

$[\zeta,\omega]$ means $s^2 + 2\zeta\omega s + \omega^2$

The units are radians, ft/sec^2 and pounds.

Type II PIO Assessment

The simplified criterion of the last section (step 3) allows us to immediately conclude that Type II PIO in this configuration is extremely unlikely. The only second order mode appearing in the acceleration transfer function is the short-period mode. But $\zeta_{sp} = 0.89$ is far in excess of the subjective predictability criterion $\zeta_R \leq 0.2$.

Type I PIO Assessment

Figure 9 is a Bode plot of the airplane's pitch attitude dynamics $\theta/F_s(j\omega)$. If we assume that the crossover frequency will lie between 2-4 rad/sec, then it is clear that the aircraft dynamics are roughly of the form K/s^2 in this region. As a rule, dynamics of these sort will lead to lightly damped closed loop oscillations and degraded pilot opinion ratings. An inspection of the data base of Reference 6 and a modicum of iteration suggests that a reasonable (not bizarre!) model for pilot dynamics in pitch tracking would be

$$Y_p(j\omega) = K_p(2.5j\omega+1)\ e^{-.385j\omega}$$

A Bode plot of the open loop system dynamics $Y_p(\theta/F_s)$ is also shown in Figure 9. Figure 9 indicates that the absolute maximum crossover frequency with this $Y_p(j\omega)$ is 3.3 rad/sec. Accordingly, $\omega_c = 2.9$ was selected and is assumed to be consistent with what would be measured in actual flight; this yields a small phase margin (about 16°). Obviously, even small increases in pilot gain will rapidly degrade system stability. This result appears to be consistent with the evaluation pilots' comments about the poor pitch handling qualities of this configuration in flight tests (Reference 8).

The corresponding closed loop dynamics $\theta/\theta_c(j\omega)$ are shown in Figure 9 for $\omega_c = 2.9$. Obviously, the closed loop system is extremely resonant at this condition. It is evident by inspection that the resonant peak of θ/θ_c will dominate the a_{z_p} power spectrum. The corresponding damping ratio for this mode is approximately 0.03. Thus, by the simplified criterion for

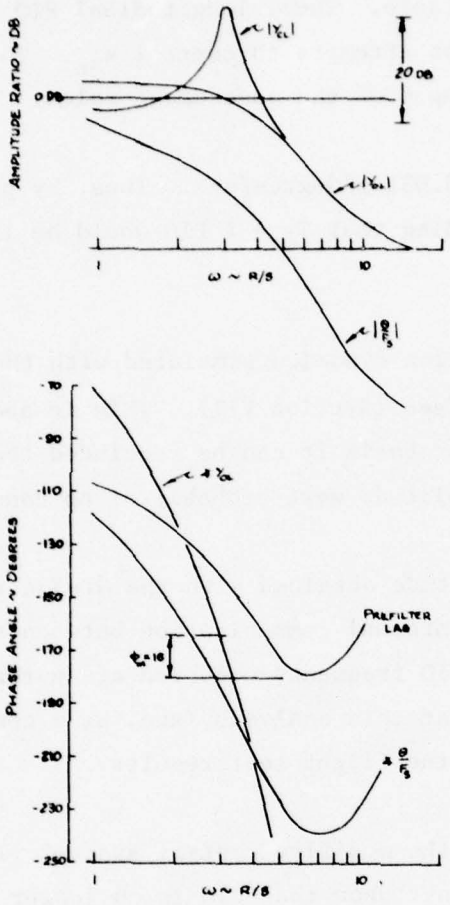

Figure 9. YF-17 Pitch Attitude Dynamics

subjective predictability of the last chapter, it must be concluded that Type I PIO cannot be ruled out on the basis of pitch control handling qualities. The resonance frequency ω_R = 3.0 rad/sec for the given $Y_p(j\omega)$. More pilot lead and higher gain would increase ω_R somewhat.

By the assessment rules, the analysis must now proceed to an investigation of stability of the $a_{z_p} \rightarrow F_s$ loop when the pilot's gain is adjusted to make $\omega_c = \omega_R$. The total $a_{z_p} \rightarrow F_s$ system phase $\phi(j\omega)$ versus frequency is plotted in Figure 10 in accordance with the rules of the PIO theory. The pilot time delay was assumed to be 0.25 seconds. At ω = 3.0 we see that

$\phi = -205°$, $180 + \phi = -25°$ (the system phase margin) and we see that the acceleration closed loop is unstable. Thus, longitudinal PIO can be initiated provided that the pilot attempts to control a_{z_p}. To see whether this is possible, proceed to step 6 of the assessment rules.

The ratio $|a_{z_p}/\dot{\theta}(3.0j)| = 0.031$ g/degree/sec. Thus, by present theory we would be justified in concluding that Type I PIO would be likely with this airplane and control system.

The actual normal acceleration dynamics simulated with the NT-33A yield $|a_{z_p}/\dot{\theta}(3.0j)| = 0.0213$ g/degree/sec (Section VII). This is about twice the criterion value of 0.012; on that basis it can be concluded that errors in the simulation of a_{z_p} motion amplitude were probably of no consequence.

The PIO frequency and amplitude obtained with the NT-33A simulation are unpublished. It is known from informal communication between the writer and Calspan staff members that the PIO frequency occurred at approximately 1/2 cps. It may therefore be concluded that this analysis (and, as a consequence, the present theory) is supported by the flight test results.

But what of the YF-17 with the modified control system? If the PIO theory is to be acceptable, it must show that PIO is no longer a probability in this flight condition. This is, indeed, the case.

A Bode phase plot is shown in Figure 10 for the two pre-filter dynamics (orginal and modified) flight tested by Calspan. It appears that the modified control system pre-filter decreases total system phase lag in the region of probable pitch system crossover by 45-70 degrees. The resulting airplane dynamics will therefore be more like K/s than the original K/s^2 form. The handling qualities are bound to be improved accordingly. No detailed analysis of pitch tracking is necessary, however, beyond the comment that, because of the improved control system dynamics, the chances are substantially reduced for obtaining resonant closed loop dynamics.

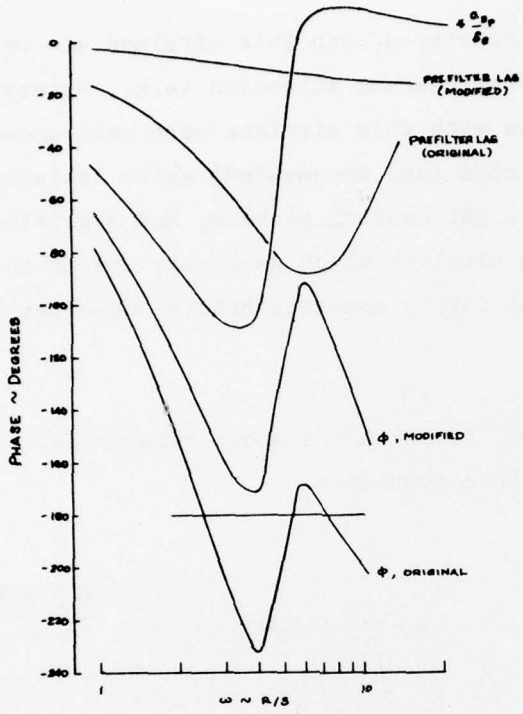

Figure 10. YF-17 Acceleration Control System Dynamics

Consider the $a_{z_p} \rightarrow F_s$ phase angle criterion. In Figure 10, $\phi(j\omega)$ is plotted with the modified control system. There are no intersections of the -180° phase condition for $\omega < 12.5$ rad/sec provided τ_a is less than about 0.3 seconds. Type I PIO would be extremely unlikely with the modified system.

It is therefore concluded that the theory of this report is substantiated by the YF-17 in-flight simulation. The reasons offered in Reference 8 for the PIO problem are confirmed, also, by these these theoretical results.

B. THE T-38A (M = 0.85 AT SEA LEVEL)

The PIO problems encountered with this airplane are well-known and have been given considerable engineering attention (e.g., References 1, 4, and 19). The PIO experiences with this airplane were well-documented, considerable analyses were conducted (and documented) which isolated the device-centered origin of the flight control problem, and significant control system changes were made to the airplane which generally appear to have solved the problems; thus, we have a fairly complete before-and-after history of this airplane's PIO behavior.

The PIO time history, cited in the above references, is reproduced in Figure 11 for the reader's convenience.

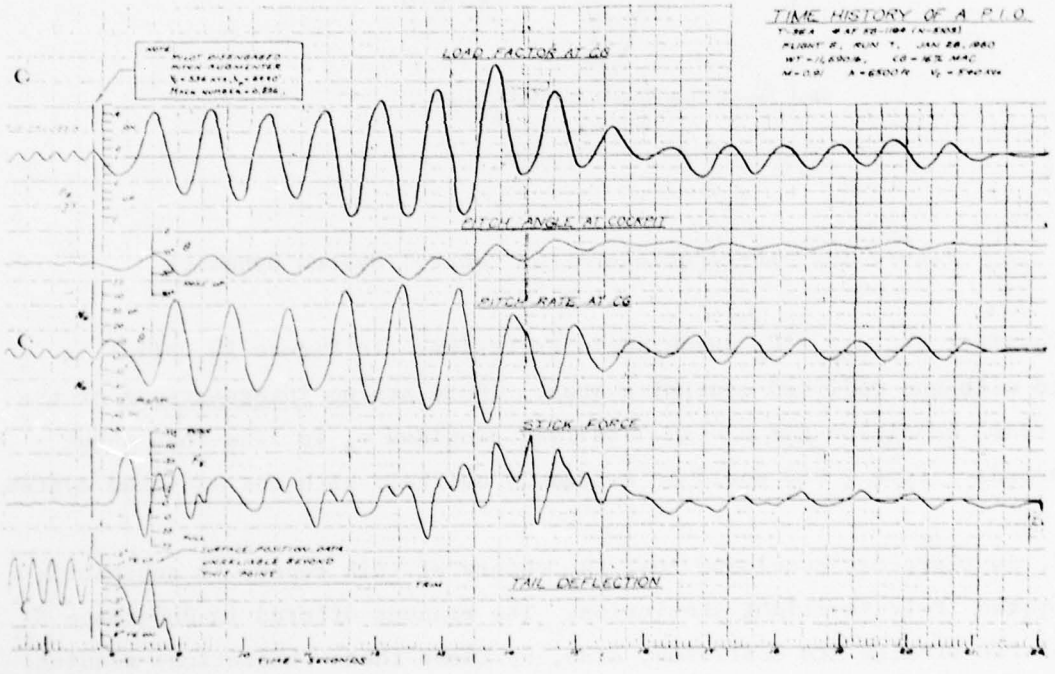

Figure 11. T-38A PIO Time History

System Dynamics--Original Control System

The dynamics of the airplane plus flight control system are complicated by

- o A normal acceleration bobweight
- o Control system friction

The bobweight had a very destabilizing influence on the short-period dynamics; this can be seen from Table 2 (p. 38). There was sufficient control system friction (break-out force = 2 pounds) to ensure that the bobweight feedback was almost completely masked for a_z less than about 1 g (the bobweight gain was 2 lb/g). The effect was to qualitatively change the airplane dynamics according to whether a_z was small or large. For small a_z the airplane's dynamics were best represented by the stick-fixed condition; for large a_z the stick-free dynamics were appropriate. The change in dynamics probably occurred very suddenly with changes in acceleration amplitude.

The structure of the airframe plus flight control system dynamics (SAS-off) is shown in Figure 12. The bobweight is modeled as a feedback of a_{z_p} to stick force. The pitch attitude dynamics $\theta/F_s(j\omega)$ are shown in Figure 13 for the two cases of no bobweight and full bobweight.

Type I PIO Assessment -- T-38A

The most difficult task in analyzing the Type I PIO behavior of the T-38A is to select suitable models for pilot dynamics in control of pitch attitude. This will be done for three cases which sufficiently cover the spectrum of pilot-vehicle system dynamics:

- o Fully-adapted pilot; small a_{z_p} ($K_B = 0$)
- o Non-equalized pilot; small a_{z_p} ($K_B = 0$)
- o Fully-adapted pilot; large a_{z_p} ($K_B = 2$)

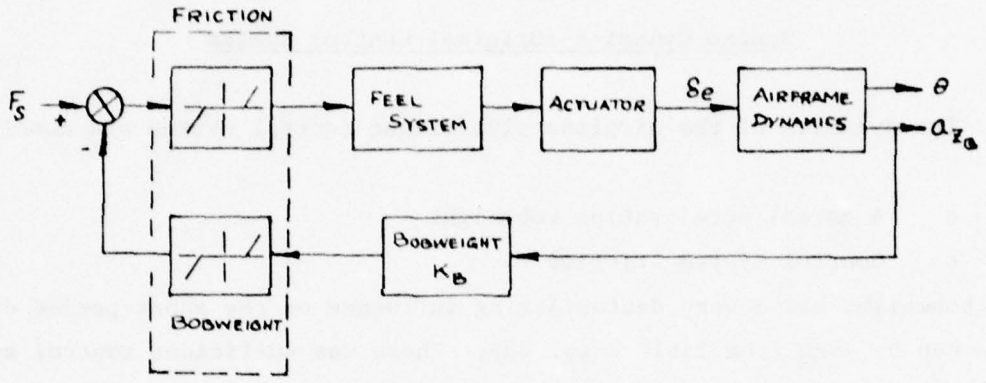

No Bobweight: $K_B = 0$

$$\frac{\theta}{F_s}(s) = \frac{.01726\left(\frac{s}{3.18}+1\right)}{s\left[\left(\frac{s}{7}\right)^2+\frac{2(.4)}{7}s+1\right]\left[\left(\frac{s}{18}\right)^2+\frac{2(.18)}{18}s+1\right]\left(\frac{s}{20}+1\right)} \sim \text{rad/lb}$$

$$\frac{a_{z_B}(s)}{F_s} = \frac{.508\left[\left(\frac{s}{24.4}\right)^2+\frac{2(.17)}{24.4}s+1\right]}{\left[\left(\frac{s}{7}\right)^2+\frac{2(.4)}{7}s+1\right]\left[\left(\frac{s}{18}\right)^2+\frac{2(.18)}{18}s+1\right]\left(\frac{s}{20}+1\right)} \sim \text{g/lb}$$

Full Bobweight: $K_B = 2$

$$\frac{\theta}{F_s}(s) = \frac{.0084\left(\frac{s}{3.18}+1\right)}{s\left[\left(\frac{s}{9.8}\right)^2+\frac{2(.10)}{9.8}s+1\right]\left[\left(\frac{s}{17.7}\right)^2+\frac{2(.23)}{17.7}s+1\right]\left(\frac{s}{21.8}+1\right)} \sim \text{rad/lb}$$

$$\frac{a_{z_B}(s)}{F_s} = \frac{.248\left[\left(\frac{s}{24.4}\right)^2+\frac{2(.17)}{24.4}s+1\right]}{\left[\left(\frac{s}{9.8}\right)^2+\frac{2(.10)}{9.8}s+1\right]\left[\left(\frac{s}{17.7}\right)^2+\frac{2(.23)}{17.7}s+1\right]\left(\frac{s}{21.8}+1\right)} \sim \text{g/lb}$$

Figure 12. T-38A Airframe-Control System Dynamics

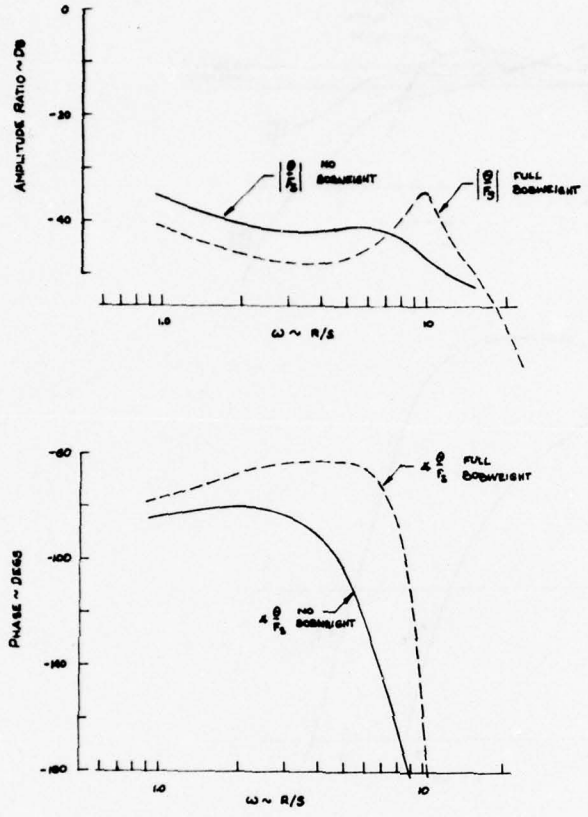

Figure 13. T-38A Pitch Attitude Dynamics; Effect of Bobweight

Reference 4 suggests that prior to PIO initiation, a reasonable model for the fully-adapted pilot in control of pitch attitude is

$$Y_p(s) = \frac{K_p\, e^{-.2s}}{\frac{s}{3.2} + 1}$$

The lag time constant was selected to cancel the $\theta/F_s(s)$ numerator time constant; the resulting open-loop dynamics of the $\theta \rightarrow F_s$ loop are therefore approximately equal in form to K/s in the region of expected crossover frequency as required by the adjustment rules of Reference 6.

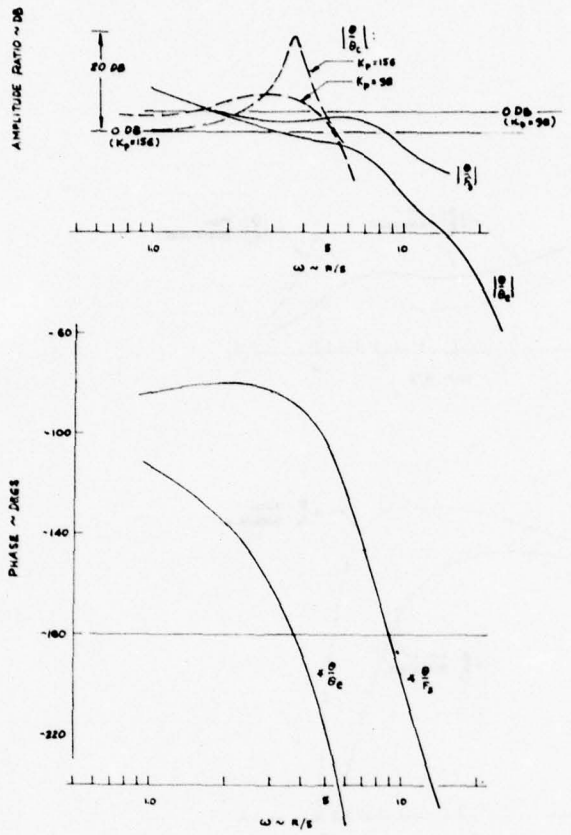

Figure 14. T-38A Pitch Control Dynamics; Lag-Equalized Pilot, No Bobweight; Effect of Pilot Gain

The open-loop $\theta \rightarrow F_s$ system dynamics with the fully adapted, lag equalized pilot are shown in the Bode plot of Figure 14.; the stick-free airplane dynamics $\theta/F_s(j\omega)$ are repeated there for comparison. Figure 14 also shows the closed loop system amplitude ratio $|\theta/\theta_c(j\omega)|$ for two values for pilot gain; the value K_p = 156 lb/rad was the one suggested in Reference 4. Recall that the pitch attitude command θ_c is an equivalent command due to turbulence for conventional VFR flight; it could also be a command input with a flight director system or an "internally generated" command by the pilot himself. Actually, θ_c is nearly immaterial to the PIO analysis. The important criterion is to determine the nature of the closed loop responses <u>if</u> the pilot elects (or is forced) to execute precision control of θ -- the existence or non-existence of command or disturbance inputs is irrelevant to this purpose; it is an analytical convenience to "invent" θ_c.

The closed loop response ratio $|\theta/\theta_c(j\omega)|$ shown in Figure 14 may be used to compute the a_{z_p} power spectral density from the equation

$$\Phi_{a_z a_z}(\omega)$$

$$= \left| \frac{Z_{\delta_e} - \ell_x M_{\delta_e}}{M_{\delta_e}} \; \frac{M_w \omega_Z^2}{\frac{1}{T_{\theta 2}} \omega_{sp}^2} \right|^2 \left| \frac{s\left[\left(\frac{s}{24.4}\right)^2 + \frac{2(17)}{24.4}\, s + 1\right]}{\left(\frac{s}{3.18} + 1\right)\left[\left(\frac{s}{7}\right)^2 + \frac{2(.4)}{7}\, s + 1\right]} \right|_{s=j\omega}^2 \left| \frac{\theta}{\theta_c}(j\omega) \right| \Phi_{w_g w_g}(\omega)$$

where

$$\left| \frac{Z_{\delta_e} - \ell_x M_{\delta_e}}{M_{\delta_e}} \; \frac{M_w \omega_Z^2}{\frac{1}{T_{\theta 2}} \omega_{sp}^2} \right|^2 = (0.5)^2 \; (\text{ft/sec}^2)^2 - \text{sec}$$

It is assumed that the pilot's location forward of the c.g. is the same as the effective bobweight location (ℓ_x = 12.83 ft, Reference 19). In view of the uncertainties surrounding θ_c and the choice of an appropriate turbulence model, assume that $\Phi_{w_g w_g}(\omega)$ is as shown in Figure 15. The resulting a_{z_p} power spectral densities, normalized by $\pi\sigma_{w_g}^2/10$, are shown in Figure 16 for two K_p values with the lag-equalized pilot model. These two spectra are repeated in Figure 17 with a linear frequency scale for ease in interpretation. Values of $\sigma_{a_{z_p}}$ are tabulated for two realistic levels of σ_{w_g}; the index ν of subjective predictability is also given for each case. The values of $\sigma_{a_{z_p}}$ were obtained by direct, approximate integration of the normalized $\Phi_{a_z a_z}(\omega)$.

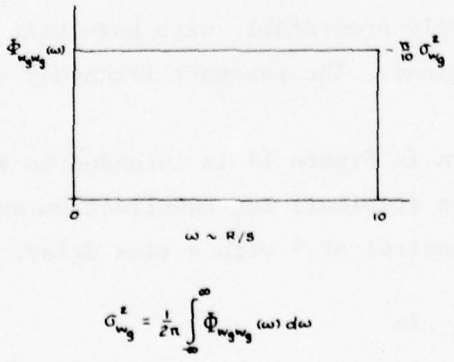

Figure 15. Simplified Turbulence Model

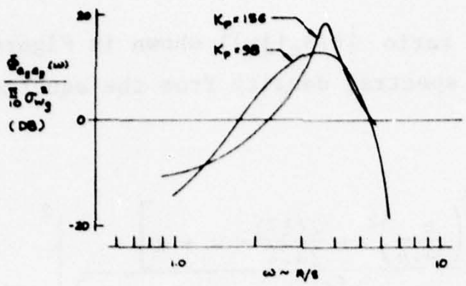

Figure 16. PSD of a_{z_p}; No Bobweight; Lag-Equalized Pilot

K_p LB/RAD	$(T_2)^{-1}$ sec^{-1}	$\sigma_{\theta p}/\sigma_{w_g}$ $(FT/S^2)/(FT/S)$	$\sigma_{a_{z_p}}$ (G) $\sigma_{w_g}=5$	$\sigma_{a_{z_p}}$ (G) $\sigma_{w_g}=10$	ν
156	3.2	1.17	.18	.36	.15
98	3.2	1.09	.17	.34	.25
98	0	1.40	.22	.45	.10
156	0	UNSTABLE	—	—	—

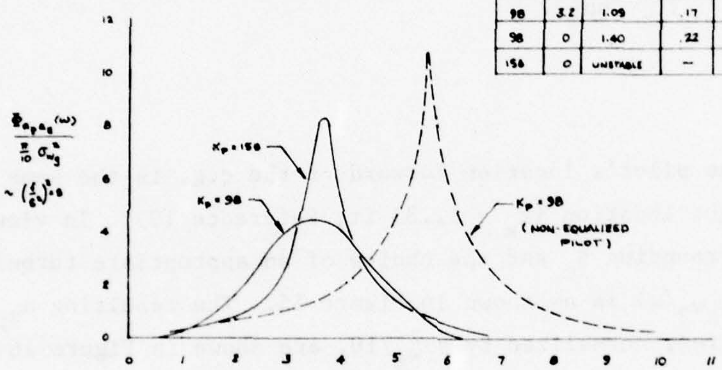

Figure 17. PSD of a_{z_p}

Based on the criterion $\nu \leq 0.3$, it appears that $a_{z_p}(t)$ is sufficiently resonant to be subjectively predictable with both pilot gains--although the case for $K_p = 98$ is marginal. The resonant frequency $\omega_R \cong 3.5\text{-}3.6$ rad/sec.

The third case shown in Figure 17 is intended to simulate the situation where the pilot drops the (typical) lag equalization and reverts to the more primitive proportional control of θ with a time delay. That is

$$Y_p(s) = K_p e^{-.2s}$$

This might occur, for example, when the pilot becomes "tense" or overly concerned about pitch errors. It could also occur when the pilot does not track θ, at all, but tracks only $\dot{\theta}$; there is some basis for such a model, but it is beyond the scope of present interest and will not be considered further. The open and closed loop $\theta \rightarrow F_s$ dynamics for this pilot model are shown in Figure 18. Note that the pitch attitude loop closure is unstable for $K_p = 156$; it is marginally stable (gain margin = 1 db) for $K_p = 98$. The power spectrum of $a_z(t)$, for the rectangular $\Phi_{w_g w_g}(\omega)$ spectrum, is shown in Figure 19 and, as previously indicated, in linear form in Figure 17. It is clear from Figure 17 that the dominant effect of reducing lag equalization is to markedly increase the resonance and resonance frequency of uncontrolled $a_{z_p}(t)$. Figure 17 indicates that with no equalization the resonance frequency $\omega_R = 5.6$ rad/sec.

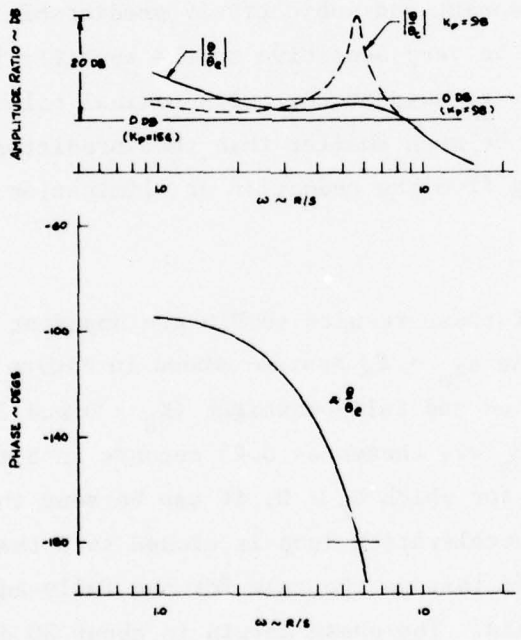

Figure 18. T-38A Pitch Control Dynamics; Non-Equalized Pilot; No Bobweight

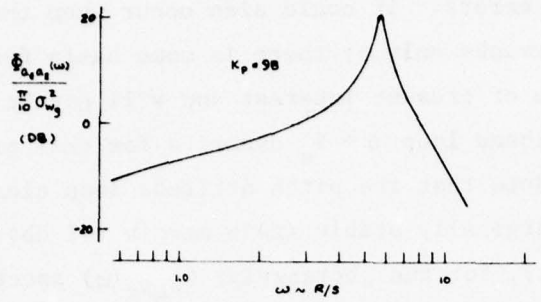

Figure 19. PSD of a_{z_p}; No Bobweight; Non-Equalized Pilot

It is clear that with realistic choices for $Y_p(j\omega)$ the pilot-felt acceleration will be resonant and subjectively predictable. The resonant frequency ω_R appears to be very sensitive to the specific form chosen for $Y_p(j\omega)$; it is reasonable to suspect that with nominal pilot dynamics, the resonant frequency will be much smaller than that predicted for off-nominal pilot dynamics resulting from the reduction or elimination of lag equalization.

The implications of these results to PIO are apparent from inspection of $\phi(j\omega)$--total phase of the $a_{z_p} \rightarrow F_s$ system--shown in Figure 20. Two cases are shown corresponding to no- and full-bobweight (K_B = 0 and 2, respectively). The pilot's time delay τ_a was chosen as 0.25 seconds in both cases. For the small acceleration case for which $K_B \cong 0$, it can be seen that $a_{z_p} \rightarrow F_s$ is quite stable if the acceleration loop is closed such that it resonates at frequency ω_R = 3.5 - 3.6; this is the case for the fully-adapted, lag equalized pilot with reasonable gain. The phase margin is about 80 degrees. For the non-equalized pilot, however, the phase margin is markedly decreased; for the case of K_p = 98 and ω_R = 5.6, it can be seen that the phase margin is about 20 degrees. Thus, it is plausible that

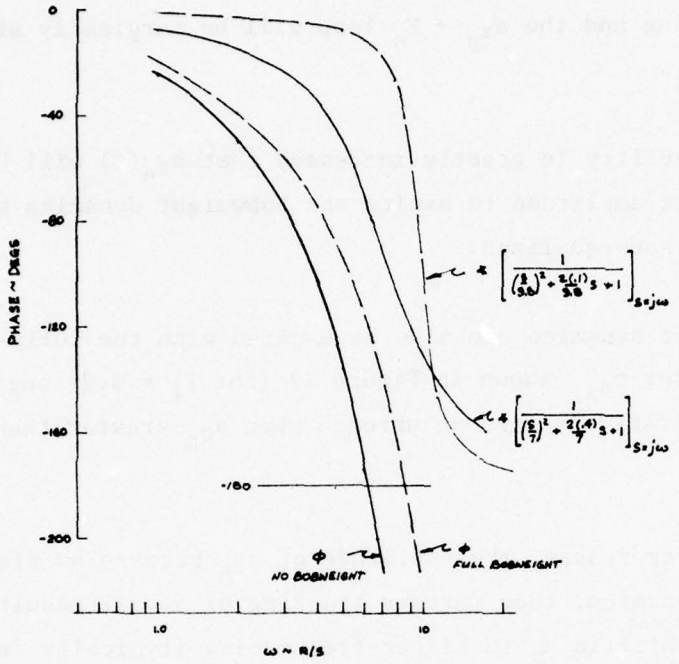

Figure 20. T-38A: Total Phase Angle of the Acceleration Control Loop; Effect of Bobweight

1. With "normal" pilot dynamics, and for initially small $a_{z_p}(t)$, the control of θ can lead to a_{z_p} resonance.

2. If the pilot attempts to track the a_{z_p} cue, the resulting $a_{z_p} \rightarrow F_s$ loop dynamics will be stable and a_{z_p} amplifications are not likely to result.

3. With a non-equalized pilot, the control of θ can lead to very resonant, but stable, a_{z_p} responses.

4. The resonant frequency ω_R due to control of θ with a non-equalized pilot will be substantially greater than that resulting from pilot-adapted lag and the $a_{z_p} \rightarrow F_s$ loop will be marginally stable at the larger ω_R.

5. The probability is greatly increased that $a_{z_p}(t)$ will become of sufficient amplitude to excite the bobweight dynamics when the pilot is non-equalized.

Of course, bobweight dynamics can also be excited with the fully-adapted pilot; the values for $\sigma_{a_{z_p}}$ shown in Figure 17 (for $T_I = 3.2$) suggest that it would be a comparatively rare occurrence when a_{z_p} greater than 1 g occurs.

If, for whatever reason, the amplitude of a_{z_p} becomes sufficient to excite bobweight dynamics, then further tracking of θ will result in

1. A large shift in ω_R to higher frequencies (typically from about 3.5 to about 8 rad/sec).
2. Closed loop instability of $a_{z_p} \rightarrow F_s$.

This appears to be true even when lag equalization is used <u>provided</u> that the pilot's adaptation is with respect to the airplane dynamics corresponding to $K_B = 0$. This situation is shown on the Bode diagrams of Figure 21; open and closed loop Bode diagrams are shown for two values of K_p with

$$Y_p(s) = \frac{K_p\, e^{-.2s}}{\frac{s}{3.2} + 1}$$

as before. The value $K_p = 156$ is approximately equal to the value for zero closed loop damping ratio; however, even with $K_p = 98$ the closed loop is highly resonant with $\omega_R = 9.2$ rad/sec. By comparison with previous results it is clear that $a_{z_p}(t)$ would qualify as subjectively predictable for these

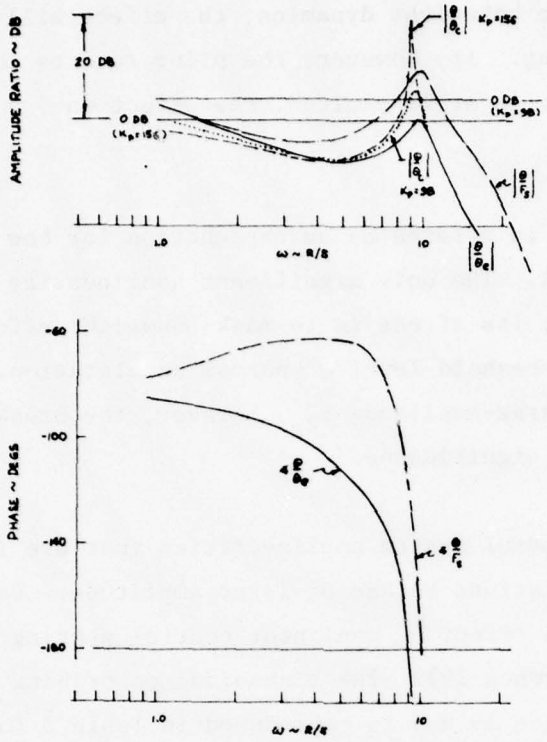

Figure 21. T-38A Pitch Control Dynamics; Lag-Equalized, Unadapted Pilot; Full Bobweight

cases. Inspection of $\phi(j\omega)$ from Figure 20 confirms that $a_{z_p} \rightarrow F_s$ would be unstable with this form of $Y_p(s)$ with an active bobweight; it is clear that closed loop instabilities in $a_{z_p} \rightarrow F_s$ will occur for ω_R greater than about 8.5 rad/sec.

Figure 20 bears further comment. The only significant difference between the $a_{z_p}/F_s(j\omega)$ dynamics with and without the bobweight is due to the short-period mode. The phase components of $\phi(j\omega)$ due to the short-period with and without the bobweight are shown in Figure 20; it is clear that, <u>for a given frequency of closure</u>, $a_{z_p} \rightarrow F_s$ is actually more stable with than without the bobweight due to the sizable reduction in phase lag resulting from the bobweight feedback (chiefly, the stick-free, short-period damping ratio). Thus, by present theory, if the pilot attempts to track a_{z_p} starting with small motions and no effective bobweight and, in the process, creates

a_{z_p} sufficient to excite bobweight dynamics, the effect will be to increase the $a_{z_p} \rightarrow F_s$ loop damping. If, however, the pilot reverts to the $\theta \rightarrow F_s$ loop while the bobweight is still excited, the effect on $\theta \rightarrow F_s$ loop stability is disastrous.

The above analysis is offered as an explanation for how Type I PIO was initiated with the T-38A. The only significant nonlinearity involved is control system friction; its effect is to mask bobweight effects on stick-free dynamics below a threshold level of normal acceleration. Once the pilot begins to track large-amplitude a_{z_p}, however, the breakout force will no longer be of primary significance.

There are other control system nonlinearities that are important to consider when the oscillations become of large amplitude. Chief among these is probably the combined effect of nonlinear control gearing and control system hysteresis (Reference 19). The sinusoidal describing function for this is given in Reference 19 and is reproduced in Table 3 for the case of oscillations about trim. The a_{z_p} control system may be modeled as indicated in Figure 22a. It can be shown that an equivalent form for the indicated system dynamics is that depicted in Figure 22b; this is the form required for the determination of system limit cycles via the gain-phase analysis. By inspection,

TABLE 3. SINUSOIDAL DESCRIBING FUNCTION FOR T-38A CONTROL SYSTEM

$\lvert F_s \rvert_{max}$ (lb)	Gain $\lvert N \rvert$		Phase $\angle N$ (deg)
	(deg/lb)	(db)	
5	.10	-20	-32
10	.18	-14.9	-12
20	.32	-9.9	-13

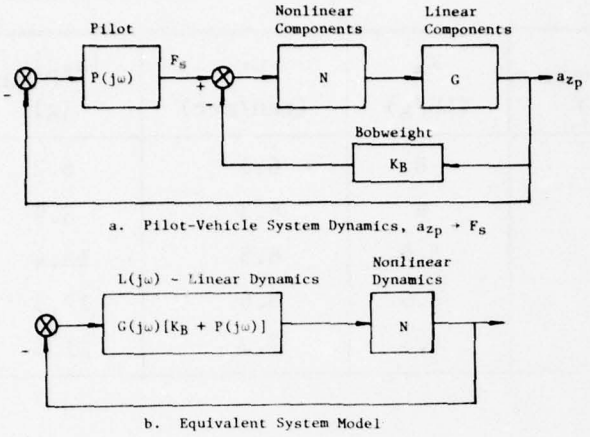

Figure 22. T-38A: A Model for Large-Amplitude Acceleration Control Dynamics

$L(j\omega) = G(j\omega)[K_B+P(j\omega)]$ = dynamics of the linear portion of the system.

N = feel system describing function (Table 3).

$G(j\omega)$ forward path dynamics of the linear control system and airframe;

$$G(j\omega) = \frac{.508[.17,24.4]}{[.40,7.0][.18,18](20)} \quad g/lb \text{ ; (the static gain is 0.508 g/lb).}$$

K_B = bobweight gain for large amplitude motion; for the original T-38A control system K_B = 2 (lb/g).

$P(j\omega) = K_a e^{-\tau_a j\omega}$ = pilot dynamics for a_{z_p} control; it is assumed that τ_a = 0.25 sec.

The gain-phase plots for both $L(j\omega)$ and -1/N are shown in Figure 23; five values of the pilot gain K_a were used for the computation of $L(j\omega)$. It can be seen that a stable limit cycle can exist with amplitude and frequency dependent upon pilot gain; typical results are shown in Table 4. The acceleration amplitudes shown in Table 4 were computed directly from the $a_{z_p}/F_s(j\omega)$ transfer function. If aerodynamic nonlinearities at high angles of attack were included in this analysis, then the unrealistic accelerations

TABLE 4. T-38 LIMIT CYCLE CHARACTERISTICS

$\lvert F_s \rvert_{max}$ (lb)	K_a (lb/g)	ω_L (rad/sec)	$\lvert a_{z_p} \rvert_{max}$ (g)
9	8	6.1	6.2
13	6	6.3	8.9
20	3.9	6.5	13.4
26	2.6	6.6	17.3
35	1.3	7.2	21.6

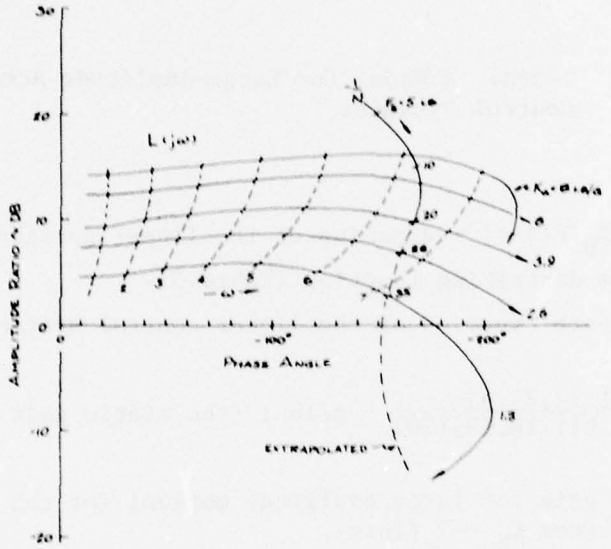

Figure 23. T-38A: Gain-Phase Diagrams for the Nonlinear $a_{z_p} \rightarrow F_s$ System Dynamics

shown would not be predicted; it was stated in Reference 19 that the nonlinear $M_\alpha(\alpha)$ curve would be sufficient to limit a_{z_p} to less than about 7g. Compare these results with the T-38A PIO time history (Figure 11). The comparison is seen to be very reasonable.

Now, according to the PIO theory described previously in this report, a Type I PIO can develop provided the accelerations resulting from pitch attitude control are sufficiently periodic (and it was shown above that they are, in general) and that the resonance frequency ω_R is approximately equal to or greater than ω_L. It was shown above that ω_R is highly variable depending upon pilot adaptation and whether or not the bobweight dynamics are excited. For those conditions believed to be related to the pre-PIO phase, however, the $\theta \rightarrow F_s$ loop analyses suggests that ω_R will lie, typically, between 5.6 and 9.5 rad/sec. We conclude, therefore, that if large amplitude motions are initiated and if the pilot attempts to track a_{z_p}, then a stable limit cycle will be very likely. The control system hysteresis at large amplitudes is sufficient to sustain the limit cycle.

The third and final necessary condition for Type I PIO was that

$$\left|\frac{a_{z_p}}{\dot{\theta}} (j\omega_R)\right| \geq 0.012 \quad \text{g/degree/sec}$$

This ratio for the T-38A is given in Table 5 for various possible ω_R. Clearly, the amplitude criterion is satisfied.

TABLE 5. $\left|\frac{a_{z_p}}{\dot{\theta}} (j\omega)\right|$ vs ω_R

ω_R (rad/sec)	$\left\|\frac{a_{z_p}}{\dot{\theta}}\right\|$ (g/deg/sec)
3	.370
4	.313
5	.267
6	.228
7	.196
8	.171
10	.132

It is concluded that Type I PIO is possible for this airplane, that the incipient-PIO frequency will be variable (from about 5.6 to 9.5 rad/sec), and that the fully-developed PIO frequency will be that of a stable limit cycle occurring in the $a_{z_p} \rightarrow F_s$ loop of frequency ω_{PIO} = 6.1 to 7.2 rad/sec. Present theory substantiates the basic conclusions of previous investigations of the system-oriented causes of the problem (notably References 1, 4, and 19); the present explanation of the phenomenon is, however, qualitatively different.

Type II PIO Assessment--T-38A

From the T-38A data summarized in Table 2, it can be seen that for large amplitude control or disturbance inputs the stick-free short-period damping ratio ζ'_{sp} = 0.1; by the simplified criterion for subjective predictability of a_{z_p}, conclude that the pilot can recognize the periodicity of the dominant mode response for abrupt inputs and he may attempt to close the $a_{z_p} \rightarrow F_s$ loop at $\omega_R \cong 9.8$ rad/sec. This, however, can result in a large-amplitude limit cycle as shown above. It can be seen from Table 5 that the amplitude criterion is satisfied at ω_R = 9.8 rad/sec. It is therefore apparent by present theory that the T-38A with the original control system was susceptible to Type II PIO.

PIO Assessment--Modified Control System

A number of modifications were made to the original T-38A control system in an attempt to cure the airplane's PIO problems. The most significant of these, so far as present theory is concerned, were

1. Increased feel spring rate at small stick deflections.
2. Decreased bobweight gain from about 2.0 to 1.0 lb/g measured at the control stick grip.

The intent of these modifications was to reduce the pilot's tendency toward "overcontrol" and to reduce the large variation in stick-free dynamics from small to large levels of normal acceleration, while maintaining approximately the same level of stick force per g (References 1 and 4).

It is clear from Table 2 that with the modified control system there is no longer a substantive difference between the stick-fixed and the stick-free dynamics. Consequently, the $\theta \rightarrow F_s$ analyses previously discussed for the case of small amplitude motion ($K_B = 0$) are also approximately valid for motion of any amplitude with the modified control system. It can be concluded, then, that while closed loop resonance can still occur, the chances for it are greatly reduced. The most important consideration, however, is that for realistic pilot dynamics (with or without fully-adapted equalization) the resonant frequency will be less than that required for instability of the acceleration loop $a_{z_p} \rightarrow F_s$ when control system nonlinearities are ignored. In such cases, Type I PIO is impossible by present theory.

The modifications made to the control system do not appear to have had a substantial effect on the large-amplitude control system nonlinearities. Figure 24 is a gain-phase plot of the linear and nonlinear portions of the $a_{z_p} \rightarrow F_s$ system dynamics for the modified system. The only difference assumed between this analysis and the one summarized in Figure 23 is that the bobweight gain is 1.0 lb/g rather than 2.0. It is clear from the gain-phase portrait that if large amplitude resonant motions can be initiated for any reason with ω_R greater than about 6.0 rad/sec, and if the pilot attempts to track a_{z_p}, then a stable limit cycle can still occur with the modified flight control system.

A recent PIO occurrence with the modified T-38A does appear to corroborate the present theoretical conclusion. This incident occurred with Air Training Command Aircraft SN 64-3253 in November 1975. The flight condition was M = 0.87 at an altitude of 15,000 feet. The aircraft was successfully recovered. Other, similar, problems with the T-38A have apparently occurred; these were the subject of Reference 21. Subsequent investigation determined that a flap-stabilator interconnect cable had broken prior to the PIO and that the probable effect of this breakage was to increase the pitch control gain by a factor of as much as 3.0 from the normal value. The resulting pitch sensitivity led to the excursions in acceleration. The instructor pilot was at the controls when the PIO occurred. If it is assumed that the pilot was fully adapted with respect to the normal aircraft dynamics, then

the previous analysis with the lag-equalized pilot ($1/T_I = 3.2$), shown in Figure 14, is approximately equivalent to this situation as a model for pitch loop dynamics. (Note that the no-bobweight case with the unmodified control system is dynamically similar to the full-bobweight case with the modified system.) If a realistic value for K_p is 98 lb/rad, then it can be seen from Figure 14 that a factor of 3 increase in open loop gain (i.e., 9.5 db) will yield an unstable pitch loop closure; the resulting motions in θ will be a divergent oscillation with frequency approximately equal to 7.4 rad/sec. Inspection of $\phi(j\omega)$ (Figure 20) indicates that the acceleration loop $a_{z_p} \rightarrow F_s$ will also be unstable when closed at this frequency. Thus, linear analysis indicates that the non-gain-adapted pilot will create large amplitude motions due to the control system linkage failure. Figure 24 suggests that a large amplitude limit cycle would be the probable steady state form of the motion. It was indicated that in this PIO encounter the pitch oscillations continued for several seconds and that the post-flight accelerometer readings were plus 5.2 and minus 6.0 g's. By comparison with past T-38A PIO case histories, this suggests that a stable, large-amplitude limit cycle, resulting from a_{z_p} loop closure, is a reasonable explanation for the facts surrounding this incident. Note the consistency between the g's obtained in the PIO and those indicated in Figure 24 or Table 4 for a factor of three increase in nominal pilot gain; i.e., the g level decreases with increasing gain.

Type II PIO would, by present theory, appear to have been eliminated since the dominant, stick-free mode damping ratio $\zeta'_{sp} = 0.28$ and is greater than the criterion value of 0.2. It is therefore concluded that if PIO is to be initiated with the modified control system, then it must result from a misadaptation by the pilot (excessive gain or lag drop-out in the control of pitch) together with a concern for load factor control.

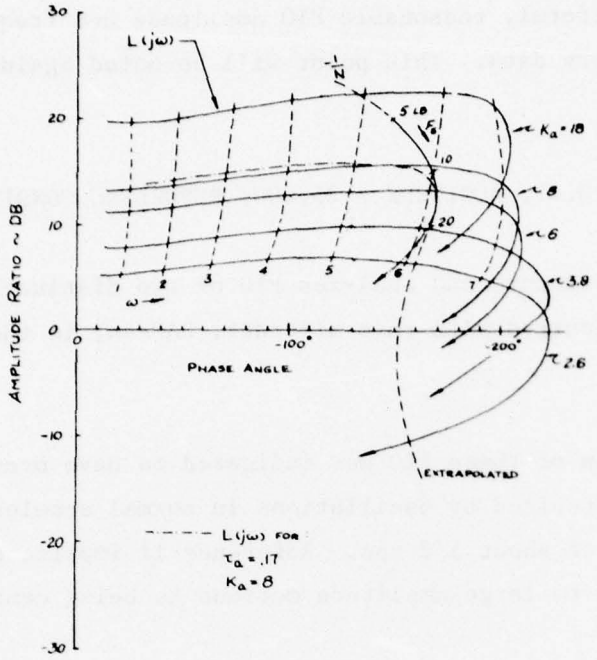

Figure 24. T-38A: Gain-Phase Diagrams for the Nonlinear $a_{z_p} \rightarrow F_s$ System Dynamics; Modified Control System

Comment on Pilot Time Delay

It was indicated in Section III that with a physiologically acceptable model for pilot dynamics, it is not necessary to resort to the assumption that, in PIO, the pilot is synchronous (i.e., has no time delay or equalization). It has been assumed that a small pilot delay exists in the $a_{z_p} \rightarrow F_s$ loop and that a reasonable value for this delay might be 0.25 seconds for want of better data.

In fact, present theory requires a minimum value of τ_a in order to support a PIO. This can be seen with the present example. In Figure 24 the dashed curve is the gain-phase plot for $L(j\omega)$ with $K_a = 8$ lb/g and $\tau_a = 0.17$. The two curves (L and -1/N) are tangent at $8 \leq \omega \leq 9$ but are otherwise non-intersecting. The conclusion, therefore, is that to obtain PIO by present

theory τ_a must be greater than 0.17 seconds. The value $\tau_a = 0.25$ was selected to give uniformly reasonable PIO amplitude and frequencies for the available case history data. This point will be noted again in the YF-12 analysis.

C. THE YF-12 (M = 0.77, ALTITUDE = 25,000; REFUELING CONDITION)

Reference 11 documents and analyzes PIO of two distinct types that are suspected to have occurred with this aircraft, SAS-on, in the same flight condition.

The more serious of these PIO was indicated to have occurred at least twice. It is characterized by oscillations in normal acceleration of about ±2 g at a frequency of about 1/2 cps. Reference 11 implicates saturation of the pitch damper due to large amplitude motions as being central to its development.

The second PIO mode was indicated to be of about 1 cps in frequency with an amplitude of about ±1/4 g. Reference 11 states that this oscillation is rather commonly encountered during refueling and that, while it is annoying to the pilot and quite beyond his ability to control, it is otherwise benign. Its origin was attributed to coupling between structural dynamics and rigid body, short-period dynamics.

Reference 11 presents an analysis of both these PIO modes based on dynamic properties of the closed loop pitch attitude control system. The pilot model used is a pure gain, following Reference 19 and others. The results of Reference 11 are essentially qualitative; they serve to illustrate the importance of SAS amplitude or rate limits to the initiation of large-amplitude oscillations. The authors note, in addition, that their analysis and similar past analyses of the PIO problem are not capable of PIO prediction but serve instead to identify causal factors after PIO is known to occur.

It is intended in the present application of the PIO theory of this report to explain both PIO modes of the YF-12, thereby confirming both the theory and the principal results of Reference 11. This is only possible in part, unfortunately, due to analytical complications posed by the SAS nonlinearities and to the almost complete lack of an analytical model for the effects of structural dynamics on the a_{z_p}/F_s transfer function. It will be shown in the following that the large amplitude, potentially catastrophic PIO is rather easily predicted by present theory. The "nuisance" PIO cannot be quantitatively confirmed by direct application of the theory due to the lack of a suitable model for structural dynamics. It will be shown, however, that its character can be assessed with a "plausible" model for structural effects and that the resulting implications to pitch attitude and pilot's control response dynamics are consistent with the flight test results published in Reference 11. In fact, the analysis offered here for the "nuisance" PIO appears to be the simplest and most straightforward method by which a theoretical understanding of the control deflection power spectral density, obtained in flight tests of the YF-12, can be derived.

System Dynamics

The dynamics of the YF-12 control system are complicated by a flexible fuselage structure and by SAS nonlinearities. It is assumed that an appropriate block diagram for the pitch attitude closed loop is as shown in Figure 25. The rigid-body modal response θ_R is considered to be the appropriate SAS input, since the rate gyro is placed near a point of zero slope on the first-mode fuselage bending curve. The pilot, however, is assumed to sense the combined attitude θ due to rigid-body motions and first mode bending.

In general, the analysis of such a system is impossible except by computer. Fortunately, it is possible to ascertain the qualitative nature of the pilot's control problem by examining only the limiting cases of very small motion amplitudes for which the SAS is completely linear and large motions for which the SAS may be considered to be always saturated and, therefore, nonfunctional. Thus, the models required are θ/δ_e and a_{z_p}/δ_e in the SAS-on and SAS-off conditions.

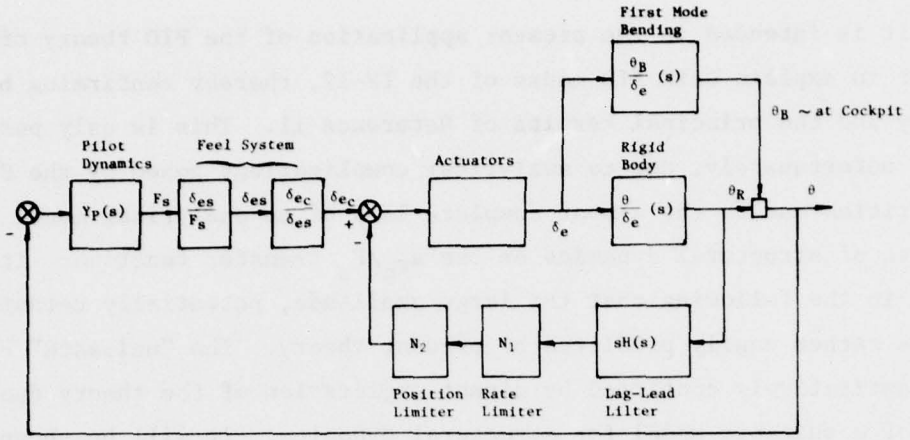

Figure 25. YF-12 Pitch Attitude Control Model

It should be noted that the YF-12 elevon controls are much more complicated than indicated by Figure 25. The differences are believed to be unimportant for an analysis of manual control. At most, higher frequency dynamics associated with the actuators contribute a small, equivalent time delay of about 0.06 seconds to the θ loop dynamics. Actuator dynamics will be neglected in the remainder of this analysis.

The first-mode structural bending curve is reproduced below (Figure 26) from Reference 11. In private communications with the authors of Reference 11, it was disclosed that this curve was analytically derived.

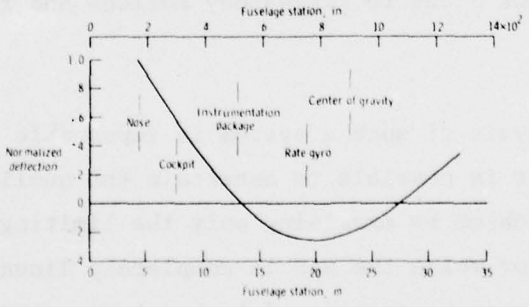

(From Reference 11)

Figure 26. YF-12 First Mode Fuselage Bending Curve

The stability derivatives given in Reference 11 are related to those used in this report (all of which are consistent with the notation of Reference 20) according to Table 6.

TABLE 6. STABILITY DERIVATIVES FOR THE YF-12

This Report	(Reference 2) NASA TN D-7900
Z_w	$-L_\alpha$
Z_{δ_e}	$-U_o L_{\delta_e}$
M_q	$M_{\dot{\theta}}$
M_α	M_α
M_{δ_e}	M_{δ_e}
U_o = 786 ft/sec ℓ_x = 50 ft (from Fig. 26) M = 0.8 h = 25,000 ft	

Airframe Dynamics (No SAS; Rigid Body)

$$\frac{\theta_R}{\delta_{e_c}}(s) = \frac{-6.08\ (s + 0.8)}{s[s^2 + 2(.376)(2.01)s + 2.01^2]} \quad \text{rad/rad}$$

$$\frac{a_{z_p}}{\delta_{e_c}}(s) = \frac{162.6[s^2 + 2(.113)(5.16)s + 5.16^2]}{[s^2 + 2(.376)(2.01)s + 2.01^2]} \quad \text{ft/sec}^2\text{/rad}$$

Airframe Dynamics (With SAS; Rigid Body)

$$H(s) = \frac{-.375(s + 8)}{(s + 4)}$$

$$\left[\frac{\theta_R}{\delta_{e_c}}(s)\right]_{SAS} = \frac{\frac{\theta}{\delta_e}}{1 + sH(s)\frac{\theta}{\delta_e}} = \frac{-6.08(s + 0.8)(s + 4)}{s(s + 1.478)[s^2 + 2(.692)(4.56)s + 4.56^2]}$$

rad/rad

$$\frac{a_{z_p}}{\delta_{e_c}}(s) = \frac{N_{\delta_e}^{a_{z_p}}}{N_{\delta_e}^{\theta}}\left[\frac{\theta_R}{\delta_e}(s)\right]_{SAS} = \frac{162.6(s+4)[s +2(.113)(5.16)s+5.16^2]}{(s+1.478)[s^2+2(.692)(4.56)s+4.56^2]}$$

ft/sec^2/rad

Airframe Dynamics (No SAS; First Bending Mode Included)

$$\frac{\theta}{\delta_{e_c}}(s) = \frac{\theta_R}{\delta_{e_c}}(s) + \frac{\theta_B}{\delta_{e_c}}(s)$$

From Reference 20,

$$\frac{\theta_B}{\delta_{e_c}}(s) = \frac{-5.15}{[s^2 + 2(.050)(15.7)s + 15.7^2]} \quad \text{rad/rad}$$

Then

$$\frac{\theta}{\delta_{e_c}}(s) = \frac{-11.23(s+.79)[s^2+2(.051)(11.61)s+11.61^2]}{s[s^2+2(.376)(2.01)s+2.01^2][s^2+2(.050)(15.7)s+15.7^2]} \quad \text{rad/rad}$$

If the pilot's displacement, due to fuselage bending, from the line of zero bending (Figure 26) is z_p, then

$$z_p = - \ell_o \theta_B$$

$$\ddot{z}_p = - \ell_o \ddot{\theta}_B$$

where the pilot's location forward of the node of the first bending mode curve is $\ell_o \cong 19.3$ feet. If a_{z_p} is assumed to result only from the rigid body acceleration plus the bending-induced acceleration, then

$$\frac{a_{z_p}}{\delta_{e_c}}(s)$$

$$= \frac{262[s^2+2(.114)(5.35)s+5.35^2][s^2+2(.044)(11.91)s+11.91^2]}{[s^2+2(.376)(2.01)s+2.01^2][s^2+2(.050)(15.7)s+15.7^2]} \quad \text{ft/sec}^2/\text{rad}$$

Unfortunately, this result neglects the heave-induced component of a_{z_p} for which there is insufficient data available for a reliable estimation. Furthermore, there is no way to assess the error that neglecting this mode might entail. For this reason, the results of this section are qualitative.

Airframe Dynamics (With SAS and First Bending Mode)

$$\frac{\theta}{\delta_{e_c}}(s) = \left[\frac{\theta_R}{\delta_{e_c}}(s)\right]_{SAS} + \frac{\theta_B}{\delta_{e_c}}(s)$$

$$\frac{\theta}{\delta_{e_c}}(s)$$

$$= \frac{-11.23(s+.79)(s+3.89)[s^2+2(.10)(11.78)s+11.78^2]}{s(s+1.478)[s^2+2(.692)(4.56)s+4.56^2][s^2+2(.050)(15.7)s+15.7^2]} \quad \text{rad/rad}$$

With the previous assumption that bending-induced heave is neglected, obtain

$$\frac{a_{z_p}}{\delta_{e_c}}(s)$$

$$= \frac{262(s+3.97)[s^2+2(.088)(5.30)s+5.30^2][s^2+2(.092)(12.07)s+12.07^2]}{(s+1.478)[s^2+2(.692)(4.56)s+4.56^2][s^2+2(.050)(15.7)s+15.7^2]} \quad \text{ft/sec}^2/\text{rad}$$

Feel System Dynamics

The feel system dynamics are indicated by Reference 20 to be very nonlinear as follows:

- o There is a large breakout force (about 5 pounds).
- o The input of sinusoidal stick force $F_s(t)$ produces a sizable hysteresis loop in the control stick deflection response.
- o The control gearing ratio $\delta_{e_c}/\delta_{e_s}$ is nonlinear.

The series combination of feel system hysteresis and nonlinear control gearing was used in Reference 11 to develop a sinusoidal describing function. This is reproduced in Figure 27.

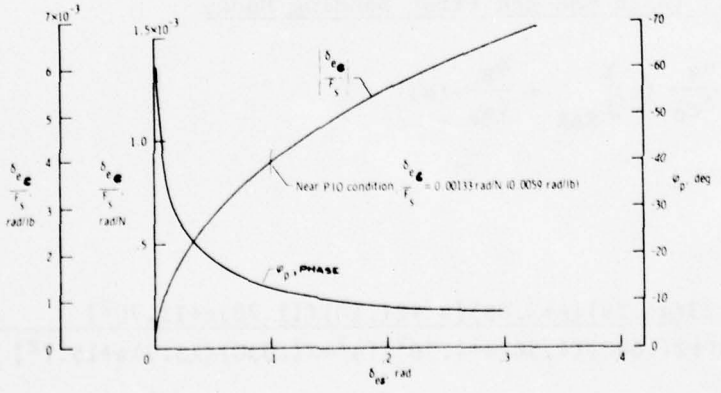

Figure 27. Describing Function for YF-12 Control System

Type I PIO Assessment--YF-12

The assessment of the YF-12's potential for Type I PIO is analogous to that for the T-38A. The pitch dynamics of the YF-12 qualitatively change when pitch rate becomes sufficient to saturate the position- and rate-limited SAS; the bobweight and control friction produced similar behavior in the case of the T-38A.

Figure 28 is a Bode plot of the linear θ/δ_{e_c} dynamics for the YF-12 with and without the SAS and including flexibility effects. Also shown is the computer-predicted, nonlinear frequency response taken from Reference 11 for the case where the SAS is assumed to be position limited to 2.5 degrees authority and with a rate limit of 12.6 degrees/sec. It is clear that when the SAS limits are encountered the resulting pitch dynamics are given to a good approximation by the SAS-off dynamics--a very fortuitous result! It was stated in Reference 11 that variations in the position limits of SAS authority do not greatly affect the nonlinear frequency response; the rate limit is the essential SAS parameter.

Inspection of Figure 28 suggests that, to a good approximation, θ/δ_{e_c} is of the form K/s in the vicinity of the probable crossover frequency (3-4 rad/sec) when the SAS is on and not limiting (the dashed curve). Thus, an appropriate pilot model for the control of pitch, with small amplitudes of $\dot{\theta}$, would be

$$Y_p(s) = K_p\, e^{-.2s}$$

i.e., a gain with time delay. It can be seen from Figure 28 that the maximum, permissible gain for stability of the pitch loop is reduced by a factor of about 3.75 (11.5 db) when the motions become of size sufficient to saturate the SAS. Also shown in Figure 28 is a closed-loop pitch response transfer function for the case where the SAS is unsaturated and the pilot gain is large. It is clear that the pitch dynamics can be resonant with a frequency $\omega_R \cong 4.5 - 4.9$ rad/sec; this is also the most likely range of maximum values for ω_R.

AD-A056 982 SYSTEMS RESEARCH LABS INC DAYTON OHIO F/G 5/8
A THEORY FOR LONGITUDINAL SHORT-PERIOD PILOT INDUCED OSCILLATIO--ETC(U)
JUN 77 R H SMITH F33615-77-C-3011
UNCLASSIFIED AFFDL-TR-77-57 NL

2 OF 2
AD
AD56 982

END
DATE
FILMED
9-78
DDC

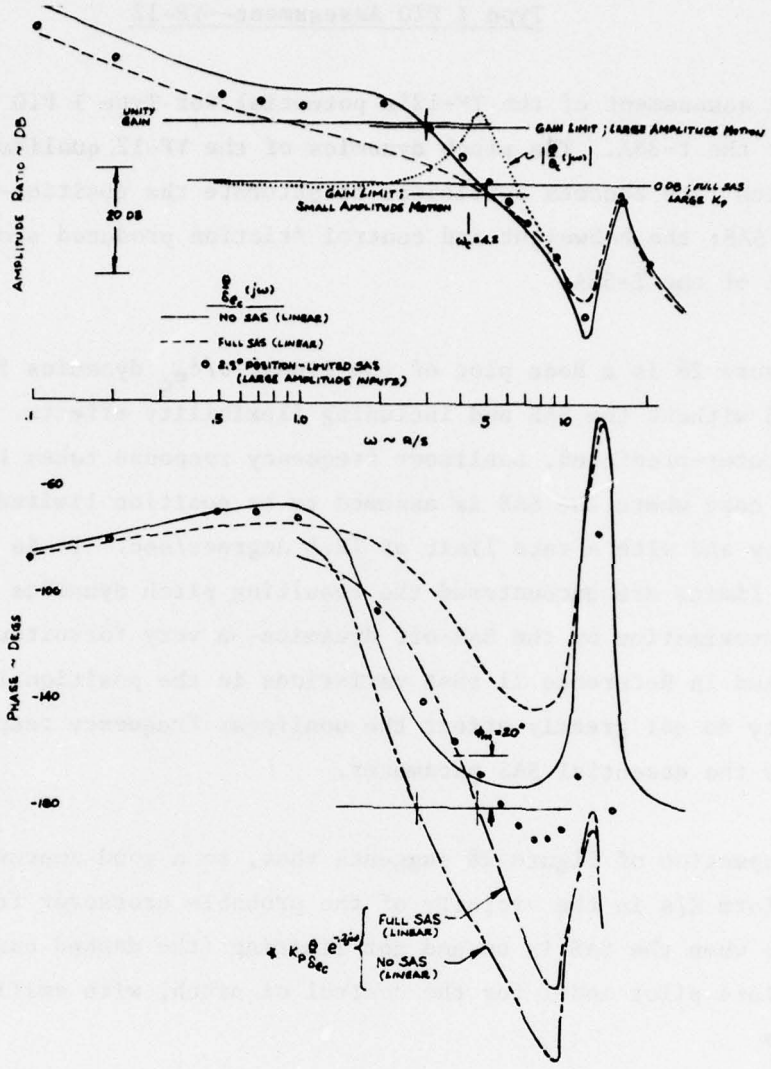

Figure 28. YF-12 Pitch Attitude Dynamics

In Figure 29 the open-loop transfer function is plotted for the $a_{z_p} \rightarrow F_s$ loop with a linear (i.e., unsaturated) SAS;

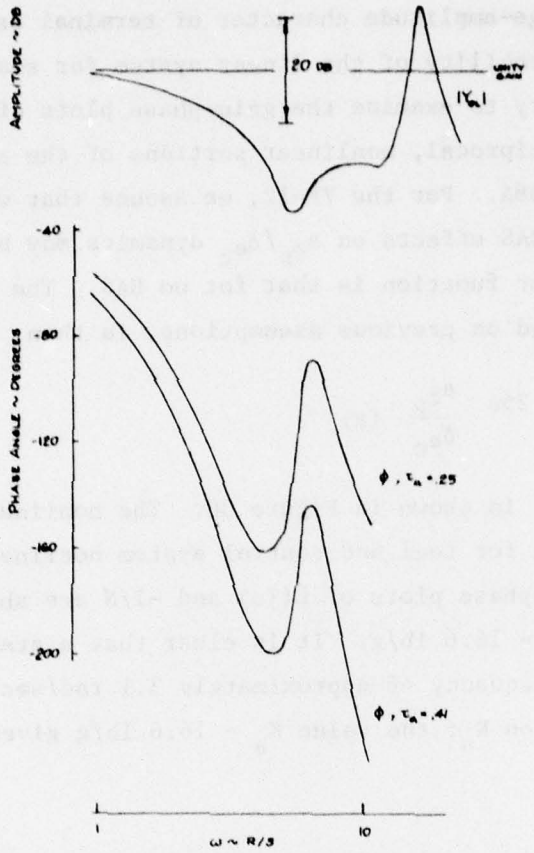

Figure 29. YF-12 $a_{z_p} \rightarrow F_s$ Dynamics; SAS-On

$$Y_{OL}(s) = K_p e^{-.25s} \frac{a_{z_p}}{\delta_{e_c}}(s)$$

The total open-loop phase angle is shown for two cases: one with no phase lag due to control and feel system dynamics and one with a time delay of 0.16 seconds (0.06 seconds due to the actuator lags and 0.10 seconds due to the feel system lag). In both cases the pilot delay is assumed to be 0.25 seconds.

It is apparent from Figure 29 that $a_{z_p} \rightarrow F_s$ system instability is possible at a resonant frequency ω_R = 4.5 - 4.9 rad/sec when the loop time delay is about 0.32 seconds. This could occur when the control system delays are approximately equal to or greater than 0.07 seconds--not an unreasonable value for the YF-12 control system.

To assess the large-amplitude character of terminal oscillations resulting from any instability of the linear system for small-amplitude motions, it is necessary to examine the gain-phase plots of the serialized linear and negative reciprocal, nonlinear portions of the $a_{z_p} \rightarrow F_s$ system, as was done for the T-38A. For the YF-12, we assume that with large-amplitude motions the SAS effects on a_{z_p}/δ_{e_c} dynamics may be neglected and the appropriate transfer function is that for no SAS. The linear part of the $a_{z_p} \rightarrow F_s$ loop, based on previous assumptions, is then

$$L(s) = K_a \, e^{-.25s} \, \frac{a_{z_p}}{\delta_{e_c}} \quad (s)$$

The Bode plot for $L(j\omega)$ is shown in Figure 30. The nonlinear part $N(A)$ is the describing function for feel and control system nonlinearities shown in Figure 27. The gain-phase plots of $L(j\omega)$ and $-1/N$ are shown in Figure 31 for a pilot gain of $K_a = 16.6$ lb/g. It is clear that a stable limit cycle can be obtained at a frequency of approximately 3.1 rad/sec; the control amplitude is dependent on K_a; the value $K_a = 16.6$ lb/g gives $|\delta_{e_c}| \cong 8.6$ degrees.

Note, also, that Figure 31 indicates that $L(j\omega)$ and $-1/N$ are <u>tangent</u> but otherwise non-intersecting for $K_a = 16.6$ when $\tau_a = 0.22$ (the dashed curve). This result is not too sensitive to K_a. This is further evidence to support the assumption that $\tau_a = 0.25$ is a generally valid delay for study of the normal acceleration dynamics.

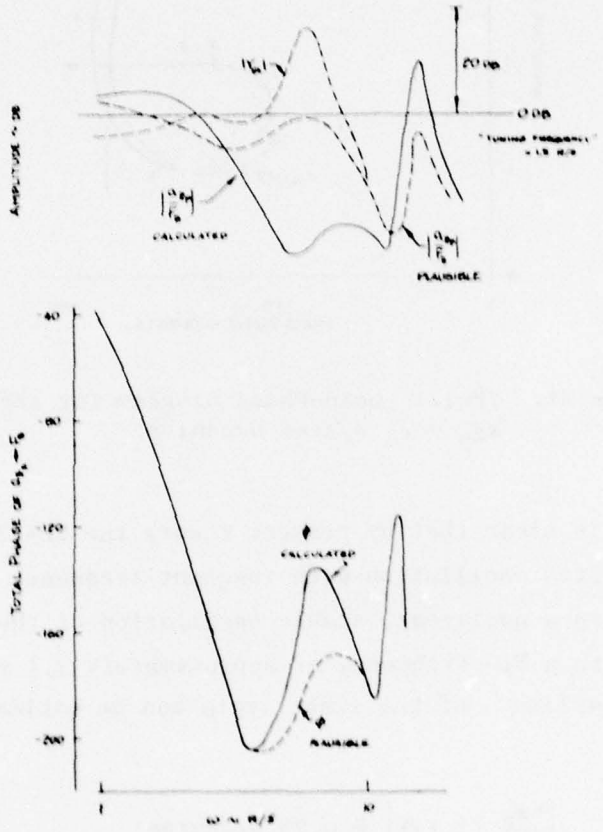

Figure 30. YF-12 $a_{z_p} \rightarrow F_S$ Dynamics; SAS-Off

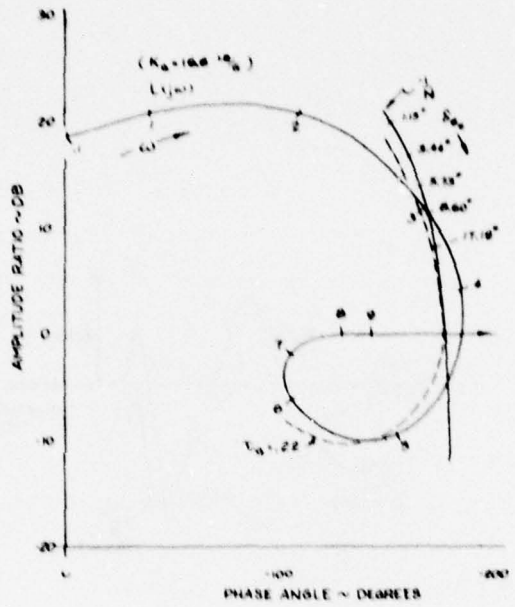

Figure 31. YF-12: Gain-Phase Diagram for the Nonlinear $a_{z_p} \rightarrow F_s$ System Dynamics

Thus, it is clear that by present theory the YF-12 PIO can be initiated as a linear, pitch oscillation with resonant frequency at about 4.5 rad/sec and terminate in a nonlinear, stable oscillation of the normal acceleration closed loop with a PIO frequency of approximately 3.1 rad/sec. At $\omega \cong 3.1$ rad/sec, the amplitude of the limit cycle can be estimated as follows:

$$\left|\frac{a_{z_p}}{\delta_{e_c}}(3.1j)\right| \cong 0.23 \text{ g/degree}$$

$$|\delta_{e_c}| \cong 8.6^\circ \quad \text{(from the } -1/N \text{ plot)}$$

$$|a_{z_p}| \cong 2 \text{ g}$$

Thus, the estimated peak-to-peak oscillations in the terminal limit cycle are 4 g. These predictions of initial frequency, terminal frequency, and PIO amplitude closely match the YF-12 large-amplitude PIO time history published in Reference 20 and reproduced here as Figure 32.

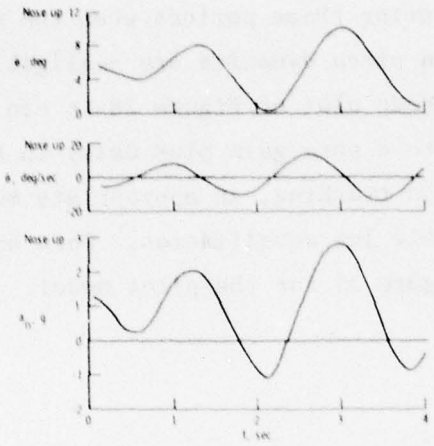

(From Reference 11)

Figure 32. YF-12: Large-Amplitude PIO Time History

The large amplitude PIO can also be initiated by large amplitude, high gain tracking. If, due to turbulence or large amplitude control, the motions become large enough to saturate the SAS then it is clear from Figure 28 that the pitch loop can be destabilized unless the pilot reduces his θ-loop gain by a factor of about 4. If the SAS is saturated then it can be seen from Figure 30 that the $a_{z_p} \rightarrow F_s$ loop is unstable when tuned to any frequency greater than about 3 rad/sec. It is therefore apparent that the large amplitude YF-12 PIO can result from either $a_{z_p} \rightarrow F_s$ loop instability when the $\theta \rightarrow F_s$ loop is driven to resonance with unsaturated SAS, or from $\theta \rightarrow F_s$ loop instability due to SAS saturation with misadapted pilot gain. In either case the terminal state of motion is a stable limit cycle.

The small amplitude YF-12 PIO is more difficult to analyze in a definitive manner. It is not clear from a priori considerations that it is a true PIO as defined in Chapter II.

Figures 33 and 34 are adapted from Reference 11 to show the flight test measured power spectral densities of θ and δ_{e_s} during refueling while the YF-12 is actually connected with the tanker. The implications of these data to human pilot dynamics offer additional understanding of the PIO phenomenon.

If it is assumed that, during those periods when the small amplitude PIO exists, the SAS effects on pitch dynamics are negligible (e.g., if it is saturated), then from the Bode plot of Figure 28 it can be seen that θ/δ_{e_c} is approximately equal to a pure gain plus delay in the region of 2 rad/sec. Thus, for precision tracking, an appropriate model for pilot dynamics might include a sizable lag equalization. Open and closed loop Bode diagrams are shown in Figure 35 for the pilot model

$$Y_p(s) = \frac{K_p e^{-.2s}}{s+1}$$

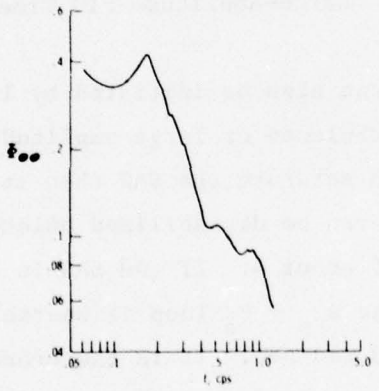

(From Reference 11)

Figure 33. YF-12: PSD of Pitch Attitude During Refueling

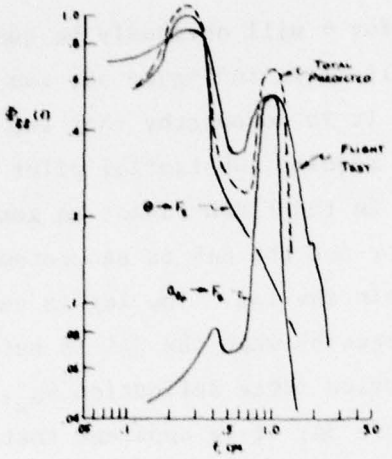

Figure 34. YF-12: PSD of Elevator Stick Deflection; Comparison of Theory and Flight Test Results

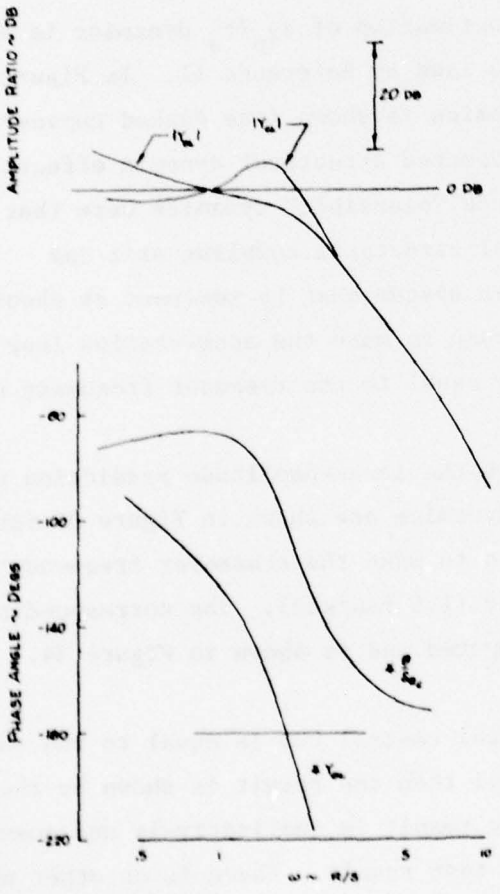

Figure 35. YF-12 Pitch Control Dynamics; Saturated SAS; Lag-Equalized Pilot

The corresponding power spectrum for θ will obviously be qualitatively consistent with the flight test result shown in Figure 33; the calculation for this will not be shown, however. It is noteworthy that the replication of these data by analysis appears to require substantial pilot lag equalization; otherwise, the low frequency peak in the θ PSD cannot be generated. This result is independent of whether or not the SAS is saturated; it is sufficient that the pilot model contain the lag. The lag is easier to justify on empirical grounds (viz., Reference 6) when the SAS is saturated. The corresponding PSD of the pilot's stick force deflection δ_{e_s}, due to pitch attitude control, is shown in Figure 34; it is apparent that the pitch loop closure accounts for the low frequency peak in $\Phi_{\delta\delta}(\omega)$. It does not appear that the $\Phi_{\delta\delta}$ peak at 1 cps can be explained on the basis of pitch control.

It has been noted that the estimation of a_{z_p}/F_s dynamics is not really possible with the information provided by Reference 11. In Figure 30, a sketch of "plausible" a_{z_p}/F_s dynamics is shown (the dashed curves) which are realistic in view of known or suspected structural dynamic effects. The ground rules for selection of these "plausible" dynamics were that

- They produce substantial structural coupling at 1 cps
- The $a_{z_p} \rightarrow F_s$ closed loop system must be resonant at about 1 cps when the pilot's gain is chosen to make the acceleration loop crossover frequency approximately equal to the resonant frequency of the pitch loop
- They are consistent with the large-amplitude prediction of PIO

The closed loop $a_{z_p} \rightarrow F_s$ system dynamics are shown in Figure 30 for the case where the pilot's gain is selected to make the crossover frequency equal to the pitch loop resonance frequency (1.5 rad/sec). The corresponding control deflection power spectrum was computed and is shown in Figure 34.

If we now assume that the total control PSD is equal to the sum of the components due to θ and a_{z_p} control then the result is shown by the dashed curve in Figure 34. Clearly, this result is qualitatively and quantitatively consistent with the flight test result. There is no other method to explain these results that is obvious to this writer. There are two noteworthy features of these postulated θ and a_{z_p} loop dynamics. First, at the

frequency of resonance of the a_{z_p} loop (1 cps) the pitch attitude response is negligible; thus, there is no loop coupling from $a_{z_p} \rightarrow F_s$ to $\omega \rightarrow F_s$. Second, if the pilot's acceleration loop gain were selected to make the crossover frequency equal the a_{z_p} resonance frequency (1 cps) then a closed loop instability could result; this apparently does not happen. We haven't the data to determine why it does not. One possibility, of course, is that the a_{z_p}/F_s dynamics (if these were known in detail) would support a stable closure at 1 cps. This seems implausible. Another possibility is that the amplitude of a_{z_p} resonance at 1 cps is simply too small to permit the pilot to subjectively predict a_{z_p} or is too small to be of overriding concern to him. This possibility cannot be evaluated without a reliable model for structural dynamics.

It is concluded that by present theory the 1 cps oscillation of the YF-12 documented in Reference 11 is, indeed, a PIO by the definition of this report. It is a lightly-damped resonance in acceleration that results from attempts by the pilot to stablize the normal acceleration motions resulting from closed loop dynamics of the pitch loop.

Type II PIO Assessment--YF-12

According to the simplified theory, Type II PIO is not possible in the refueling configuration. The stick-free, dominant mode damping ratio is $\zeta_{sp} = 0.376$ (SAS-off); this is greater than the criterion value of 0.2.

D. CALSPAN PIO IN-FLIGHT SIMULATIONS

Reference 17 documents an in-flight simulation with the variable stability NT-33A of approximately 150 combinations of short-period frequency, damping ratio, and speed. Stick force per g and elevator-to-stick deflection gearing were pilot selected. The purpose of these experiments was, in part, to examine the suitability of the parameter

$$\frac{2\zeta_{sp}\omega_{sp}}{L_\alpha}$$

as a measure of PIO susceptibility. It had been proposed that values of this ratio less than one were a prerequisite for PIO, and that values greater than one would be sufficient to preclude the development of PIO. This criterion originated from the notion that in PIO the pilot is a synchronous controller of pitch attitude (discussed previously in Section II).

Sustained PIO was obtained for only six of the short-period dynamic configurations tested. One of these (flight 583) violated the above criterion. Sustained PIO was defined, in Reference 17, to correspond to a PIO rating (PIOR) of 4 or greater according to the PIOR scale devised (apparently) at McDonnell Aircraft during flight tests of the F-4. This scale is shown in Figure 36. These six configurations are summarized in Table 7.

The theory of this report may be easily applied to these configurations. This analysis will not be shown here since it is similar to those previously shown. The dynamics and feel system characteristics, as simulated, were completely linear. The feel system dynamics were those of a conventional

DESCRIPTION	NUMERICAL RATING
NO TENDENCY FOR PILOT TO INDUCE UNDESIRABLE MOTIONS	1
UNDESIRABLE MOTIONS TEND TO OCCUR WHEN PILOT INITIATES ABRUPT MANEUVERS OR ATTEMPTS TIGHT CONTROL. THESE MOTIONS CAN BE PREVENTED OR ELIMINATED BY PILOT TECHNIQUE	2
UNDESIRABLE MOTIONS EASILY INDUCED WHEN PILOT INITIATES ABRUPT MANEUVERS OR ATTEMPTS TIGHT CONTROL. THESE MOTIONS CAN BE PREVENTED OR ELIMINATED BUT ONLY AT SACRIFICE TO TASK PERFORMANCE OR THROUGH CONSIDERABLE PILOT ATTENTION AND EFFORT	3
OSCILLATIONS TEND TO DEVELOP WHEN PILOT INITIATES ABRUPT MANEUVERS OR ATTEMPTS TIGHT CONTROL. PILOT MUST REDUCE GAIN OR ABANDON TASK TO RECOVER	4
DIVERGENT OSCILLATIONS TEND TO DEVELOP WHEN PILOT INITIATES ABRUPT MANEUVERS OR ATTEMPTS TIGHT CONTROL. PILOT MUST OPEN LOOP BY RELEASING OR FREEZING THE STICK	5
DISTURBANCE OR NORMAL PILOT CONTROL MAY CAUSE DIVERGENT OSCILLATION. PILOT MUST OPEN CONTROL LOOP BY RELEASING OR FREEZING THE STICK	6

Figure 36. The PIO Rating Scale

TABLE 7. CALSPAN PIO CONFIGURATIONS

Flt	U_o (IAS) (kts)	Pilot	ω_{sp}	ζ_{sp}	$\frac{1}{T_{\theta_2}}$ (L_α)	$\frac{2\zeta_{sp}\omega_{sp}}{L_\alpha}$	$\frac{F_s}{n_z}$	POR	PIOR
583	365	AF	8.98	.66	3.04	3.90	4.86	3	4
595	365	CAL	3.72	.24	3.08	.58	--	9	4.5
596	300	CAL	6.08	.13	1.78	.89	15.8	8	5
601	365	CAL	2.16	.44	3.07	.62	16.2	9	4.5
605	365	AF	3.72	.19	3.07	.46	4.15	7.5	4.0
610	365	AF	5.47	.05	2.88	.18	8.12	8.5	4.0

(From Reference 17)

spring-mass-damper system. Unfortunately, Reference 17 does not document a_{z_p}/δ_e; it was estimated as follows:

$$\frac{a_{z_p}}{\delta_e}(s) = \frac{K(s^2 + 2\zeta_Z\omega_Z s + \omega_Z^2)}{\Delta_{sp}(s)}$$

$$\omega_Z^2 \cong \frac{2U_o}{\ell_x}\frac{1}{T_{\theta_2}}$$

$$2\zeta_Z\omega_Z \cong \frac{1}{T_{\theta_2}}$$

For the six configurations, above, ω_Z was sufficiently greater than ω_{sp} that any errors in the approximation of ω_Z or ζ_Z will not significantly affect the following results.

Type I PIO

An appropriate pilot model for each of the six configurations was selected for the $\theta \rightarrow F_s$ loop. From these, estimates of the pitch loop resonance frequencies ω_R were made and the phase criterion checked for the $a_{z_p} \rightarrow F_s$ loop to ascertain PIO susceptibility. The results are shown in Table 8. Two values of ω_R are shown for each case corresponding to a nominal choice of pilot dynamic equalization for optimized tracking and for an unequalized pilot (gain plus time delay)--$\omega_{R_{NOM}}$ and ω_{R_o}, respectively.

TABLE 8. ESTIMATED PIO PARAMETERS FOR CALSPAN CONFIGURATIONS; TYPE I PIO

FLT	Pilot Equalization	$\omega_{R_{NOM}}$	ω_{R_o}	$\phi(j\omega_{R_{NOM}})$	$\phi(j\omega_{R_o})$	PIOR	PIOR Justified?
583	small lag	4	7.3	-110	-210	4	Yes
595	small lead	4.1	3.8	-186	-176	4.5	Yes
596	moderate lag	4.5	5.0	-100	-120	5	NO
601	large lead	4.2	2.3	-226	-141	4.5	Yes
605	large lead	3.9	3.8	-170	-156	4	Yes
610	lag-lead	4	5.5	-81	-214	4	Yes

It is concluded from these data that five of the six PIO configurations satisfy the Type I PIO phase criterion of present theory. Present theory suggests that the configuration of flight 596 is not prone to the development of PIO as the result of closed loop tracking of pitch attitude.

Reference 17 notes the apparent contradiction between the Cooper-Harper POR and the PIOR obtained for flight 583. For this configuration the ratio $2\zeta_{sp}\omega_{sp}/L_\alpha$ is greater than one and the Cooper-Harper rating of pitch dynamics was Level 1 (POR = 3). Even so, the PIOR rating obtained was indicative of a definite tendency to develop PIO. The pilot's inexperience with the rating scales and with the flight test procedure was cited as a probable reason for this discrepancy.

According to the present PIO theory there is no reason to believe that the PIOR/POR results for flight 583 are necessarily contradictory. If the pilot rated only his ability to control pitch attitude in the simulated IFR tracking task described in Reference 17, then a Cooper-Harper rating of 3 might be reasonable (although there is no way to be certain); if the pilot rated PIO tendencies strictly according to the PIOR scale then, following abrupt control inputs with tight attitude control, present theory indicates

that unstable or nearly unstable oscillations of the $a_{z_p} \rightarrow F_s$ loop can develop. This result emphasizes how inadequate our understanding of the basis for pilot rating really is; it suggests that great care must be taken in assessing pilot rating data when more than one cue or mode of control may exist.

No check was made of the amplitude criterion $|a_{z_p}/\dot{\theta}(j\omega_{PIO})| \geq 0.012$ since errors in estimation of the acceleration transfer function could invalidate the result. Future investigators are encouraged to publish all their data in future experiments of these sort.

Type II PIO

The susceptibility of the six PIO configurations to the open loop initiation of PIO was tested using the simplified criterion based on dominant mode damping ratio; viz., if $\zeta_{sp} \leq 0.2$, then the configuration is sufficiently resonant at frequency ω_{sp} to initiate a_{z_p} tracking. If, further, $\phi(j\omega_{sp}) \leq -180°$ then the configuration is susceptible to Type II PIO. The results are summarized in Table 9. Note that for these experiments the stick-free and stick-fixed dynamics were the same for the frequency range of interest here.

It is apparent that the poor PIOR obtained for flight 596 could have resulted from the pilot attempting to track oscillations of a_{z_p} at frequency ω_{sp} following control or atmospheric inputs sufficient to excite the short-period dynamics. When closed at this frequency, the $a_{z_p} \rightarrow F_s$ loop is unstable. It is seen that flight 610 is also prone to Type II PIO.

TABLE 9. TYPE II PIO SUSCEPTIBILITY EVALUATION OF CALSPAN CONFIGURATIONS

Flt	ω_{sp}	ζ_{sp}	$\zeta_{sp} \leq .2$?	$\phi(j\omega_{sp})$	PIOR	Potential for Type II PIO
583	8.98	.66	No	n.a.	4	Not possible
595	3.72	.24	No	-158	4.5	Not likely
596	6.08	.13	Yes	-200	5	Possible
601	2.16	.44	No	n.a.	4.5	Not possible
605	3.72	.19	Yes	-148	4	Not likely
610	5.47	.05	Yes	-253	4	Possible

Summary

The data provided by Reference 17 appear to support the present PIO theory. These same data do not appear to validate $2\zeta_{sp}\omega_{sp}/L_{\alpha}$ (or its more recent variations) as a reliable metric for the prediction or assessment of PIO. To this author, it is clear that this parameter is an indication of pitch handling qualities but, according to theory of this report, this is merely a necessary consideration for PIO assessment--not a sufficient one.

What these data do clearly illustrate is how carefully we should treat Cooper-Harper or PIOR scale data to avoid misconstruing the messages they may provide due to our lack of a unified understanding of the handling qualities problem of longitudinal mode control.

These data appear to support the simplified criterion $\zeta_R \leq 0.2$ as an indication of Type II PIO susceptibility.

E. A-7A (M = 1.1, h = 15,000 ft)

The A-7 series of aircraft have no history of longitudinal PIO problems. It is of interest to test this airplane against the PIO theory to ascertain why PIO is not a problem (at least at this one flight condition).

The flight condition selected for study is not one that is typical of A-7 operations. It was chosen because the corresponding airframe dynamics are similar to those for the T-38A. This flight condition could be reached as the result of a supersonic dive from high altitude.

With no stability augmentation the required airframe dynamics are (from Reference 18):

$$\frac{\theta}{\delta_e}(s) = \frac{-44.3(s + 2.02)}{s[s^2 + 2(.185)(8.81)s + 8.81^2]} \quad \text{rad/rad}$$

$$\frac{a_{z_p}}{\delta_e}(s) = \frac{222.7[s^2 + 2(.072)(21.6)s + 21.6^2]}{[s^2 + 2(.185)(8.81)s + 8.81^2]} \quad \text{ft/sec}^2\text{/rad}$$

(it is assumed that ℓ_x = 10 ft).

The pitch dynamics are shown on the Bode plot of Figure 37; these are approximately equal to a pure gain in the region of probable crossover frequency. A reasonable mode for pilot dynamics for pitch tracking would be

$$Y_p(s) = \frac{K_p}{1.0s + 1} \; e^{-.2s} = \frac{F_s}{\theta_e}(s)$$

The open-loop, pilot-airplane dynamics are shown in Figure 37 for the case where no control or feel system dynamics exist. The open-loop phase is also shown for the unequalized pilot. Without further discussion, it is clear

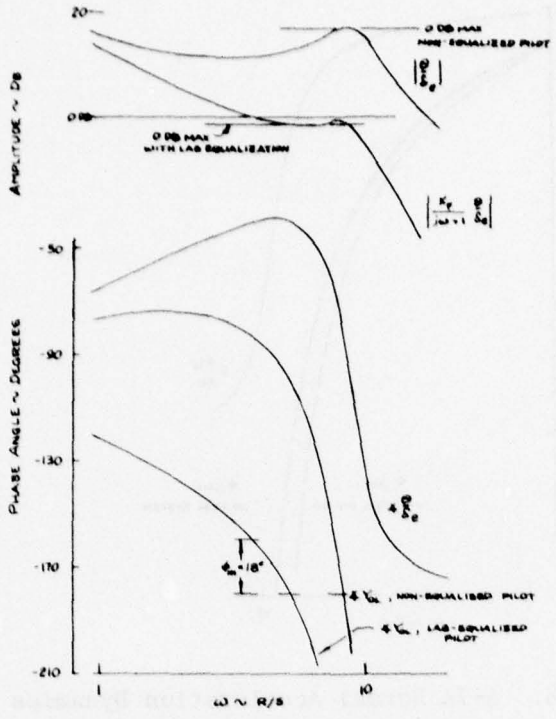

Figure 37. A-7A Pitch Attitude Dynamics

that the closed-loop pitch dynamics can become resonant at ω_R = 4-5.3 rad/sec with the given pilot dynamics. From the $a_{z_p} \rightarrow \delta_e$ dynamics (Figure 38) it is clear that PIO cannot develop over this range of frequencies, in the absence of control and feel system dynamics.

If the pilot decreases the level of lag equalization at a constant static gain, then the resonant frequency can become greater than 5.3 rad/sec. For the unequalized pilot, the resonant frequency for pitch oscillations must become greater than about 8 rad/sec (from Figure 38) in order for a PIO to develop.

Resonances in pitch due to abrupt control or large aerodynamic input can occur at the short-period frequency ω_{sp} = 8.81. Since ζ_{sp} = 0.185 is <0.2 it appears that these short-period responses would be subjectively predictable (according to the simplified Type II PIO criterion). From Figure 38 we see that the acceleration loop dynamics would be unstable if tuned to a crossover frequency of 8.81 rad/sec. Also,

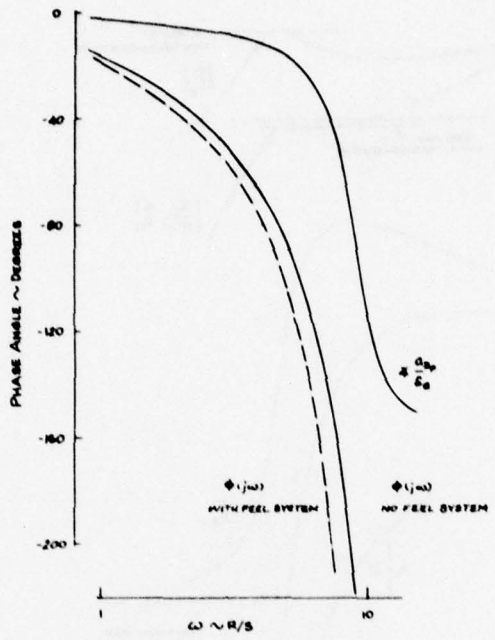

Figure 38. A-7A Normal Acceleration Dynamics

$$\left|\frac{a_{zp}}{\dot{\theta}}(8.81j)\right| = 0.14 > 0.012 \text{ g/degree/sec}$$

Therefore, conclude that the A-7, <u>with no control or feel system dynamics</u>, is PIO-prone at this flight condition.

However, the A-7 does have significant control and feel system dynamics--even without stability augmentation. The airplane has two bobweights which respond to $\ddot{\theta}$ and a_z to create equivalent stick forces; the stick-free dynamics are therefore substantially different from the stick-fixed dynamics. Figure 39 illustrates the first-approximation system schematic. The system parameters were supplied to this author by Vought Aircraft. When all four feedback loops are closed, the resulting stick-free dynamics at this flight condition become (using the short-hand notion):

$$\frac{\theta}{F_s}(s) = \frac{-69.6(2.02)}{(0)[.207,7.28][.448,32.4]} \qquad \text{rad/lb}$$

$$\frac{a_{z_p}}{F_s}(s) = \frac{350[.072,21.6]}{[.207,7.28][.448,32.4]} \qquad \text{ft/sec}^2\text{/lb}$$

The analysis of pilot-vehicle system dynamics will not be repeated; it is seen that the bobweight feedbacks have the principal effects of increasing the short-period damping ratio and decreasing the natural frequency. Since $\zeta_R > 0.2$, and since $\phi(7.28j)$ is very nearly equal to -180 degrees, it appears that the probability for PIO initiation is significantly reduced when account is taken of the feel and control system dynamics.

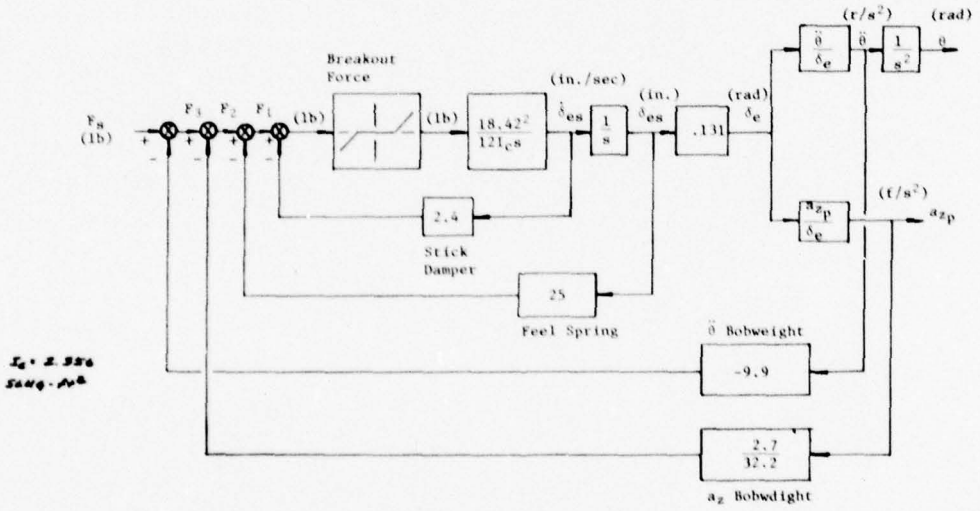

Figure 39. A-7A Feel and Control System Schematic Description

The facts that the stick-free short-period damping ratio ζ_{sp} is 0.207, and no PIO problems exist, are taken to be further support for the subjective predictability criterion $\zeta_R \leq 0.2$.

One final point is worth noting about the bobweight effects on the A-7 dynamics. Since control system friction is unavoidable, then for small amplitude motions the pilot actually flys the stick-fixed dynamics. If the motion become large enough to excite the bobweights, then the airplane dynamics are those of the stick-free responses. This change in airplane dynamics can suddenly occur. Since the stick-free, short-period natural frequency is less than the stick-fixed value, then the sudden change in aircraft dynamics is actually stabilizing in the sense that, with constant pilot gain, the closed-loop system becomes more stable when the bobweight feedbacks are initiated following small amplitude motion tracking. This effect is exactly opposite that previously seen in the T-38A example with the original control system. It is proposed that this mechanism provides a reasonable theoretical basis to support the empirically derived criterion of Neal (Reference 22) for the optimized design of bobweights.

SECTION VII

THE IDENTIFICATION OF PIO IN FLIGHT TEST OR SIMULATION

A. GROUND-BASED SIMULATION

According to the theory of this report, longitudinal, short-period PIO cannot exist in a fixed-base simulation; the normal acceleration cue is essential to the mechanics of PIO. The sorts of pilot-vehicle system oscillations that occur in fixed-base simulations of pitch tracking, for example, and which have been called PIO in past work, have been purposely excluded from the PIO classification by the definition proposed in this report. The reasons for doing this have been previously discussed.

However, the use of fixed-base simulation and the PIO theory may enable the early diagnosis of PIO. This would require that pitch attitude tracking experiments be devised in a manner to excite the extremes of piloting behavior; if it can be determined by measurement that closed-loop resonances can occur, then an analytical check of the acceleration loop phase criterion

$$\phi(j\omega_R) \leq -180^\circ$$

at each resonant frequency may be sufficient to ascertain whether or not PIO would be obtained in flight. These results from a combination of fixed-base simulation and from analysis could also be used for the preparation of specifications for the motion drive system of a moving-base simulation. This might permit the use of a moving-base simulator to verify the PIO tendencies of an aircraft configuration during its development and prior to its flight.

A moving-base simulator can only approximate the dynamics of flight. The chief limitation is the allowable range of cockpit travel. The usual method for limiting the travel is to introduce acceleration washout in the motion drive system software interface between the computed aircraft acceleration and the servos and actuators that physically move the cockpit. Thus, the acceleration dynamics become:

$$\left[\frac{a_{zp}}{F_s}(s)\right]_{simulated} = \left[\frac{a_{zp}}{F_s}(s)\right]_{airplane} \times W(s)$$

W(s) = washout dynamics

The typical washout system will therefore add a phase lead to the pilot-felt acceleration dynamics that would not actually exist in flight. According to the theory of this report, this could eliminate the possibility for finding PIO in a moving base simulator (assuming that it existed in actual flight) if, with no washout

$$\phi(j\omega_{PIO}) < -180°$$

and if, with washout

$$\phi(j\omega_{PIO}) + W(j\omega_{PIO}) > -180°$$

Consider the YF-17 example previously discussed. PIO was not diagnosed as a potential problem with that aircraft based upon moving-base simulation of the approach and landing problem; yet the in-flight simulation of the airplane resulted in serious PIO. It has been suggested elsewhere that lack of resolution of the visual system presentation in the near-flare condition might have invalidated Northrop's landing simulation of the YF-17. This is conceivable. It is also conceivable that the "pucker factor" was not sufficient to make the simulator pilot excite PIO. It is the opinion of this author, however, that the real problem was likely to have been with the motion drive system.

Sinacori (Reference 23) describes the motion drive logic in use at Northrop at the time of the YF-17 simulation; he also lists the motion drive system parameters appropriate for the YF-17. If it is assumed that these are representative of those actually used for the YF-17 approach and landing simulation, then the normal acceleration washout dynamics were, to a first approximation,

$$W(s) = \frac{.15s^2}{s^2 + 2(.7)(1)s + 1}$$

The effect of these dynamics on the total phase angle of the $a_{z_p} \rightarrow F_s$ loop is illustrated in Figure 40. The total system phase angle ϕ is defined as in the previous YF-17 analysis (Figure 10); it is assumed that $\tau_a = 0.25$. Figure 40 clearly indicates two points of note:

- The acceleration washout makes the simulated YF-17 acceleration control loop significantly more stable than is the (estimated) actual YF-17 in the region of probable PIO frequencies. For $\omega \leq 3$, in fact, the simulated YF-17 with the original control system is not qualitatively different from the YF-17 with the modified control system.

- Allowing for uncertainties in estimates of YF-17 dynamics and for the actual motion drive dynamics employed, it appears that PIO may not have been possible to produce in the moving base simulator--regardless of "pucker factor" or of the fidelity of the visual system--since $\phi(3j)$ is slightly greater than -180° with washout.

An additional fidelity problem could have been created due to the use of amplitude scaling in the motion drive system:

$$\left|a_{z_p}/\dot{\theta}(3.0j)\right|_{airplane} = 0.031$$

$$|W(3.0j)| = 0.149$$

$$\left|a_{z_p}/\dot{\theta}(3.0j)\right|_{simulated} = 0.031 \times 0.149 = 0.0046 \text{ g/degrees/sec}$$

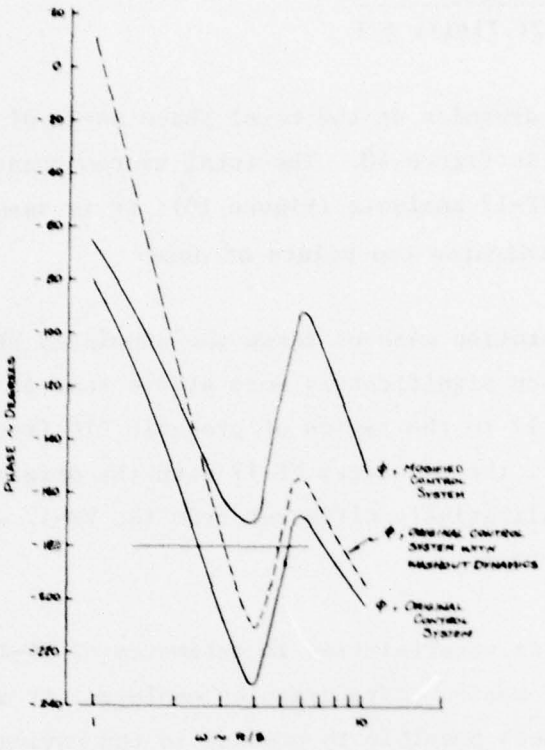

Figure 40. Effect of Motion Drive System Washout on Simulated YF-17 $a_{z_p} \rightarrow F_s$ Dynamics

This response ratio is less than the criterion value (.012) proposed for subjective predictability of normal acceleration responses.

In view of the practical constraints on simulation, it is problematical whether a PIO problem can be discovered in a simulator by an empirical, trial and error approach. The use of simulation, exclusively, as a means for assessing the PIO tendencies of an aircraft-control system design is a very risky approach to aircraft design and development.

B. IN-FLIGHT SIMULATION

The use of a variable stability airplane for the discovery or assessment of PIO may be an attractive alternative to moving base simulation. It is not a panacea, however.

It is, in general, impossible to simulate the PIO characteristics of a specific airplane without the use of direct lift control (DLC) in a variable stability aircraft. The use of DLC permits the natural dynamics of the variable stability airplane to be decoupled in pitch and heave and, therefore, to be independently controlled.

This was a potential error in the simulated YF-17 flight tests with the NT-33A conducted prior to the prototype's first flight (Reference 8). The NT-33A does not have a DLC system. In order to match the θ/δ_e dynamics of the YF-17 in approach and landing it was necessary to select the approach airspeed to give the correct L_α (or $1/T_{\theta_2}$); this could only be done to a first approximation. The parameters ω_{sp} and ζ_{sp} were matched using response feedback. Since the normal acceleration dynamics are unknown for the actual YF-17 and can only be estimated for the YF-17 as simulated by the NT-33A, it is not possible to completely evaluate the degree to which errors in simulation of a_{z_p} responses influenced the assessment of the YF-17 handling qualities. It is instructive to consider what these might have been; consider the following:

1. For the NT-33A in the approach and landing configuration selected to match the YF-17 dynamics,

   $U_o = 140$ kt $= 236$ ft/sec

   $1/T_{\theta_2} = 0.9$

   It can be determined from Reference 25 that for this condition:

   $\ell_x = 7.39$ ft

   $M_{\delta_e} = -4.49$ $1/sec^2$

   $Z_{\delta_e} = -15.34$ ft/sec^2

$M_q = -.482$ 1/sec

$M_{\dot{\alpha}} = -.216$ 1/sec

$M_\alpha = -2.84$ 1/sec^2

$Z_\alpha = -229.4$ ft/sec^2

2. Assume that response feedback techniques, only, were used in the YF-17 simulation of Reference 8 (i.e., model-following, or similar techniques, are assumed not to have been used). It follows that the numerators $N^{\theta}_{\delta_e}(s)$, $N^{a_z}_{\delta_e}(s)$ and $N^{a_{z_p}}_{\delta_e}(s)$ for the simulated YF-17 dynamics were the same as those for the basic NT-33A. It is noted that this is, in general, not true when a DLC system is used.

3. For a rigid airframe $a_{z_p} = a_z - \ell_x \ddot{\theta}$. It follows by direct synthesis that for the YF-17, as simulated by the NT-33A:

$$\boxed{\frac{a_{z_p}}{\delta_e}(s) = \frac{17.84[.072, 7.44]}{[.89, 1.98]}} \qquad (1)$$

4. For the actual YF-17 in the approach and landing configuration,

$\ell_x \cong 15.7$ ft

$U_o = 118$ kt $= 199$ ft/sec

$1/T_{\theta_2} = 0.68$

The control effectiveness derivatives are unknown. Assume those for the F-5 in a similar flight condition are reasonable approximations (errors in these will only affect the acceleration gain).

$M_{\delta_e} = -5.31$ 1/sec^2

$Z_{\delta_e} = -26.9$ ft/sec^2

5. Assume that for the YF-17

$$N^{a_{z_p}}_{\delta_e}(s) = (Z_{\delta_e} - \ell_x M_{\delta_e})\left[s^2 + \frac{1}{T_{\theta_2}}s + \frac{2U_o}{\ell_x}\frac{1}{T_{\theta_2}}\right] \qquad (2)$$

It has been this author's experience that this approximation is often accurate when $\frac{M_{\delta_e}}{Z_{\delta_e}}$ is not >>10. Note, also, that equation (2) is an excellent approximation to the numerator of the NT-33A transfer function (1). It should be noted that if the YF-17 flight control system, in landing approach uses flaps as an active control, then equation (2) is invalid.

6. Using the approximation for the acceleration transfer function numerator the estimated, actual YF-17 transfer function is:

$$\boxed{\frac{a_{z_p}}{\delta_e}(s) = \frac{56.6\ [.080, 5.04]}{[.89, 1.98]}} \qquad (3)$$

Unfortunately, there is no way to verify this result without more data.

It is apparent that if equation (2) is a valid approximation for the YF-17 then a comparison of equations (1) and (3) indicates that the NT-33A simulation of the YF-17 was possibly in error on two counts. First, the magnitude of static response was about 50 percent lower in the simulation than actual. Second, the error in ω_z simulation produced more phase lag in the simulated a_{z_p} response transfer than would actually exist in the YF-17. The numerators of transfer functions (1) and (3) are compared on the Bode plot of Figure 41. This comparison suggests that in the vicinity of probable PIO frequency the NT-33A simulation of the YF-17 may have been slightly more PIO-prone than the actual YF-17. However, the analysis of Section VI also concludes that the YF-17 with the original control system was PIO-prone--therefore substantiating Calspan's major conclusion.

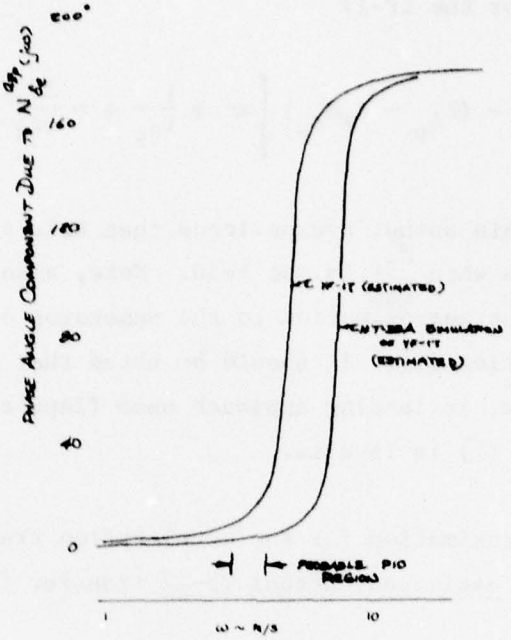

Figure 41. Phase Angle Comparison of $N_{\delta_e}^{a_{z_p}}(j\omega)$ for the YF-17 In-Flight Simulation

C. FLIGHT TEST

PIO problems with new aircraft designs often first occur in the latter stages of flight test or after the aircraft has been delivered to the operational community. This may be due to the use of flight test techniques which emphasize MIL-F-8785B compliance and the determination of the traditional measures of airplane stability and control (e.g., short-period frequency and damping ratio, stick force per g, stick deflection for trim, etc.). When tests are performed which emphasize tracking (e.g., weapons delivery, air-to-air gunnery, refueling, etc.) then PIO may appear if it is, indeed, a latent problem. It would be preferable to conduct baseline tracking tests (e.g., as proposed in Reference 24) during the initial stages of flight testing to enable an early diagnosis of PIO. Revised flight test procedures and the theory of this report should permit the rapid detection and elimination of PIO problems.

A very real problem that can arise in flight testing is to determine whether a control problem should be called a PIO or a pitch sensitivity problem. This question might appear to be in the same league with determining how many angels can stand on the head of a pin. It is not. If the balance between the pitch and heave degrees of freedom is understood, then the opportunities are increased for eliminating the control problem. In an era of multimode flight control systems, CCV, and direct force control, this is a very real benefit to the process of flight control system design.

Once an aircraft reaches the flight test stage of development, PIO may be difficult and expensive to eliminate. The normal acceleration dynamics a_{z_p}/δ_e are dominated by L_α and are therefore beyond control at that point. The elimination of PIO, once it is known to exist, should probably be done by

1. Reducing control system phase lags.

2. Minimizing abrupt changes in stick-free dynamics due to control nonlinearities or SAS saturation.

3. Improving pitch attitude handling qualities.

4. In extreme cases, adding a new dynamic element to the flight control system to attenuate pitch attitude responses.

Control stick dampers have been used without (apparently) great success as past "cures" for PIO tendencies; the documentation of these trials is poor. It has been suggested in past work that the use of dampers is to be discouraged. On the basis of this report, this author is not greatly enthusiastic about a stick damper, either. However, there may be cases where a damper can be successfully used. An example might be when a PIO results due to very small ζ_{sp}. A damper configuration which decouples the feel system dynamics might be used to attenuate the short-period response. This would be at the expense of increased stick forces.

The use of linear prefilters to heavily attenuate the pilot's (electrical) output should be discouraged as a means of preventing the transmission of large, inadvertent commands to surface actuators in a fly-by-wire system. The control system phase lags may lead to serious control problems which can escape diagnosis in fixed- and moving-base simulation. A better technique might be to use a nonlinear filtering logic which only attenuates the amplitudes of large, high-frequency signals without increasing the control system phase lags within the bandwidth of the closed loop pitch control loop.

SECTION VIII

DISCUSSION AND CONCLUSIONS

A PIO theory has been presented that is believed to be consistent with most opinions found in the literature or expressed privately about the problem. The theory appears to unify divergent viewpoints regarding the significance to PIO of airframe dynamics, feel and control dynamics, task, system nonlinearities, and motion vs visual cues. A number of PIO case histories are presented which appear to confirm the theory.

It is postulated that if in the control of pitch attitude, the pilot-vehicle system dynamics are sufficiently resonant, and if the pilot-felt normal acceleration closed-loop would be unstable when the loop gain is adjusted to make the crossover frequency equal to the resonant frequency of the pitch loop, then the airframe-control system dynamics are PIO-prone. A PIO initiated as the result of pitch attitude tracking is defined as a Type I PIO.

Aircraft configurations that feature a very lightly damped stick-fixed or stick-free dominant mode are postulated to be susceptible to the initiation of PIO following abrupt control or atmospheric disturbance inputs of magnitude sufficient to excite the dominant mode. A PIO initiated as the result of open-loop control or external inputs is defined as a Type II PIO. It is proposed that a configuration is susceptible to Type II PIO when the dominant mode damping ratio is less than 0.2.

The major difficulty in applying this theory is to determine whether the pitch loop dynamics can become sufficiently resonant as the result of precision, piloted control in tracking modes. The state of the art of pilot-vehicle system dynamics cannot entirely resolve this matter. It is, however, possible to select models for pilot dynamics and perform a closed loop analysis to bound the range of frequencies over which closed loop resonances could occur. If the acceleration loop is unstable when closed at any of these frequencies, then PIO is a possibility. This, however, may be overly conservative for design purposes. Validity probably must be

determined on a case-by-case basis. Any physical dynamic system can be driven to resonance given sufficient gain, for example; what must be assessed in a design or test is the probability that such resonances will occur in actual operational usage of the airplane. This is an engineering problem that is probably best addressed from an integrated viewpoint blending ground-based and in-flight simulation, with analysis used as a forecasting tool.

It is noteworthy, however, that subtle errors in the design of flight control systems have not been responsible for those PIO cases that have been documented. These have resulted from deficiencies that could, within the present state of the art, now be eliminated with the application of elementary pilot-vehicle system dynamic theory. A principal source of PIO has been the influence of artificial feel system dynamics and feel nonlinearities (especially friction) on the dynamic response of the airplane to pilot-applied stick force. It appears that pitch handling qualities will be poor, almost regardless of stick-fixed dynamics, when feel system nonlinearities make the stick-free dynamics sensitive to amplitude of the motion such that the maximum pilot gain required for closed loop stability is less at large than at small amplitudes. Problems of this sort have most often been due to the use of bobweights in past designs. The saturation of a rate- or position-limited SAS can produce the same effect.

Based upon the success of this theory it appears that the pilot's principal output is stick force rather than deflection. This suggests two corollaries:

1. Stick force (static and dynamic) should not become "too small."
2. Feel and control system dynamics should not result in stick deflection leading stick force. If that were to happen then the pilot's internal mechanisms for sensing and controlling force output would become unbalanced.

It is conceivable that with small stick force levels (item 1) or with lead-producing feel system dynamics (item 2) additional pilot lag is produced as

a result of neuromuscular system dynamics. If so, the effect would be to promote instabilities or closed loop resonance in the precision control of pitch attitude. A PIO can then result when the acceleration loop is unstable at the resonant frequency.

The importance of feel and control system dynamics to the PIO problem is central and cannot be overemphasized. The present theory, however, can provide no support for the notion that stick force per g is a PIO parameter, per se. As a general conclusion, PIO tendencies can be minimized by minimizing flight control system phase lags in the principal region of manual control interest (nominally $1 < \omega < 10$ rad/sec).

A major conclusion of this report is that the potential for PIO can be predicted entirely on the basis of linear systems analysis. The basic philosophy is easily stated: there can be no unwanted, large amplitude oscillations so long as the small amplitude motions are stable. The prediction of fully-developed PIO frequency and amplitude does, however, require full consideration of all major system nonlinearities; even here, the use of simple quasi-linear sinusoidal describing function analysis appears to be very successful as a diagnostic tool.

Appendix

NORMAL ACCELERATION DYNAMICS

$$a_{z_p} = a_z - \ell_x \ddot{\theta}$$

$$a_z = \dot{w} - U_o q$$

$$N_{\delta_e}^{a_z}(s) = sN_{\delta_e}^{w}(s) - U_o N_{\delta_e}^{q}(s)$$

$$N_{\delta_e}^{a_z}(s) = Z_{\delta_e}\left[s^2 - (M_q+M_{\dot{\alpha}})s - \left(M_\alpha - \frac{M_{\delta_e}}{Z_{\delta_e}} Z_\alpha\right)\right]$$

$$\ell_x N_{\delta_e}^{\ddot{\theta}}(s) = s\ell_x N_{\delta_e}^{q}(s) = s\ell_x(M_{\delta_e}+Z_{\delta_e}M_{\dot{w}})\left[s + \frac{Z_{\delta_e}M_w - Z_w M_{\delta_e}}{M_{\delta_e}+Z_{\delta_e}M_{\dot{w}}}\right]$$

$$N_{\delta_e}^{a_{z_p}}(s) = \left[Z_{\delta_e} - \ell_x(M_{\delta_e}+Z_{\delta_e}M_{\dot{w}})\right]s^2 + \left[-Z_{\delta_e}(M_q+M_{\dot{\alpha}}) - \ell_x(Z_{\delta_e}M_w - Z_w M_{\delta_e})\right]s$$
$$-Z_{\delta_e}\left(M_\alpha - \frac{M_{\delta_e}}{Z_{\delta_e}} Z_\alpha\right)$$

$$N_{\delta_e}^{a_{z_p}}(s) = \left[Z_{\delta_e} - \ell_x(M_{\delta_e}+Z_{\delta_e}M_{\dot{w}})\right]\left\{s^2 - \frac{Z_{\delta_e}(M_q+M_{\dot{\alpha}}) + \ell_x(Z_{\delta_e}M_w - Z_w M_{\delta_e})}{Z_{\delta_e} - \ell_x(M_{\delta_e}+Z_{\delta_e}M_{\dot{w}})}\, s\right.$$
$$\left. - \frac{Z_{\delta_e}\left(M_\alpha - \frac{M_{\delta_e}}{Z_{\delta_e}} Z_\alpha\right)}{Z_{\delta_e} - \ell_x(M_{\delta_e}+Z_{\delta_e}M_{\dot{w}})}\right\}$$

This expression is complete and assumes only that the short-period approximations are valid. In generic form

$$N_{\delta_e}^{a_{z_p}}(s) = K_Z(s^2 + 2\zeta_Z\omega_Z s + \omega_Z^2)$$

However,

$$\frac{1}{T_{\theta_2}} = - Z_w + M_w \frac{Z_{\delta_e}}{M_{\delta_e}}$$

Then

$$\omega_Z^2 = \frac{-U_o M_{\delta_e} \frac{1}{T_{\theta_2}}}{K_Z}$$

It often happens that $\ell_x M_{\delta_e}/Z_{\delta_e} \cong 2$; assume this to be true. Assume also that $|M_{\delta_e}| >> |Z_{\delta_e} M_{\dot{w}}|$; then

$$\boxed{\omega_Z^2 \cong \frac{2U_o}{\ell_x} \frac{1}{T_{\theta_2}}}$$

Since, to a good approximation,

$$2\zeta_{sp}\omega_{sp} = - Z_w - (M_q + M_{\dot{\alpha}})$$

it follows that

$$2\zeta_Z\omega_Z \cong \frac{-Z_{\delta_e}}{K_Z}\left[-2\zeta_{sp}\omega_{sp} + \frac{1}{T_{\theta_2}}\left(\frac{\ell_x M_{\delta_e}}{Z_{\delta_e}} + 1\right)\right]$$

or

$$\boxed{2\zeta_Z\omega_Z \cong \frac{1}{T_{\theta_2}}}$$

It is clear that ζ_Z is always very small. Typically, ω_Z is a factor of about 2-5 times greater than ω_{sp}. The phase differences between $a_z(t)$ and $a_{z_p}(t)$ will therefore be significant at frequencies greater than ω_{sp}. At flight conditions where ω_{sp} is less than, or approximately equal to, the crossover frequency of the pilot-aircraft system, the distinction between a_z and a_{z_p} as piloting cues becomes of potential significance. Note that so long as $\zeta_Z > 0$, $a_{z_p}(t)$ always leads $a_z(t)$ due to the $\ddot{\theta}$ component of a_{z_p}.

The response ratio $\dot{\theta}/a_{z_p}$ is of probable importance to longitudinal handling qualities. Using the above approximations, this ratio can be written as

$$\frac{\dot{\theta}}{a_{z_p}}(s) \cong \frac{-2}{\ell_x} \frac{s + \frac{1}{T_{\theta_2}}}{s^2 + \frac{1}{T_{\theta_2}} s + \frac{2U_o}{\ell_x} \frac{1}{T_{\theta_2}}}$$

Thus, for fixed ℓ_x and at a constant speed the ratio of attitude rate (or attitude) to the pilot's normal acceleration is entirely parameterized by $1/T_{\theta_2}$.

In cases where $\ell_x M_{\delta_e}/Z_{\delta_e} = 2$ is not a good approximation,

$$\omega_z^2 = \frac{Z_{\delta_e}\left(M_\alpha - \frac{M_{\delta_e}}{Z_{\delta_e}} Z_\alpha\right)}{Z_{\delta_e} - \ell_x(M_{\delta_e} + Z_{\delta_e} M_{\dot{w}})}$$

should be used.

BIBLIOGRAPHY

B1. Anonymous. "Aircraft Stores Compatibility Symposium Proceedings, Stability and Control Session," Vol. III, September 19-21, 1969, Eglin Air Force Base, AD 868 609.

B2. Abzug, Malcom J. "High-Speed Stability and Control Problems as They Affect Flight Testing," AGARD Report 120, May 1957.

B3. Abzug, M. J. "High Speed Stability and Control Problems," AGARD Flight Test Manual, Vol. II, Chapter 9, Douglas Aircraft Co., Inc., 1969.

B4. Abzug, M. J. and H. B. Dietrick. "Interim Report on Elimination of Pilot-Induced Longitudinal Oscillations from the Douglas Model A4D-2 Airplane," Report No. ES26613, Douglas, 20 March 1957.

B5. A'Harrah, Ralph C. "Low-Altitude, High-Speed Handling and Riding Qualities," NATO, AGARD Report 443, April 1963.

B6. A'Harrah, R. C. "Low-Altitude, High-Speed Handling and Riding Qualities," J. of Aircraft, Vol. 1, 1964, pp. 32-40.

B7. A'Harrah, Ralph C. "Reply by Author to I. L. Ashkenas," J. of Aircraft, July-August 1964, pp. 223-224.

B8. A'Harrah, R. C. and R. F. Siewert. "Pilot-Induced Instability," AGARD Conference Proceedings No. 17, Part II, 1966.

B9. A'Harrah, R. C. and R. P. Schulze. "An Investigation of Low-Altitude, High Speed Flying and Riding Qualities of Aircraft," North American Aviation, Inc., Report No. 62H-397, February 1963.

B10. Allender, J. Reverdy and Robert M. White. "F-102A Phase IV Stability Test," AFFTC-TR-57-5, April 1957.

B11. Archer, Donald D. and Charles L. Gandy, Jr. "T-37A Phase IV Performance and Stability and Control," AFFTC-TR-56-37, February 1957.

B12. Ashkenas, I. L. "Comment on 'Low-Altitude, High-Speed Handling and Riding Qualities,'" AIAA J. of Aircraft, July-August 1964, pp. 222-223.

B13. Ashkenas, I. L. "Further Comment on 'Low-Altitude, High-Speed Handling and Riding Qualities,'" AIAA J. of Aircraft, November-December 1964, p. 377.

B14. Ashkenas, I. L. and D. T. McRuer. "Optimization of the Flight Control, Airframe System," J. Aero/Space Sc., Vol. 27, No. 3, March 1960.

B15. Ashkenas, I., H. Jex, and D. McRuer. "Pilot-Induced Oscillations: Their Cause and Analysis," NORAIR Report No. NOR-64-143, Systems Technology, Inc. TR-239-2, 20 June 1964.

B16. Bihrle, William, Jr. "Longitudinal Control Surface Pumping--A Pilot's Technique for Controlling the Flight Path Precisely," AIAA Paper No. 70-567, May 1970, AIAA J. of Aircraft, Vol. 8, No. 1, pp. 56-58, January 1971.

B17. Browne, E. V. "Northrop T-38A PIO Program Review--Prepared for the Air Force T-38A PIO Review Board," AIS-65, February 1963.

B18. Brulle, R. V. and W. A. Moran. "Dynamic Flying Qualities Investigation," AFFDL-TR-74-142, November 1974.

B19. Caporali, R. L., J. P. Lamers, and J. R. Totten. "A Study of Pilot-Induced Lateral-Directional Instabilities," Aeronautical Engineering Report 604, Princeton University, May 1962.

B20. Chalk, C. R. et al. "Background Information and User Guide for MIL-F-8785B(ASG), 'Military Specification--Flying Qualities of Piloted Airplanes,'" AFFDL-TR-69-72, August 1969.

B21. Chalk, C. R. et al. "Revisions to MIL-F-8785B(ASG) Proposed by Cornell Aeronautical Laboratory Under Contract F33615-71-C-1254," AFFDL-TR-72-41, April 1973.

B22. Craig, S. J. and I. L. Ashkenas. "Background Data and Recommended Resisions for MIL-F-8785B(ASG), 'Military Specification--Flying Qualities of Piloted Airplanes,'" Systems Technology, Inc. Technical Report No. 189-1, March 1971.

B23. Crawford, Charles C. and Jones P. Seigler. "KC-135A Stability and Control Test," AFFTC-TR-58-13, May 1958.

B24. Decker, James L. "The Human Pilot and the High-Speed Airplane," J. Aero. Sciences, Vol. 23, No. 8, August 1956.

B25. DiFranco, Dante A. "Flight Investigation of Logitudinal Short Period Frequency Requirements and PIO Tendencies," AFFDL-TR-66-163, June 1967.

B26. DiFranco, Dante A. "In-Flight Investigation of the Effects of Higher-Order Control System Dynamics on Longitudinal Handling Qualities," AFFDL-TR-68-90, August 1968.

B27. Eichler, Jay. "A Regression Analysis of Pilot-Induced Oscillation Ratings," J. of A/C, 7, 4, pp. 314-319, August 1970.

B28. Finberg, Floyd, Lt. Col. "Report of the T-38 Flight Control System PIO Review Board," Aeronautical Systems Division, USAF, 15 February 1963.

B29. Finch, Thomas W. and Gene J. Matranga. "Launch, Low-Speed, and Landing Characteristics Determined from the First Flight of the North American X-15 Research Airplane," NASA TM X-195, September 1959.

B30. Fortenbaugh, Robert L. "Moving Base Simulator Evaluation of Two Quantitative PIO Criteria," SAE Aerospace Vehicle Flight Control Systems Committee Meeting No. 26, Seattle, Washington, September 23-25, 1970.

B31. Gedeon, J. "Statistical Aspects of Handling Criteria Research," Aerorevue , No. 3, March 1970, pp. 146-150.

B32. Gobert, Don O. et al. "Flying Qualities and Limited Systems Military Preliminary Evaluation of the A-7D/E with Three Hydraulic Power Control Systems," AFFTC-TR-70-10, April 1970.

B33. Grosso, Vincent A. "An Investigation to Determine the Effects of Several Parameters on Optimum Zoom Climb Performance," AFFTC-TN-59-32, September 1959.

B34. Hall, G. Warren and Robert P. Harper, Jr. "In-Flight Simulation of the Light Weight Fighters," AIAA Paper No. 75-985, August 1975.

B35. Hall, G. Warren and Rogers E. Smith. "Flight Investigation of Fighter Side-Stick Force-Deflection Characteristics," AFFDL-TR-75-39, March 1975.

B36. Harper, Robert P., Jr. "In-Flight Simulation of the Lateral-Directional Handling Qualities of Entry Vehicles," WADD TR-61-147, February 1961.

B37. Hartwick, Peter, J., Bredette C. Thomas, Jr., and George C. Nield. "T-38 Flap Interconnect Failure Tests," AFFTC-TR-76-32, September 1976.

B38. Hirsch, D. "Investigation and Elimination of PIO Tendencies in the Northrop T-38A," SAE Paper, New York, July 1964.

B39. Hirsch, D. and R. McCormick. "Experimental Investigation of Pilot Dynamics in a Pilot-Induced Oscillation Situation," AIAA Paper 65-793, November 1965, J. of Aircraft, November-December 1966, p. 567.

B40. Hoffman, Lee Gregor, Kishor V. Shah, and Dunstan Graham. "Analysis of Limited Authority Manual Control Systems," AFFDL-TR-71-6, July 1971.

B41. Jex, H. R. "Summary of T-38A PIO Analyses," Systems Technology, Inc. TM No. 239-3, 25 January 1963.

B42. Johnson, Harold I. "Flight Investigation to Improve the Dynamic Longitudinal Stability and Control Feel Characteristics of the P-63A-1 Airplane (AAF No. 42-68889) with Closely Balanced Experimental Elevators," NACA MR No. L6E20, July 1946. (Also NACA WR L-730.)

B43. Kandalaft, R. N. "Validation of the Flying Qualities Requirements of MIL-F-8785B(ASG)," AFFDL-TR-71-134, September 1971.

B44. Keith, L. A. and G. J. Marrett. "F-4C Stability and Control Tests with a TAC training Load," AFFTC-TR-67-9, 1967.

B45. Keith, L. A., R. R. Richard, and G. J. Marrett. "Evaluation of Longitudinal Control Feel System Modifications Proposed for USAF F/RF-4 Aircraft," AFFTC-TR-67-19, December 1967.

B46. Keith, L. A., G. J. Marrett, and R. R. Rickard. "F-4C Category II Follow-On Stability and Control Tests," AFFTC-TR-67-26, May 1968.

B47. Kempel, Robert W. "Analysis of a Coupled Roll-Spiral Mode, Pilot-Induced Oscillation Experienced with the M2-F2 Listing Body," NASA TN D-6496, September 1971.

B48. Kleckner, Harold F. "Preliminary Flight Research on an All-Movable Horizontal Tail as a Longitudinal Control for Flight at High Mach Numbers," NACA WR L-89, 1945.

B49. Kleckner, Harold F. "Flight Tests of an All-Movable Horizontal Tail with Geared Unbalancing Tabs on the Curtiss XP-42 Airplane," MACA TN 1139, 1946.

B50. Lau, Conrad A. and Lyman C. Josephs. "Some Experiences of a Manufacturer with Power Operated Aircraft Control Systems," Chance Vought Aircraft, May 25, 1951.

B51. Levi, O. A. and W. E. Nelson. "An Analytical and Flight Test Approach to the Reduction of Pilot Induced Oscillation Susceptibility," J. of Aircraft, July-August 1964, pp. 178-184.

B52. Lytwyn, Roman T. "An Analysis of the Divergent Vertical Helicopter Oscillations Resulting from the Physical Presence of the Pilot in the Collective Control Loop," J. of the AHS, Vol. 12, June 1967, pp. 45-52.

B53. Matranga, Gene J. "Analysis of X-15 Landing Approach and Flare Characteristics Determined from the First 30 Flights," NASA TN D-1057, July 1961.

B54. McFadden, Norman M., Frank A. Pauli, and Donovan R. Heinle. "A Flight Study of Longitudinal Control System Dynamic Characteristics by the Use of a Variable Control System Airplane," NACA RM A57L10, March 3, 1958.

B55. McPherson, T. M. and K. W. Weir. "Flight-Test Evaluations: Airplane Dynamic Longitudinal Stability in the Low Altitude, High Speed Region," AGARD Report 442, April 1963.

B56. Miyajima, Katsuyuki. "Some Considerations on Pilot Induced Oscillations," Japan Society for Aeronautical and Space Sciences, Transactions, Vol. 10, No. 16, pp. 11-22, 1967.

B57. Neal, T. Peter. "The Influence of Bobweights on Pilot-Induced Oscillations," AIAA Paper No. 70-1002, August 1970.

B58. Nelson, W. E. "A Brief Analysis of the Relationship of PIO Tendencies to Low Static Margins as Applied to the F-5A/B Aircraft," Norair Division, Northrop Corporation, Report No. FMR-65-5, June 1965.

B59. Nelson, W. E. and O. A. Levi. "An Analytical and Flight Test Approach to the Reduction of Pilot Induced Oscillation Susceptibility," Northrop-Norair Division Report, October 1963.

B60. Neubeck, F. G. High Speed Stability and Control (Pilot Induced Oscillation), textbook of the Aerospace Research Pilot School, Edwards Air Force Base, 1962.

B61. Newell, Fred. "Investigation of Phugoid Effects on GCA Landings," WADC-TR-57-650, December 1957.

B62. Newell, Fred D. and Richard Wasserman. "In-Flight Investigation of the Effect on PIO of Control System Nonlinearities, Pitch Acceleration and Normal Acceleration Bobweights," AFFDL-TR-69-3, May 1969.

B63. Ozarko, Henry S. "Preliminary Results of Tests of a 10-Ton Surface Effect Vehicle in the Artic; Pilot Induced Oscillation," Naval Ship Research and Development Center, Technical Note AL-246, April 1972. (Also AD 901 496.)

B64. Paiewonsky, B. H. "The Effects of Engine Angular Momentum on an Airplane's Longitudinal and Lateral-Directional Dynamic Stability," WADC TR 56-225, June 1956.

B65. Phillips, William H. "An Investigation of Additional Requirements for Satisfactory Elevator Control Characteristics," MACA TN 1060, 1946.

B66. Phillips, William H., B. Porter Brown, and James T. Matthews. "Review and Investigation of Unsatisfactory Control Characteristics Involving Instability of Pilot-Airplane Combination and Methods for Predicting these Difficulties from Ground Tests," MACA TN 4064, August 1957. (Also, NACA RM L53F17a, August 1953.)

B67. Phillips, W. H., W. C. Williams, and H. H. Hoover. "Measurements of Flying Qualities of a Curtis SB2C-1 Airplane (No. 00014)," NACA WR L-571, 1944.

B68. Richardson, J. D. and R. C. A'Harrah. "The Application of Flight Simulators to the Development of the A-5A Vigilante," AIAA Simulation for Aerospace Flight, National Specialists Meeting, August 1963.

B69. Sadoff, M. "Effects of Longitudinal Control System Dynamics on Pilot Opinion and Response Characteristics as Determined from Ground Simulator Studies," NASA Memo 10-1-58A, Ocrober 1958.

B70. Simmons, Carl D. and Donald M. Sorlie. "F-101B Air Force Stability and Control Evaluation," AFFTC-TR-58-11, May 1958.

B71. Smith, John W. and Donald T. Berry. "Analysis of Longitudinal Pilot-Induced Oscillation Tendencies of YF-12 Aircraft," NASA TN D-7900, February 1975.

B72. Snyder, C.T. et al. "Motion Smulator Study of Longitudinal Stability Requirements for Large Delta Wing Transport Airplanes During Approach and Landing with Stability Augmentation Systems Failed," NASA TM X-62,200, December 1972.

B73. Taylor, Lawrence W., Jr. "Analysis of a Pilot-Airplane Lateral Instability Experienced with the X-15 Airplane," NASA TN D-1059, November 1961.

B74. Terrill, W. H., J. G. Wong, and L. R. Springer. "Investigation of Pilot-Induced Longitudinal Oscillation in the Douglas Model A4D-2 Airplane," Report No. LB-25452, Douglas, 15 May 1957.

B75. Ulrich, K. W. "F9F-8 Longitudinal Stability Derivatives from Porpoising Flight Test Data," Grumman Aircraft Engineering Report XA93-119-2, July 1956.

B76. Williams, G. H. and W. T. Twinting. "F-4C Category II Stability and Control Test," AFFTC-TR-65-30, December 1965.

REFERENCES

1. Finberg, Floyd, Lt. Col., "Report of the T-38 Flight Control System PIO Review Board," Aeronautical Systems Division, USAF, 15 February 1963.

2. Bihrle, William, Jr., "Longitudinal Control Surface Pumping--A Pilot's Technique for Controlling the Flight Path Precisely," AIAA Paper No. 70-567, May 1970, AIAA J. of Aircraft, Vol. 8, No. 1, pp. 56-58, January 1971.

3. Smith, Ralph H. and Mark E. Reigle, "Toward a Pilot Model for Carrier Approach," unpublished report,U.S. Naval Air Development Center, Warminster, Pennsylvania, 1971. Presented by the principal author as an informal paper at the Eighth Annual Conference on Manual Control, University of Michigan, Ann Arbor, Michigan, May 17-19, 1972.

4. Ashkenas, I., H. Jex, and D. McRuer, "Pilot-Induced Oscillations: Their Cause and Analysis," NORAIR Report No. NOR-64-143 (also Systems Technology, Inc. TR-239-2), 20 June 1964.

5. Ashkenas, I. L., "Comment on 'Low-Altitude, High-Speed Handling and Riding Qualities,'" AIAA J. of Aircraft, July-August 1964, pp. 222-223.

6. McRuer, Duane, Dunstan Graham, Exra Krendel, and William Reisner, Jr., "Human Pilot Dynamics in Compensatory Systems: Theory, Models and Experiments with Controlled Element and Forcing Function Variations," AFFDL-TR-65-15, July 1965.

7. A'Harrah, Ralph C., "Reply by Author to I. L. Ashkenas," J. of Aircraft, July-August 1964, pp. 223-224.

8. Hall, G. Warren, and Robert P. Harper, Jr., "In-Flight Simulation of the Light Weight Fighters," AIAA Paper No. 75-985, August 1975.

9. Magaleno, R. E., H. R. Jex, and W. A. Johnson, "Tracking Quasi-Predictable Displays: Subjective Predictability Gradations, Pilot Models for Periodic and Narrowband Inputs," NASA SP-215, Fifth Annual NASA-University Conference on Manual Control, March 27-29, 1969, pp. 391-428.

10. Smith, R. H., "A Theory for Handling Qualities with Applications to MIL-F-8785B," AFFDL-TR-75-119, October 1975.

11. Smith, John W. and Donald T. Berry, "Analysis of Longitudinal Pilot-Induced Oscillation Tendencies of YF-12 Aircraft," NASA TND-7900, February 1975.

12. Smith, R. H., "LSO-Pilot Interviews on Carrier Approach," U.S. Naval Air Development Center, Warminster, Pennsylvania, TM No. AM-TM-1681, May 1973.

13. Graham, Dunstan and Duane McRuer, Analysis of Nonlinear Control Systems, Wiley, 1961.

14. Meiry, Jacob L., "The Vestibular System and Human Dynamic Space Orientation," NASA CR-628, October 1966.

15. Chalk, Charles R., Dante A. DiFranco, J. Victor Lebazqz, and T. Peter Neal, "Revisions to MIL-F-8785B(ASG) Proposed by Cornell Aeronautical Laboratory Under Contract F33615-71-C-1254," AFFDL-TR-72-41, April 1973.

16. Chalk, C. R., T. P. Neal, T. M. Harris, F. E. Pritchard and R. J. Woodcock, "Background Information and User Guide for MIL-F-8785B(ASG), 'Military Specification--Flying Qualities of Piloted Airplanes,'" AFFDL-TR-69-72, August 1969.

17. DiFranco, D. A., "Flight Investigation of Longitudinal Short-Period Frequency Requirements and PIO Tendencies," AFFDL-TR-66-163, June 1967.

18. Teper, Gary L., "Aircraft Stability and Control Data," Systems Technology, Inc. TR 176-1, April 1969.

19. Jex, H. R., "Summary of T-38A PIO Analyses," Systems Technology, Inc. TM No. 239-3, 25 January 1963.

20. Ashkenas, Irving L. and Duane T. McRuer, "Approximate Airframe Transfer Functions and Application to Single Sensor Control Systems," WADC TR 58-82, June 1958.

21. Hartwick, Peter J., Bredette C. Thomas, Jr., and George C. Nield, "T-38 Flap Interconnect Failure Tests," AFFTC-TR-76-32, September 1976.

22. Neal, T. Peter, "The Influence of Bobweights on Pilot-Induced Oscillations," AIAA Paper No. 70-1002, August 1970.

23. Sinacori, J. B., "A Practical Approach to Motion Simulation," AIAA Paper No. 73-931, September 1973.

24. Twisdale, Thomas R. and David L. Franklin, "Tracking Test Techniques for Handling Qualities Evaluation," AFFTC-TD-75-1, May 1975.

25. Hall, G. Warren and Ronald W. Huber, "System Description and Performance Data for the USAF/CAL Variable Stability T-33 Airplane," AFFDL-TR-70-71, August 1970.

*U.S.Government Printing Office: 1978 — 757-080/681